

UNCLASSIFIED

AD NUMBER

AD833215

NEW LIMITATION CHANGE

TO

**Approved for public release, distribution
unlimited**

FROM

**Distribution authorized to U.S. Gov't.
agencies and their contractors; Critical
Technology; 15 DEC 1954. Other requests
shall be referred to Soace and Missile
Systems Organiation, Los Angeles, CA.**

AUTHORITY

SAMSO USAF ltr, 28 Feb 1972

THIS PAGE IS UNCLASSIFIED

ANALYST
PREPARED BY
CHECKED BY
REVISED BY

CONSOLIDATED VULTEE AIRCRAFT CORPORATION
SAFETY DIVISION

PAGE
REPORT NO. ZA-7-065
MODEL
DATE

1-Atlas-103
6/14/63

This document is subject
to special export controls and
each transmission to foreign
governments or foreign
organizations may be made only
with prior approval of:
HQ. SAMS, IIA, Cal 90045
Attn: SMSD

Current of Breakdown, Inspection Note

and Skin Protection Data for

Proprietary Goods

CONVAIR
AERONAUTICS

SEP 24 1959

LIBRARY

M. P. Basig

15 December 1954

20060314000

Best Available Copy

ANALYSIS
PREPARED BY
CHECKED BY
REVISED BY

CONSOLIDATED VULTEE AIRCRAFT CORPORATION
SAN DIEGO DIVISION

PAGE 1
REPORT NO. A-Atlas-103
MODEL 7
DATE 15 Dec. 1954

Curves of Shockwave, Expansion Wave and
Skin Friction Data for Hypersonic Flows

1.0 Summary

This report presents curves of shockwave, expansion wave and boundary layer data plotted for use at Mach numbers up to 20. Normal and oblique shockwave parameters, conical shock parameters, expansion wave parameters, cone aerodynamic coefficients and compressible laminar and turbulent boundary layer skin friction formulas are given for Mach numbers up to at least 20. The use of these curves is briefly described in the text.

2.0 Symbols

C_D - wave drag coefficient = $\frac{\text{Wave Drag}}{q_0}$

C_f - local skin friction coefficient = $\frac{f}{g}$

C_F - wave skin friction coefficient = $\frac{\text{Wave Drag}}{q_0}$

C_N - normal force coefficient = $\frac{\text{Normal Force}}{q_0}$

C_p - coefficient of specific heat at constant pressure BTU/lb. $^{\circ}$ R

C_x - axial drag coefficient = $\frac{\text{Axial Drag}}{q_0}$

g - acceleration due to gravity ft./sec. 2

h - heat transfer coefficient BTU/ft. 2 hr. $^{\circ}$ R

H - total pressure lbs./ft. 2

J - mechanical equivalent of heat ft.-lb./BTU

k - thermal conductivity BTU/ft. hr. $^{\circ}$ R

l - wetted length ft.

l' - effective starting length ft.

M - Mach number

N - Froude number = $\frac{H}{\sqrt{g}}$

p - static pressure lb./ft. 2

P_r - Prandtl number = $\frac{\mu C_p}{k}$

ANALYSIS
PREPARED BY
CHECKED BY
REVISED BY

CONSOLIDATED VULTEE AIRCRAFT CORPORATION
SAN DIEGO DIVISION

PAGE 2
REPORT NO. A-Atlae-103
MODEL 7
DATE 15 Dec. 1954

Q - heat flux	BTU/hr. ft. ²
$\frac{q}{\rho}$ - dynamic pressure	lb./ft. ²
Re - Reynolds number = $\frac{\rho u l}{\mu}$	
S - reference area	ft. ²
T - static temperature	°R
T' - reference temperature	°R
T_e - recovery or inherent temperature	°R
u - velocity	ft./sec.
x - axial length	ft.

Greek

α - angle of attack	degrees
β - shockwave angle	degrees
γ - ratio of specific heats	
δ - flow deflection angle, boundary layer thickness	degrees, ft.
θ - boundary layer momentum thickness	ft.
θ_v - cone semi-vortex angle	degrees
ϕ_w - cone shockwave half angle	degrees
μ - coefficient of viscosity	lb. sec./ft. ²
ν - Prandtl-Mayer angle	degrees
ρ - density	lb. sec. ² /ft. ⁴
τ - shear stress	lbs./ft. ²

Subscripts

- 1 - initial or free stream
- 2 - after the shock
- s - surface of the cone
- 00 - sea level

ANALYSIS
PREPARED BY
CHECKED BY
REVISED BY

CONSOLIDATED VULTEE AIRCRAFT CORPORATION
SAN DIEGO DIVISION

PAGE 3
REPORT NO. A-Atlas-103
MODEL 7
DATE 15 Dec. 1954

w - at the wall

α - local

i - incompressible or location index

3.0 Discussion and Results

The need for a combined collection of basic supersonic aerodynamic data has long been evident to Convair Aerodynamicists working with high velocity bodies. The existing charts and tables (Reference 1, 2, 3) are either limited in some phase of Mach number and flow deflection angle or the data are not presented graphically (Reference 4). It was believed also that some convenient reference should be provided for the skin friction and heat transfer formulae associated with the reference temperature method explained in Reference 9. This report fulfills these needs.

The sections following will deal with the separate types of curves presented.

3.1 Inviscid Flow Parameters

The curves in this section are separated into one, two and three dimensional flow. The flow parameters presented, all versus initial Mach number, are Mach number after the shock, static pressure ratio, static temperature ratio, density ratio, velocity ratio, dynamic pressure ratio, Reynolds number ratio, total head ratio and shockwave angle. All ratios are quantities after the wave divided by the value of the same quantity before the wave.

Force coefficients are given for both unyawed and yawed cones. C_N , $\frac{dC_N}{d\alpha}$ and C_x are given for cones in Newtonian flow (Reference 4, 5, 6).

The Reynolds numbers presented in Figure 1.6, 2.8 and 3.8 were found from

$$\frac{P_{e2}}{P_{e1}} = \frac{\rho_2 u_2}{\rho_1 u_1} \left(\frac{T_1}{T_2} \right)^{0.7}$$

where an exponential viscosity - temperature relation

$$\frac{\mu_2}{\mu_1} = \left(\frac{T_1}{T_2} \right)^{0.7}$$

was assumed.

ANALYSIS
PREPARED BY
CHECKED BY
REVISED BY

CONSOLIDATED VULTEE AIRCRAFT CORPORATION
SAN DIEGO DIVISION

PAGE 4

* REPORT NO. A-Atlas-103
MODEL 7
DATE 15 Dec. 1954

The data for these curves were obtained from Reference 1 through Reference 6 or were computed for high Mach number-deflection angle combinations when they were not tabulated.

3.2 Viscoelastic Flow Parameters By The Reference Temperature Method

The curves presented in this section are primarily for use with the reference temperature method of calculating heat transfer and skin friction. Figures 4.1 - 4.7 include: local and mean incompressible flow skin friction coefficients for laminar, transition and turbulent flow vs. Reynolds number (Reference 7); reference temperature ratio T'/T_∞ vs. Mach number; and reference temperature $(T')^{1/7}$ vs. T' . For use in the heat balance equation the inherent (recovery) temperature rise ΔT_1 is given versus velocity. The theoretical laminar boundary layer stability curve (Reference 8) is shown in Figure 4.5 to indicate the type of boundary layer flow which might be expected for various R , T_w/T_∞ and Re combinations. Figures 4.6 and 4.7 present the NACA-NBS variation of C_p with T and variation of μ with T as given by the Sutherland viscosity rule.

The reference temperature method and its associated equations will be presented below in outline form. A complete derivation of these equations may be found in Reference 9, which also contains a critical evaluation of the method. The concept of an "effective length", needed for the application of this method to bodies other than flat plates, is discussed by Sieff (Reference 10) and Romig (Reference 11). Therefore the following sections are primarily on the use of the method in obtaining the heat transfer and skin friction.

The reference temperature method is based on the assumption that the use of a characteristic temperature in the compressible equations for drag and heat transfer will eliminate their outward dependence on temperature and Mach number, i.e., convert them to the incompressible, constant-property equation. Under this assumption the T' method is thus described as: if all temperature-dependent properties in the incompressible equations for heat transfer and drag are based on the reference temperature T' then the incompressible equations will yield the compressible friction or heat transfer coefficients. Use of this method therefore obviates solving the compressible laminar and turbulent boundary layer equations. The equations for the reference temperature are

$$T' = T_\infty \left[0.42 + 0.032 M_\infty^2 + 0.58 \frac{T_w}{T_\infty} \right], M_\infty \leq 5.5 \quad (1)$$
$$T' = T_\infty \left[0.70 + 0.023 M_\infty^2 + 0.58 \frac{T_w}{T_\infty} \right], M_\infty \geq 5.5$$

where the ratio T'/T_∞ may be found in Figure 4.2 vs. Mach number for integral values of $1 \leq T_w/T_\infty \leq 4$. The eq. (1) are valid for both laminar and turbulent flow.

ANALYSIS
PREPARED BY
CHECKED BY
REVISED BY

CONSOLIDATED VULTEE AIRCRAFT CORPORATION
SAN DIEGO DIVISION

PAGE 5
REPORT NO. 4-Atlas-103
MODEL 7
DATE 15 Dec. 1954

3.2.1 Basic Equations for Two-Dimensional Flow

The compressible skin friction may be obtained either as the ratio of compressible to incompressible, C_f/C_{f_i} , or explicitly as a function of the Reynolds number based on T' . For practical considerations explicit relationships will be developed first for the local and mean compressible friction.

Assume all air properties in the incompressible drag equations are based on f' so that according to the assumption stated in 3.2,

$$(\text{compressible}) C_{f_\infty} \frac{q_\infty}{\rho_\infty} \equiv \gamma \equiv (\text{incompressible}) C_{f_i} \frac{q'}{\rho_0}$$

where the primes denote that air properties are based on T' .

or

$$C_{f_\infty} = C_{f_i}' \frac{\rho'}{\rho_0}$$

Using the perfect gas equation at constant pressure,

$$C_{f_\infty} = \frac{T_\infty}{T'} C_{f_i}' \quad (2)$$

where C_{f_i}' is given either by the Blasius formula

$$\text{LAMINAR } C_{f_i}' = \frac{0.664}{\sqrt{\frac{\rho' u^2}{\mu'}}} \quad (3)$$

or the Karman equation

$$\text{TURBULENT } (C_{f_i}')^{-1/2} = 1.7 + 4.15 \log_{10} \frac{\rho' u L}{\mu'} C_{f_i}' \quad (4)$$

These laminar and turbulent incompressible friction coefficients (Eq. 3 & 4) are plotted in Figure 4.1 versus Reynolds number. The Reynolds number to be used with Eq. (3) & (4) and hence in evaluating Eq. (2) is a function of T' . The expression for $R_{T'}$ is given as

$$R_{T'} = \frac{\rho' u L}{\mu'}$$

ANALYSIS
PREPARED BY
CHECKED BY
REVISED BY

CONSOLIDATED VULTEE AIRCRAFT CORPORATION
SAN DIEGO DIVISION

PAGE 6
REPORT NO 1-Atlas-103
MODEL 7
DATE 15 Dec. 1954

or, using the power law for viscosity, $\mu \propto (T)^{0.7}$ and using ambient conditions as a reference,

$$Re_{T'} = \left(\frac{T_\infty}{T'} \right)^{1.7} Re_\infty \quad (5)$$

If the perfect gas law is used and sea level ($T = 518.4^\circ R$) conditions are used in the power law,

$$Re_{T'} = 12.44 \times 10^4 \frac{\rho_\infty \mu_\infty l}{(T')^{1.7}} \quad (6)$$

Thus it is only necessary to enter Figure 4.1 with $Re_{T'}$, computed by Eq. (5) or Eq. (6), locate the desired C_{f_i}' and compute C_{f_∞} by Eq. (2). For convenience in computing $Re_{T'}$, the function $(T')^{1.7}$ is plotted versus T' in Figure 4.3.

The mean skin friction coefficients may be obtained in much the same way from the drag equation. For both laminar and turbulent flow

$$C_{f_\infty} = \frac{T_\infty}{T'} C_{f_i}' \quad (7)$$

where C_{f_i}' is given by the Blasius formula

$$\text{LAMINAR } C_{f_i}' = \frac{1.328}{\sqrt{Re_{T'}}} \quad (8)$$

and the Prandtl-Schlichting equation

$$\text{TURBULENT } C_{f_i}' = \frac{0.455}{(\log_{10} Re_{T'})^{2.58}} \quad (9)$$

Eqs. (8) and (9) are also plotted versus Reynolds number in Figure 4.1. The same procedure is used in evaluating the mean coefficient as was used for the local.

The compressible heat transfer rate can be obtained from the definition of the heat equation

$$Q = h(T_i - T_w) \quad (10)$$

ANALYSIS
PREPARED BY
CHECKED BY
REVISED BY

CONSOLIDATED VULTEE AIRCRAFT CORPORATION
SAN DIEGO DIVISION

PAGE 7
REPORT NO. A-Atlas-103
MODEL 7
DATE 15 Dec. 1954

where the heat transfer coefficient is defined as

$$h = \frac{Nu k}{l} \quad (11)$$

If the air properties in h are based on T' and the following incompressible relationships for Nusselt number are used,

$$\text{LAMINAR } Nu_{\infty} = 0.332 \sqrt{Pr'} \sqrt{R_{\infty}} \quad (12)$$

and

$$\text{TURBULENT } Nu_{\infty} = 0.0296 (R_{\infty})^{0.8} \quad (13)$$

then after considerable algebraic manipulation the following heat transfer equations are found

$$\text{LAMINAR } h = 0.0074 \left[\frac{Pr_{\infty} U_{\infty}}{l} \right]^{0.5} \quad (14)$$

$$\text{TURBULENT } h = \frac{0.02498 (Pr_{\infty} U_{\infty})^{0.8}}{l^{0.2} (T')^{0.51}} \quad (15)$$

It was assumed in Eq. (14) and (15) that the air properties varied in the following way

$$\frac{\mu}{\mu_{\infty}} = \left(\frac{T}{T_{\infty}} \right)^{0.7}, \quad \frac{k}{k_{\infty}} = \left(\frac{T}{T_{\infty}} \right)^{0.85}, \quad Pr = 0.72 \quad p = \rho R T \quad (15a)$$

The validity of Eq. (14) in particular and the exponents in the power laws were substantiated in the investigations of Reference (9). It was found that these heat transfer equations are correct as long as the boundary layer air is not dissociated.

Curves of $\Delta T_1 = T_1 - T_1'$, where T_1 is the free stream static temperature, are plotted versus free stream velocity in Figure 4.4a - 4.4c for use in eq. (10).

Thus to compute the compressible laminar or turbulent heat, it is only necessary to find the reference temperature and solve eq. (14) or (15). These values of h are used along with the temperatures obtained from Figure 4.4a - 4.4c in eq. (10) to find the heat rate Q .

ANALYSED
FOR SPARED BY
CHECKED BY
REVISED BY

CONSOLIDATED VULTEE AIRCRAFT CORPORATION
SAN DIEGO DIVISION

PAGE 8
REPORT NO. A-Atlas-103
MODEL 7
DATE 15 Dec. 1954

3.2.2 Two Dimensional Flow With Discontinuities

The equations (1) - (15) written above apply in strict sense only to flat plate flow. Any condition which would tend to make the external flow discontinuous at a point, such as transition from laminar to turbulent flow, or passing through a shockwave or expansion, renders the equations inapplicable.

In order to use eq. (1) - (15) it is necessary, therefore, to somehow refer the boundary layer characteristics at the point of discontinuity to a flat plate boundary layer with identical characteristics but with no flow discontinuities. This can be accomplished by forcing, as it were, the momentum loss of the boundary layer flow to remain constant across any discontinuity. This momentum-loss method will give an effective starting length for the boundary layer characteristics to the point of discontinuity.

The momentum loss equations are discussed at length in Reference (10) and (11) and only a brief outline of them are given here. If the momentum loss through the boundary layer is defined as

$$\int_0^{\delta} \rho u (u_{\infty} - u) dy$$

then across any point of discontinuity it is assumed that

$$\int_0^{\delta_1} \rho u (u_1 - u) dy = \int_0^{\delta_2} \rho u (u_2 - u) dy \quad (16)$$

This is equivalent to stating that

$$\Theta_1 g_1 = \Theta_2 g_2 \quad (17)$$

where Θ is the boundary layer momentum thickness and g the stream dynamic pressure. The laminar or turbulent equations for Θ allow (17) to be solved for ℓ_2 , the effective starting length. For convenience in nomenclature ℓ_2 is designated as ℓ' hereafter.

Therefore let

$$\Theta_{LM} = \frac{1.328}{(\frac{\rho_0 u_0 \ell}{\mu_0})^{1/2}} \left(\frac{C_F}{C_{F_L}} \right)_{LM} \ell \quad (18)$$

ANALYSIS
PREPARED BY
CHECKED BY
REVISED BY

CONSOLIDATED VULTEE AIRCRAFT CORPORATION
SAN DIEGO DIVISION

PAGE 9
REPORT NO. A-Atlas-103
MODEL 7
DATE 15 Dec. 1954

and

$$\Theta_{TURB} = \frac{0.072}{\left(\frac{\rho_0 u_0}{\mu_0}\right)^{0.2}} \left(\frac{C_F}{C_{F_i}}\right)_{TURB} l \quad (19)$$

where l is the length along the body to the point of discontinuity. The turbulent expression for Θ is based on the $1/7$ th power law for velocity. It is adequate for $5 \times 10^5 \leq Re \leq 10^7$. The more exact solution (Eq. (9)) would not be amenable for computation of l' . These equations giving Θ can be simplified by making the same assumptions used in the heat equations (14) and (15) in the skin friction derivation to get

$$\left(\frac{C_F}{C_{F_i}}\right)_{LAM} = \left(\frac{T_\infty}{T'}\right)^{0.15} \quad \& \quad \left(\frac{C_F}{C_{F_i}}\right)_{TURB} = \left(\frac{T_\infty}{T'}\right)^{0.66} \quad (20)$$

Substitution of (20) into (18) and (19) and use of Eq. (15a) gives

$$\Theta_{LAM} = 0.003765 \left[\frac{\rho_0 u_0}{(T_\infty)^{1/7}} \right]^{-0.5} \left(\frac{T_\infty}{T'} \right)^{0.15} l^{0.5} \quad (21)$$

and

$$\Theta_{TURB} = 0.006892 \left[\frac{\rho_0 u_0}{(T_\infty)^{1/7}} \right]^{-0.2} \left(\frac{T_\infty}{T'} \right)^{0.66} l^{0.8} \quad (22)$$

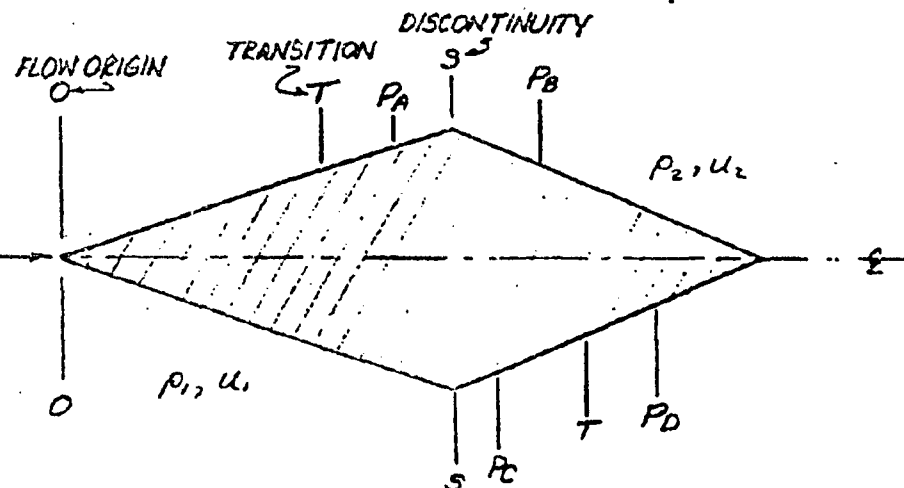
These equations can then be used in (17) to obtain l' .

Two types of flow discontinuities can be encountered in two dimensional flow. These are (a) transition from laminar to turbulent flow and (b) shockwave or an expansion. The equations for l' for combinations of these cases are obtained from Eq. (17) - (22) and are summarized in the following table for flow on an infinite double-wedge airfoil, a typical two-dimensional body.

ANALYSIS
PREPARED BY
CHECKED BY
REVISED BY

CONSOLIDATED VULTEE AIRCRAFT CORPORATION
SAN DIEGO DIVISION

PAGE 10
REPORT NO. A-Atleg-103
MODEL 7
DATE 15 Dec. 1954



The following effective starting lengths are given to the points P of interest

$$\text{TO } P_A \quad l'_A = \bar{T} \bar{P}_A + 0.4696 \left[\frac{p_1 u_1}{(T_1')^{1.7}} \right]^{-0.375} (\bar{O} \bar{T})^{0.625} \quad (23)$$

$$\text{TO } P_B \quad l'_B = \bar{S} \bar{P}_B + (\bar{S} \bar{P}_A + l'_A) \frac{p_1}{p_2} \left(\frac{u_1}{u_2} \right)^{1.5} \left(\frac{T_2'}{T_1'} \right)^{0.825} \quad (24)$$

$$\text{TO } P_C \quad l'_C = \bar{S} \bar{P}_C + \bar{O} \bar{S} \frac{p_1}{p_2} \left(\frac{u_1}{u_2} \right)^3 \left(\frac{T_2'}{T_1'} \right)^{0.3} \quad (25)$$

$$\text{TO } P_D \quad l'_D = \bar{T} \bar{P}_D + (l'_C + \bar{P}_C \bar{T})^{0.625} \cdot 0.4696 \left[\frac{p_2 u_2}{(T_2')^{1.7}} \right]^{-0.375} \quad (26)$$

Eq. (23) - (26) may then be used to evaluate the l' , which in turn can be used in Eq. (2) - (15) along with local conditions to evaluate the desired coefficients. Since Eq. (1) is independent of length this method does not involve iteration.

ANALYSIS
PREPARED BY
CHECKED BY
REVISED BY

CONSOLIDATED VULTEE AIRCRAFT CORPORATION
SAN DIEGO DIVISION

PAGE 11
REPORT NO. A-Atlas-103.
MODEL 7
DATE 15 Dec. 1954

3.2.3 Three Dimensional Flow

Since the boundary layer at any point on a cone is much thinner than the boundary layer of a flat plate which has otherwise the same boundary layer characteristics as the cone, the Eq. (2) - (15) do not apply to conical flow unless some correction is made in order to correlate the boundary layer thicknesses. This correction can be made by working directly with the three-dimensional boundary layer equations in the laminar case. Hantzsche and Wenzel (Reference 12) found that the conical equations transformed directly into the two dimensional equations if the factor 1/3 were inserted in the cone length. Therefore, for laminar flow, if

$$\text{LAMINAR: } l_{\text{cone}} = \frac{1}{3} l_{\text{FLAT PLATE}} \quad (27)$$

then Eq. (2) - (15) (with slight modification in the mean friction coefficient) can be used. Van Driest (Reference 13) made the same type of investigation of the three-dimensional turbulent equations and found that the effective starting length for a cone in fully turbulent flow is

$$\text{TURBULENT } l_{\text{cone}} = \frac{1}{2} l_{\text{FLAT PLATE}} \quad (28)$$

Summarized below, for convenience, are eq. (2) - (15) for conical flow. The length used for the actual cone wetted length is

$$\text{laminar } R_{e_T} = 4.147 \times 10^4 \frac{P_s U_e L}{(T')^{1/7}} \quad (29)$$

$$\text{turbulent } R_{e_T} = 6.22 \times 10^4 \frac{P_s U_e L}{(T')^{1/7}} \quad (30)$$

$$\text{Local skin friction (unchanged)} \quad C_{f_\infty} = \left(\frac{T_e}{T'} \right) C'_{f_\infty}$$

$$\text{mean laminar } C_{f_\infty} = \frac{2}{3} \cot \theta_v \left(\frac{T_e}{T'} \right) C'_{f_\infty} \quad (31)$$

referred to base area of cone

$$\text{mean turbulent } C_{f_\infty} = 1.02 \cot \theta_v \left(\frac{T_e}{T'} \right) C'_{f_\infty} \quad (32)$$

referred to base area of cone
(using the 1/5 or 1/7 power law for
gives identical results)

$$\text{laminar } f = 0.1281 \left(\frac{P_s U_e}{l} \right)^{0.5} \quad (33)$$

ANALYSIS
PREFARED BY
CHECKED BY
REVISED BY

CONSOLIDATED VULTEE AIRCRAFT CORPORATION
SAN DIEGO DIVISION

PAGE 12
REPORT NO. A-Atlas-103
MODEL 7
DATE 15 Dec. 1954

and turbulent $\theta = \frac{0.02866 (\rho_s u_s)^{0.8}}{(l)^{0.2} (T')^{0.51}}$ (34)

Eq. (29) - (34) are then solved in the same manner as the equations (2) - (15) for two dimensional flow.

3.2.4 Three Dimensional Flow with Discontinuities

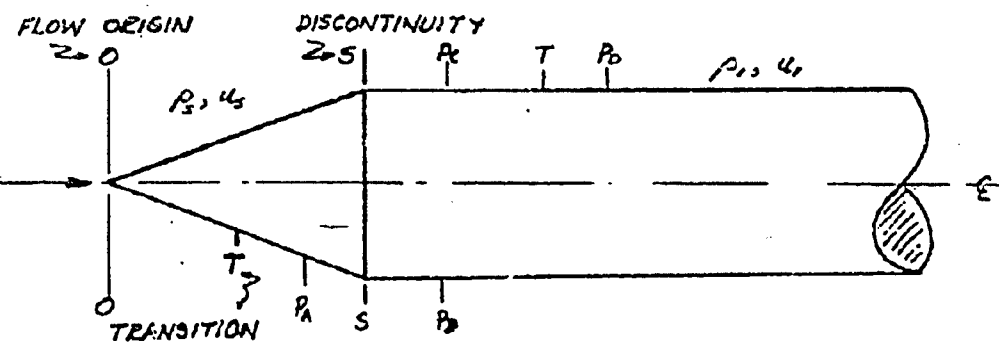
The constant momentum-loss method of section 3.2.2 can be applied to the case of three-dimensional flow. The only changes which need be made are in the equations for the momentum thickness where the factors $1/3$ and $1/2$ must be inserted in the laminar and turbulent θ , respectively. Making this change we have

$$\text{LAMINAR } \theta_{cone} = 0.002174 \left(\frac{\rho_s u_s}{(T_s)^{1.7}} \right)^{-0.5} \left(\frac{T_s}{T'} \right)^{0.15} l^{0.5} \quad (35)$$

$$\text{TURBULENT } \theta_{cone} = 0.003959 \left(\frac{\rho_s u_s}{(T_s)^{1.7}} \right)^{-0.2} \left(\frac{T_s}{T'} \right)^{0.66} l^{0.8} \quad (36)$$

These equations are used in Eq. (17) to find l' , the effective length, which is then used in Eq. (2) - (15) to obtain friction and heat transfer.

The types of discontinuities usually encountered in conical flow would be found, say, on a cone-cylinder. The equations for various starting lengths found from Eq. (17), (35) and (36) are summarized for that body in the following table:



ANALYSIS
PREPARED BY
CHECKED BY
REVISED BY

CONSOLIDATED VULTEE AIRCRAFT CORPORATION
SAN DIEGO DIVISION

PAGE 13
REPORT NO. A-Atlas-103
MODEL 7
DATE 15 Dec. 1954

ASSUMED PRESSURE GRADIENT ON THE CYLINDER

$$AT P_A : \quad l'_A = \frac{TP_A}{2} + 0.4727(\bar{O})^{0.625} \left[\frac{p_s u_s}{(T_s')^{1.7}} \right]^{-0.375} \quad (37)$$

$$AT P_B : \quad l'_B = \bar{S}P_B + 0.57435 \left(k'_A + \frac{\bar{S}P_A}{2} \right) \frac{p_s}{p_i} \left(\frac{u_s}{u_i} \right)^{0.5} \left(\frac{T_s'}{T_i'} \right)^{0.825} \quad (38)$$

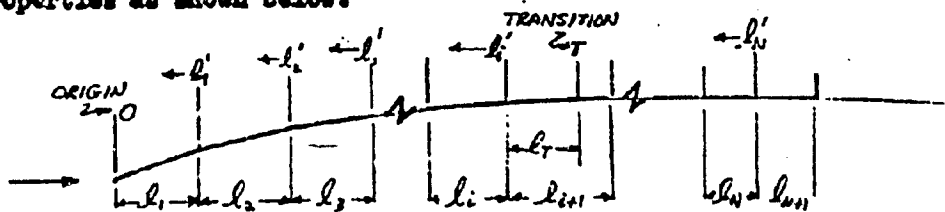
$$AT P_C : \quad l'_C = \bar{S}P_C + 0.57735 \frac{\bar{O}\bar{S}}{3} \frac{p_s}{p_i} \left(\frac{u_s}{u_i} \right)^3 \left(\frac{T_s'}{T_i'} \right)^{0.3} \quad (39)$$

$$AT P_D : \quad l'_D = \bar{I}P_D + 0.4696 \left[l'_C + \bar{I}P_C \right]^{0.625} \left[\frac{p_s u_s}{(T_e')^{1.7}} \right]^{-0.375} \quad (40)$$

to be used in Eq. (2) - (15) to find the friction and heat transfer.

3.2.5 Flow With Streamwise Gradients

In section 3.2.4 the flow on the cylinder portion of the body investigated was assumed to be at constant pressure in order to obtain the simple equations (38), (39) and (40). For the case where a streamwise gradient is to be considered the body must be broken into small segments of constant flow properties. If this is done then the equations (17), (21) and (22) can be applied to each section and equivalent starting lengths can be found for any point on the body. For flow of such a type consider a semi-infinite biconvex airfoil broken into small segments of constant stream properties as shown below:



ANALYSIS
PREPARED BY
CHECKED BY
REVISED BY

CONSOLIDATED VULTEE AIRCRAFT CORPORATION
SAN DIEGO DIVISION

PAGE 14
REPORT NO. A-Atlas-103
MODEL 7
DATE 15 Dec. 1954

Each segment has the stream properties $p_1, u_1; p_2, u_2; p_3, u_3, \dots$ etc.

To derive the general equation for the effective length along the body at a point preceded by completely laminar flow, apply Eq. (21) and (22) to Eq. (17). For segment ℓ_1 ,

$$\partial_1 g_1 = \partial_2 g_2$$

So

$$0.003765 \left[\frac{p_1 u_1}{(T_1)^{1.7}} \right]^{0.5} \left(\frac{T_1}{T_1'} \right)^{0.15} \ell_1^{0.5} g_1 = 0.003765 \left[\frac{p_2 u_2}{(T_2)^{1.7}} \right]^{0.5} \left(\frac{T_2}{T_2'} \right)^{0.15} (\ell_1')^{0.5} g_2$$

or

$$(\ell_1')^{0.5} = \ell_1^{0.5} \left(\frac{p_2 u_2}{p_1 u_1} \right)^{0.5} \left(\frac{T_1}{T_2} \right)^{0.15} \left(\frac{T_1}{T_1'} \right)^{0.15} \frac{g_1}{g_2}$$

$$\ell_1' = \ell_1 \left(\frac{p_2 u_2}{p_1 u_1} \right) \left(\frac{T_1}{T_2} \right)^2 \left(\frac{T_1}{T_1'} \right)^{0.3} \left(\frac{g_1}{g_2} \right)^2$$

Apply the perfect gas law to the g -ratio

$$\frac{g_1}{g_2} = \frac{p_1 u_1^2}{p_2 u_2^2} = \frac{p_1 u_1^2 T_2}{p_2 u_2^2 T_1}$$

and insert in the above equation to get

$$\ell_1' = \ell_1 \left(\frac{p_1 u_1^2}{p_2 u_2^2} \right)^2 \left(\frac{p_2 u_2}{p_1 u_1} \right) \left(\frac{T_1}{T_1'} \right)^{0.3} \left(\frac{T_1}{T_2} \right)^2 \left(\frac{T_2}{T_1} \right)^{-1}$$

or
$$\ell_1' = \ell_1 \frac{p_1}{p_2} \left(\frac{u_1}{u_2} \right)^2 \left(\frac{T_1}{T_1'} \right)^{0.3}$$

ANALYSED
PREPARED BY
CHECKED BY
REVISED BY

CONSOLIDATED VULTEE AIRCRAFT CORPORATION
SAN DIEGO DIVISION

PAGE 15
REPORT NO. A-Atlas-103
MODEL 7
DATE 15 Dec. 1954

This procedure can be repeated for each segment, i.e.,

$$l_i' = (l_2 + l_1') \frac{p_2}{p_1} \left(\frac{u_2}{u_1} \right)^3 \left(\frac{T_2'}{T_1'} \right)^{0.3}$$

or

$$l_i' = l_2 \frac{p_2}{p_1} \left(\frac{u_2}{u_1} \right)^3 \left(\frac{T_2'}{T_1'} \right)^{0.3} + l_1' \frac{p_1}{p_2} \left(\frac{u_1}{u_2} \right)^3 \left(\frac{T_1'}{T_2'} \right)^{0.3}$$

and in general

$$l_i' = \sum_{k=1}^{k=i} l_k \frac{p_k}{p_i} \left(\frac{u_k}{u_i} \right)^3 \left(\frac{T_i'}{T_k'} \right)^{0.3} \quad (41)$$

Let transition occur at some point T in segment l_{i+1}' at some distance l_T from the beginning of the segment. Then the effective length to T is

$$l_T' = (l_T + l_i')^{0.625} \cdot 0.4694 \left[\frac{p_{i+1} u_{i+1}}{(T_{i+1}')^{1.7}} \right]^{-0.375} \quad (42)$$

and for any general turbulent section thereafter

$$l_N' = \sum_{k=i+2}^{k=N} l_k \frac{p_k}{p_N} \left(\frac{u_k}{u_N} \right)^{1.5} \left(\frac{T_N'}{T_k'} \right)^{0.025} + (l_T' + l_{i+1}' - l_T) \frac{p_{i+1} u_{i+1}}{p_N u_N} \left(\frac{T_N'}{T_{i+1}'} \right)^{1.5} \left(\frac{T_N'}{T_{i+1}'} \right)^{0.025} \quad (43)$$

These generalized formulas for l' may then be used along with local conditions to evaluate the friction and heat transfer at any point from Eq. (2) - (15).

REVIEWED
APPROVED
CHECKED
REVISED BY

CONSOLIDATED VULTEE AIRCRAFT CORPORATION
SAN DIEGO DIVISION

PAGE 16
REPORT NO A-Atlas-163
MODEL 7
DATE 15 Dec. 1954

4.0 Conclusions

A collection has been made of aerodynamic flow characteristics for one, two and three dimensional hypersonic flow. The Mach number range is from $0 \leq M \leq 20$. The flow parameters are shown as functions of initial Mach number and deflection angle in sections 1, 2, 3; Figures 1.0 through 3.16.

Equations for compressible skin friction and heat transfer using the reference temperature method were presented for two and three dimensional flow, flow with discontinuities and flow with streamwise gradient. Figures necessary in using the formulae are in section 4, Figure 4.1 - 4.7.

5.0 References

1. Dailey, C. C. and Wood, F. C. "Computation Curves for Compressible Fluid Problems". 1949.
2. "Notes and Tables For Use in the Analysis of Supersonic Flow". Staff of the 1 x 3 foot Supersonic Wind Tunnel Section, Ames Aeronautical Laboratory. NACA TN 1428, 1947.
3. "Charts and Tables for Analysis of Supersonic Flow". GALCIT Memo #4. Pasadena, 1951.
4. Kopal, Z., ed. Tables of Supersonic Flow Around Cones. MIT Technical Report No. 1, 1947.
5. Grimminger, G., et. al., "Lift on Inclined Bodies of Revolution in Hypersonic Flow". Journal of Aeronautical Sciences, November, 1950.
6. Young, G. B. W. and Siska, C. P., "Supersonic Flow Around Cones at Large Yaw". RAND Report P-198, March 1951.
7. Von Karman, T. "Turbulence and Skin Friction", Journal of Aeronautical Sciences, January 1934.
8. Van Driest, E. R. "Calculation of the Stability of the Laminar Boundary Layer in a Compressible Fluid on a Flat Plate With Heat Transfer", Journal of Aeronautical Sciences, December 1952.
9. Rosig, M. F. "The Reference Temperature Method for Calculating Skin Friction and Heat Transfer in Compressible Flow". Convair Memo A-Atlas-151, 3 December 1954.
10. Sieff, A. "Examination of the Existing Data on the Heat Transfer of Turbulent Boundary Layers at Supersonic Speeds From the Point of View of Reynolds Analogy". NACA TN 3284, August 1954.
11. Rosig, M. F. "Survey and Analysis of Experimental Data on Boundary Layer Transition in Supersonic Flow". Convair Memo A-Atlas-142, 5 November 1954. (Confidential)

SEARCHED
INDEXED
FILED
SERIALIZED

CONSOLIDATED VULTEE AIRCRAFT CORPORATION
SAN DIEGO DIVISION

PAGE 17
REPORT NO A-Atlas-103
MODEL 7
DATE 15 Dec. 1954

12. Hantzsche, W. and Wandt, H. "The Laminar Boundary Layer on a Cone in a Supersonic Air Stream at Zero Angle of Attack". Translation R&T-6, RAND Corporation, 1947.
13. Van Driest, E. R. "Turbulent Boundary Layer on a Cone in a Supersonic Flow at Zero Angle of Attack". Journal of Aeronautical Sciences, January 1952.

Prepared by: Mary F. Romig
M. F. Romig

Checked by: R. C. Huyett
R. C. Huyett

Approved by: William H. Dorrance
W. H. Dorrance

cc:
H. P. Dunholter
C. S. Amos
D. Pollard
W. Schwidetzky
H. Friedrich
W. P. Radcliffe
L. Jirsa
D. Collins
H. Steele
R. Shorey
W. H. Dorrance
File
R. J. Kirby
E. C. Huyett
M. F. Romig
R. G. Morell
W. B. Mitchell
W. J. Gaudtner
H. Garbin
F. M. Perkins
C. H. Eaton
P. I. Dickey

P. E. Culbertson
J. Q. Wenzel
G. Hoble
S. Lexington
J. Farber
V. Kebely
D. Otis
K. Marcks
MIT (Attn. Security Officer) Copy #31
P. S. Tip
J. Sherley
R. Wentink
J. Bowyer
H. U. Eckert
W. P. Radcliffe
R-W Library via M. Rosenbaum
Avco Mfg. Co. via M. Rosenbaum

MADE AND
MANUFACTURED BY
CONSOLIDATED
AVIATION COMPANY
DESIGNED BY

CONSOLIDATED VULTEE AIRCRAFT CORPORATION
SAN DIEGO DIVISION

PAGE 18
REPORT NO A-Atlas-103
MODEL 7
DATE 15 Dec. 1954

Index to Figures

Section 1. One-Dimensional Flow Characteristics

Plotted versus Initial Mach Number

Figure No.	Page
1.1 - Mach number after shock	20
1.2 - Static pressure ratio	21
1.3 - Static temperature ratio	22
1.4 - Density ratio	23
1.5 - Velocity and dynamic pressure ratio	24
1.6 - Reynolds number ratio	25
1.7 - Total head ratio	26
1.8 - Area Ratio	27

Section 2. Non-Dimensional Flow Characteristics

A. EXPANSION

Plotted versus Initial Mach Number with Wedge Angle a Parameter

Figure No.	Page
2.0 - Maximum cone, wedge angles for attached shock	28
2.1 - Mach number after shock	29
2.2 - Static pressure ratio	30
2.3 - Static temperature ratio	31
2.4 - Density ratio	32
2.5 - Shockwave angle	33
2.6 - Velocity ratio	34
2.7 - Dynamic pressure ratio	35
2.8 - Reynolds number ratio	36
2.9 - Total head ratio	37

B. EXPANSION

2.10a - Mach number versus Prandtl-Meyer angle	38
2.10b - Continued	39
2.11a - Static pressure to total head ratio versus	40
- 2.11i Prandtl-Meyer angle	48 to

Section 3. Conical Flow

A. Flow Characteristics, Unwaved Cone

Plotted versus Free Stream Mach Number with Cone Semi-Vertex Angle a Parameter

REVISIONS
PREPARED BY
CHECKED BY
REVIEWED BY

CONSOLIDATED VULTEE AIRCRAFT CORPORATION
SAN DIEGO DIVISION

PAGE 19
REPORT NO A-Atlas-103
MODEL 7
DATE 15 Dec. 1954

Figure No.

Page

- 3.1 - Surface Mach number 49
3.2 - Surface static pressure ratio 51
3.3 - Surface static temperature ratio 52
3.4 - Surface density ratio 53
3.5 - Shock wave angle 54
3.6 - Surface velocity ratio 55
3.7 - Surface dynamic pressure ratio 56
3.8 - Surface Reynolds Number ratio 57
3.9 - Surface total head ratio 58

B. Force Coefficients. Unshaped Cone

Figure No.

Page

- 3.10a - Wave drag coefficient versus 59 to
- 3.10d Cone half-angle 62
3.11 - Initial Axial Force coefficient, $C_{x0} / \sin^2 \theta_v$ versus Mach number 63
3.12 - Initial normal force coefficient slope, $(dC_n/d\alpha)_{\alpha=0} / C_{x0}^2 \theta_v$, vs. Mach number 64

C. Force Coefficients. Sharp Cone

Figure No.

Page

- 3.13 - Additional axial force coefficient due to 65
angle of attack/ α' versus Mach number
3.14 - Normal force coefficient/ $C_n \sin^2 \theta_v$ versus 66
angle of attack (Newtonian Flow)
3.15 - Normal force coefficient slope/ $C_n \sin^2 \theta_v$ 67
versus angle of attack (Newtonian Flow)
3.16 - Axial force coefficient versus angle of 68
attack (Newtonian Flow)

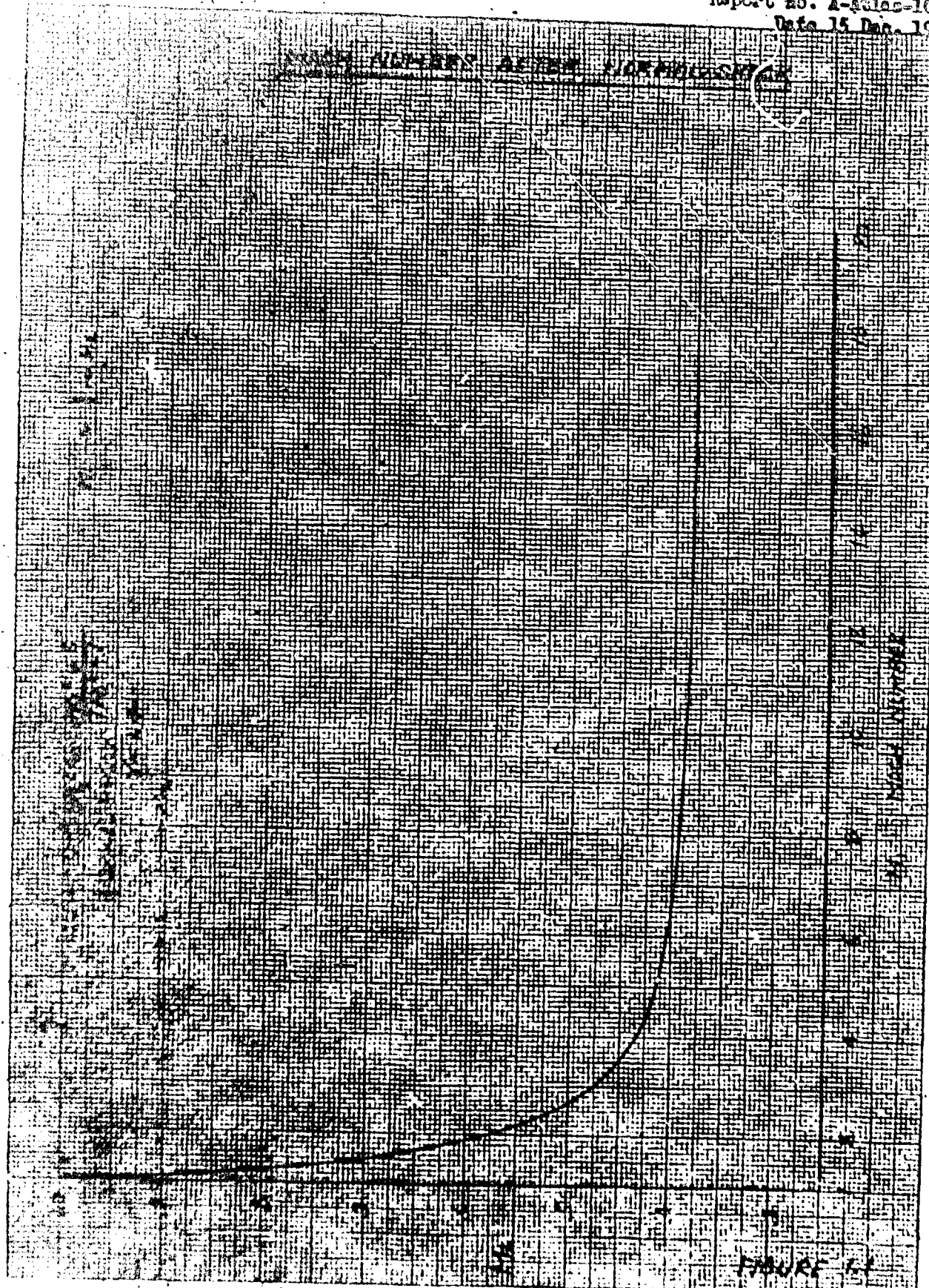
Section 4. Viscous Flow Phenomena

Figure No.

Page

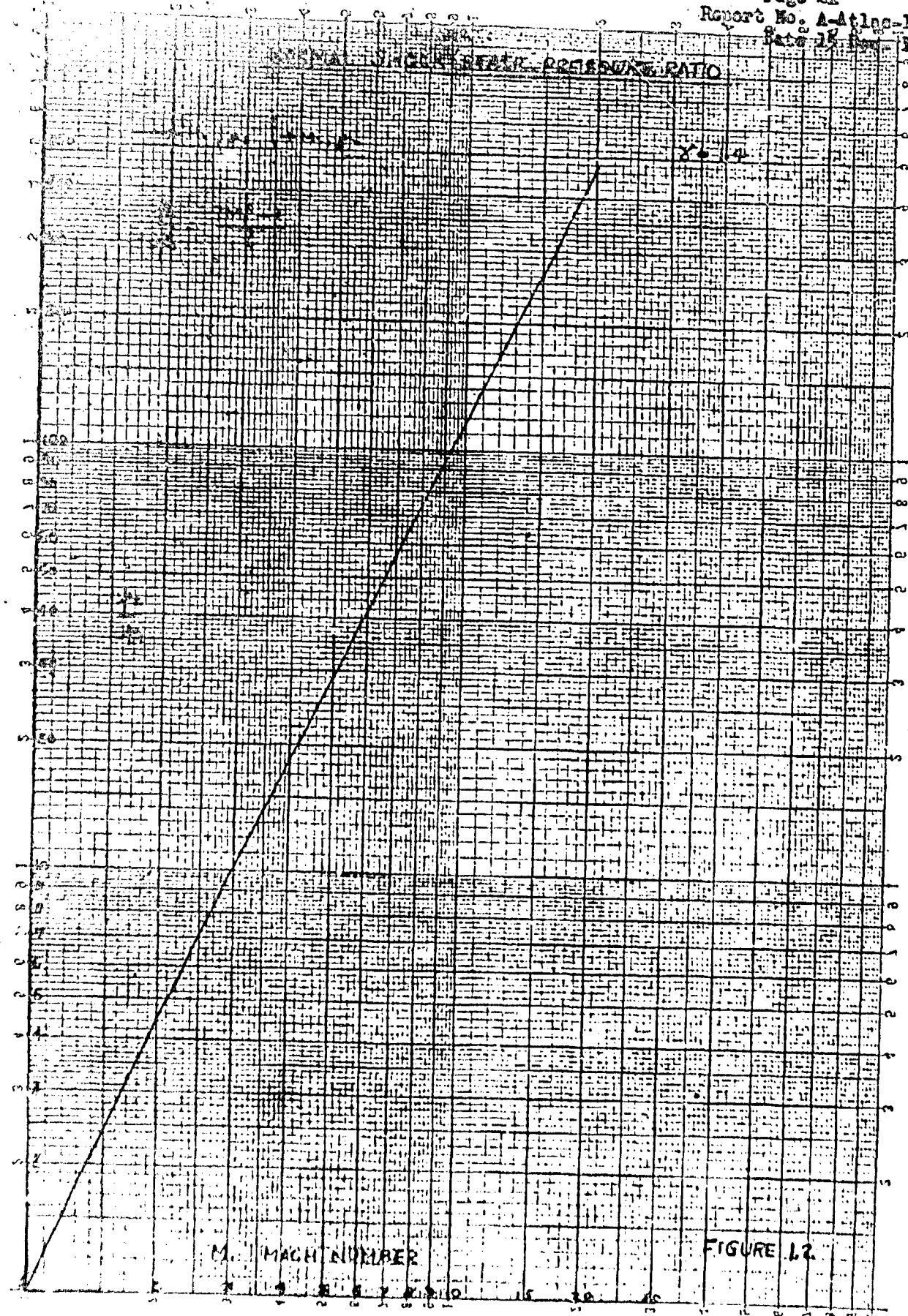
- 4.1 - Incompressible laminar and turbulent mean and 69
local skin friction coefficients versus
Reynolds number
4.2 - T'/T_∞ versus Mach number 70
4.3 - $(T')^{1/7}$ versus T' 71
4.4 - Adiabatic Temperature rise, ΔT_i , versus 72 - 74
velocity
4.6 - Specific heat of air versus temperature 75
4.8 - Minimum critical Reynolds number for stability 76
of the laminar boundary layer
4.7 - Coefficient of viscosity versus temperature for 77
the Sutherland Viscosity Law

Page 20
Report No. A-Atlas-103
Date 15 Dec. 1954

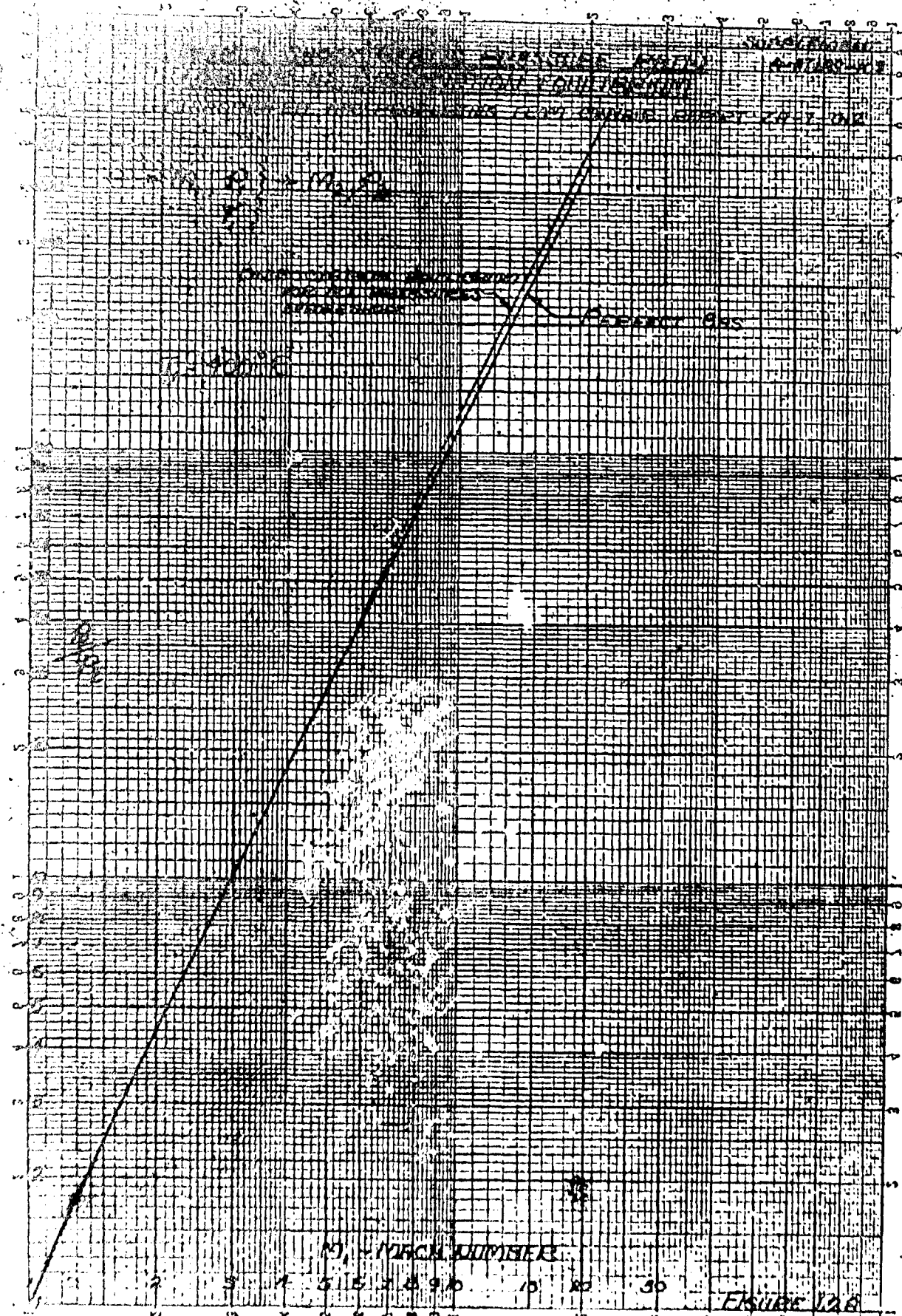


Page 21

Report No. A-Atlas-103
Date 18 Sept 1954



PAGE 21A



K-E
KODAK SAFETY FILM
EXPOSURE 328-115

Page 22
Report No. Audit-100
Date 12 Dec 1964

1	2	3	4	5	6	7	8	9	10	11	12	13	14	15	16	17	18	19	20	21	22	23	24	25	26	27	28	29	30	31	32	33	34	35	36	37	38	39	40	41	42	43	44	45	46	47	48	49	50	51	52	53	54	55	56	57	58	59	60	61	62	63	64	65	66	67	68	69	70	71	72	73	74	75	76	77	78	79	80	81	82	83	84	85	86	87	88	89	90	91	92	93	94	95	96	97	98	99	100
---	---	---	---	---	---	---	---	---	----	----	----	----	----	----	----	----	----	----	----	----	----	----	----	----	----	----	----	----	----	----	----	----	----	----	----	----	----	----	----	----	----	----	----	----	----	----	----	----	----	----	----	----	----	----	----	----	----	----	----	----	----	----	----	----	----	----	----	----	----	----	----	----	----	----	----	----	----	----	----	----	----	----	----	----	----	----	----	----	----	----	----	----	----	----	----	----	----	----	-----

PAGE ONE

SUPPLEMENT
A-ATLAS-105NORMAL SHOCK DENSITY RATIO
FOR AIR AT DISSOCIATION EQUILIBRIUM

DISSOCIATED AIR PROPERTIES FROM CONVAIR REPORT ZD-7-02

$$\begin{array}{ccc} M_1 & \rightarrow & P_2 \\ P_1 & \rightarrow & P_2 \\ T_1 & \rightarrow & T_2 \\ \rho_1 & \rightarrow & \rho_2 \end{array}$$

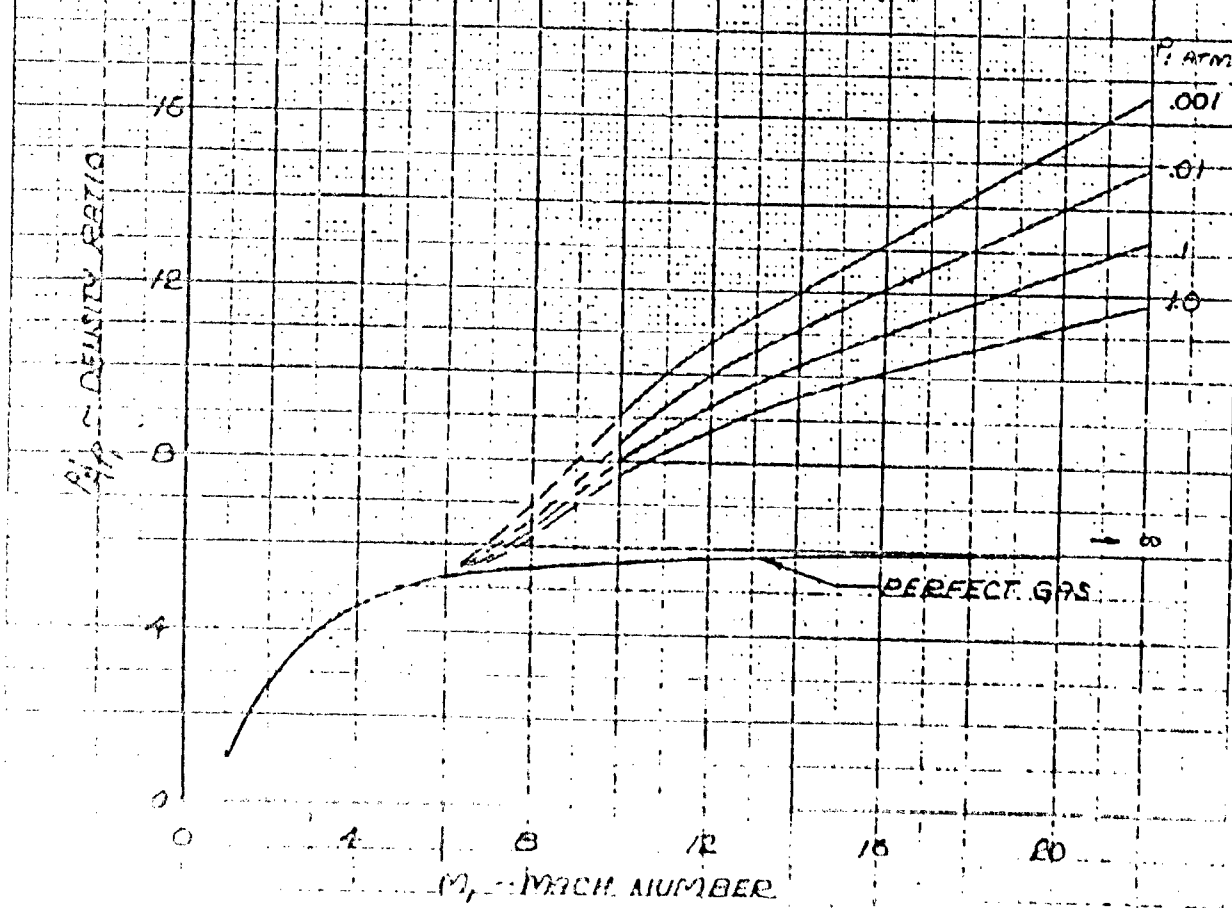
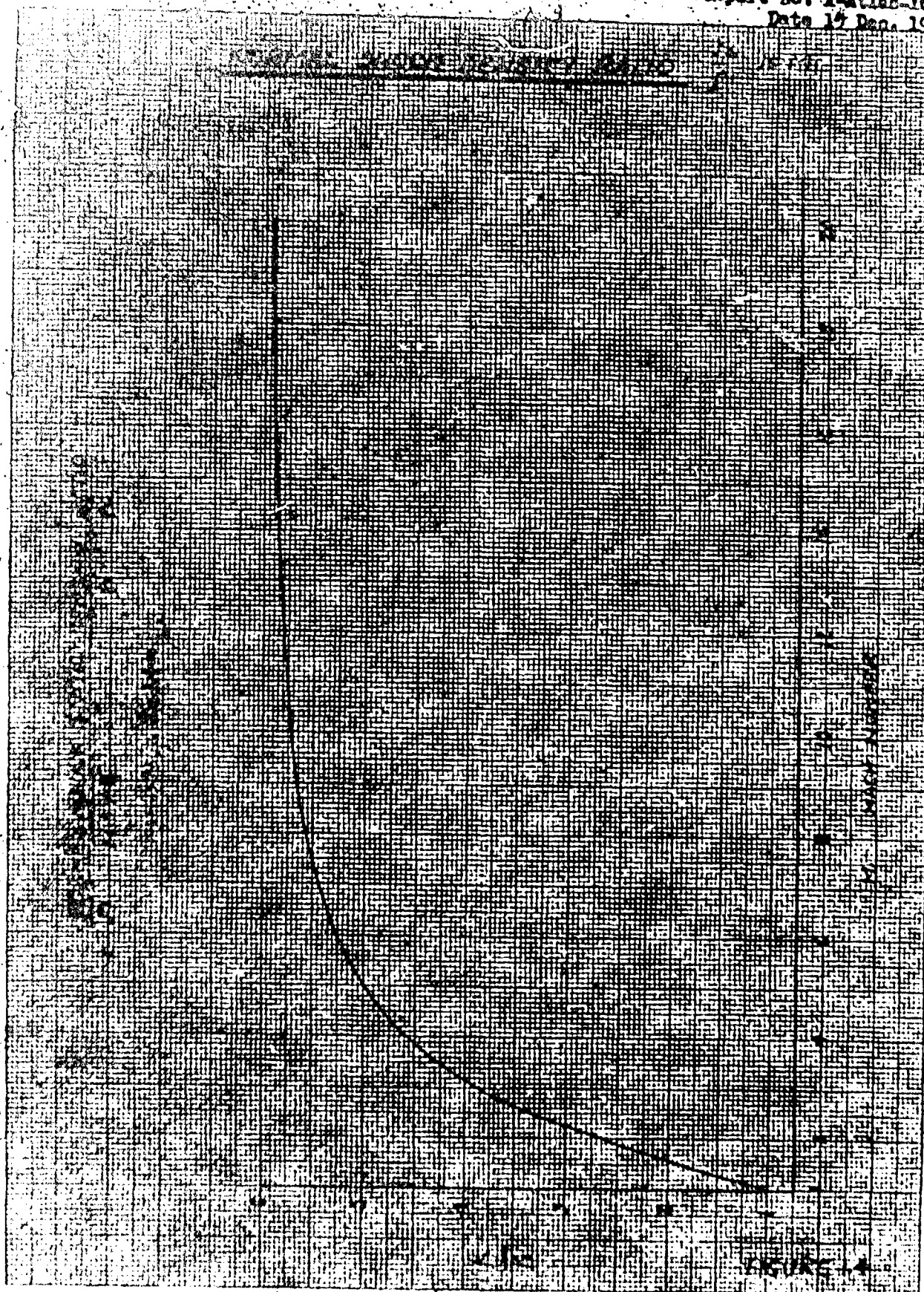
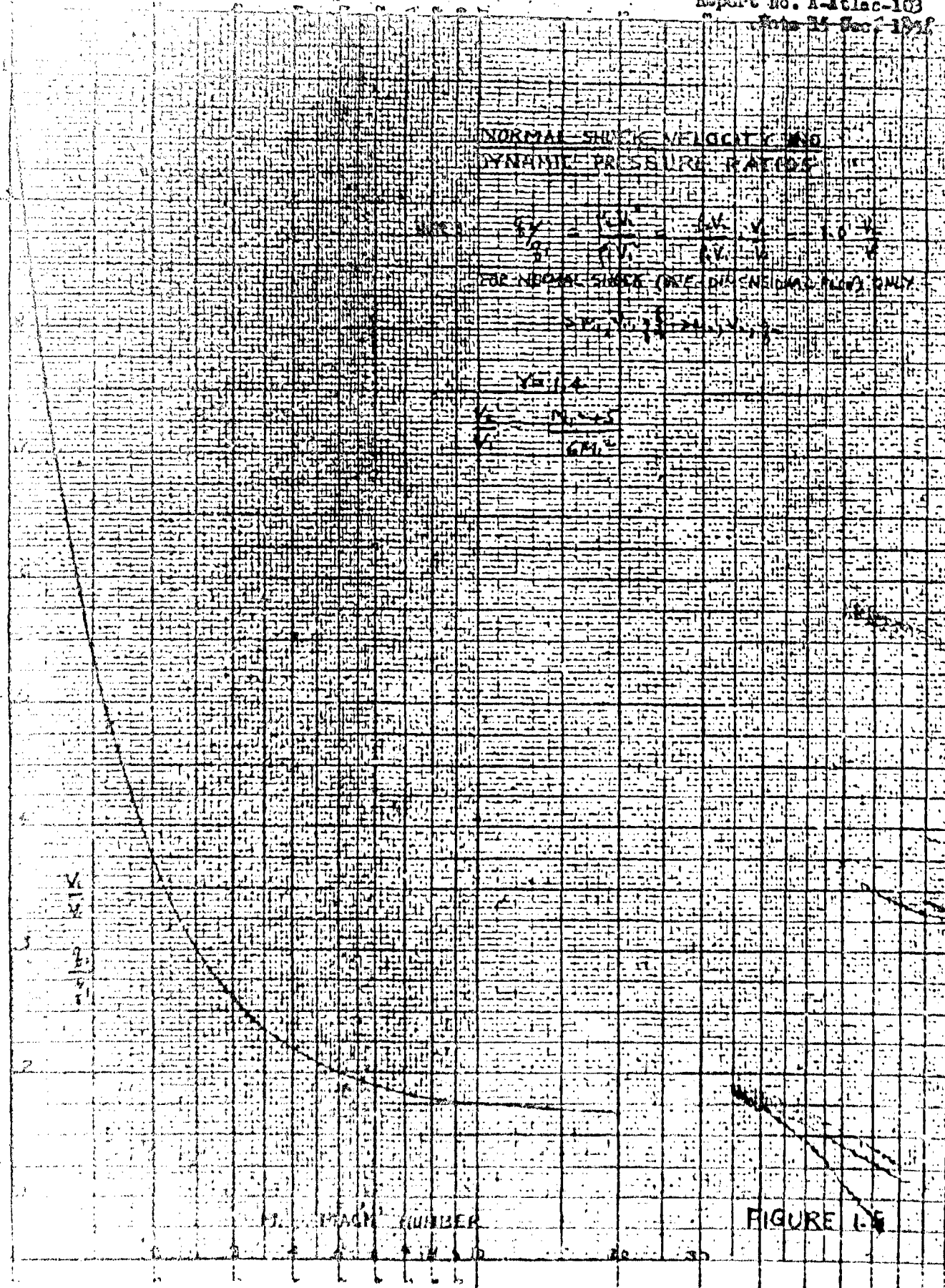
 $T_2 = 400^\circ R$ 

FIGURE 1.4A

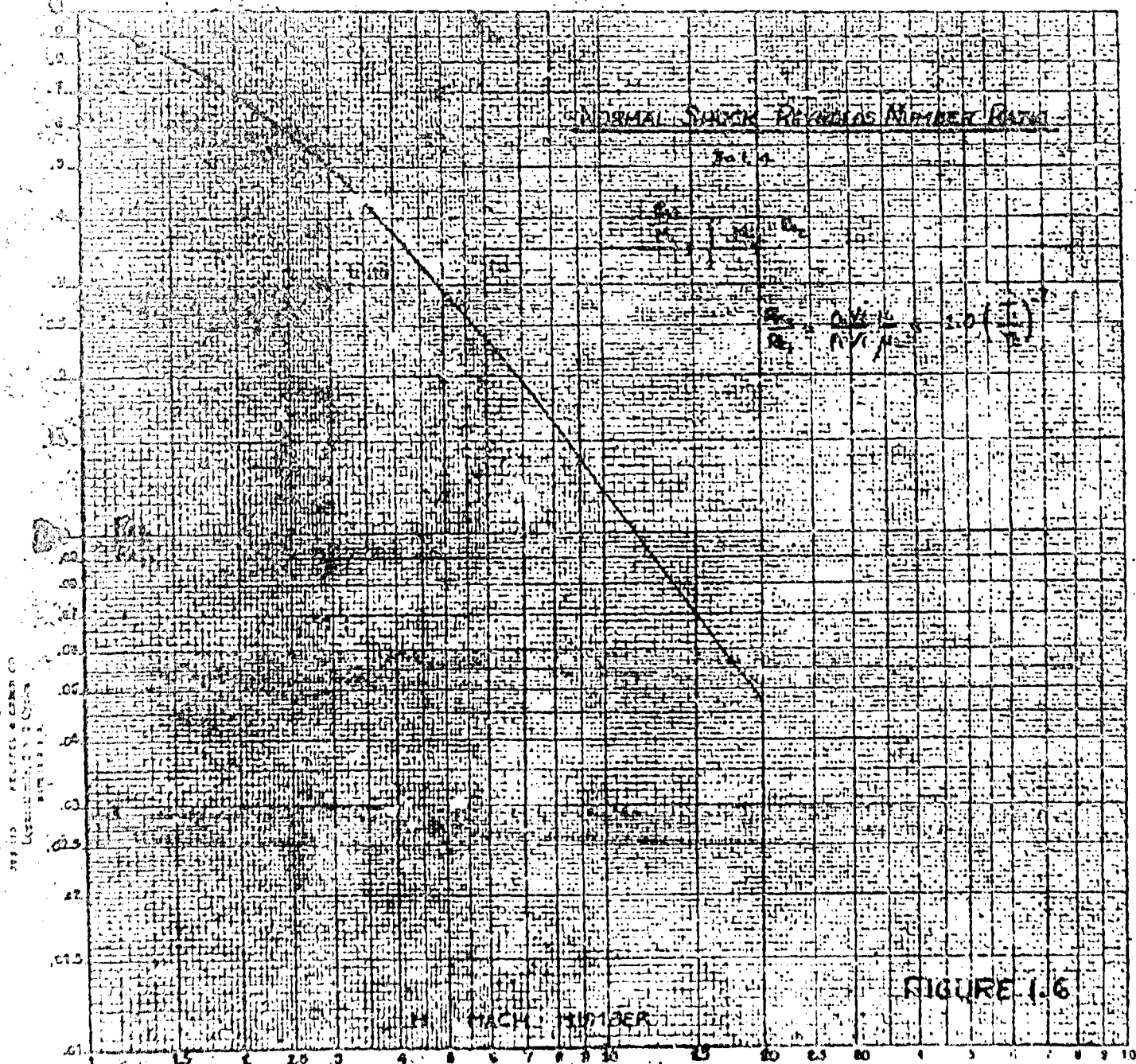
Page 29
Report No. 1-Atlas-103
Date 14 Dec. 1954



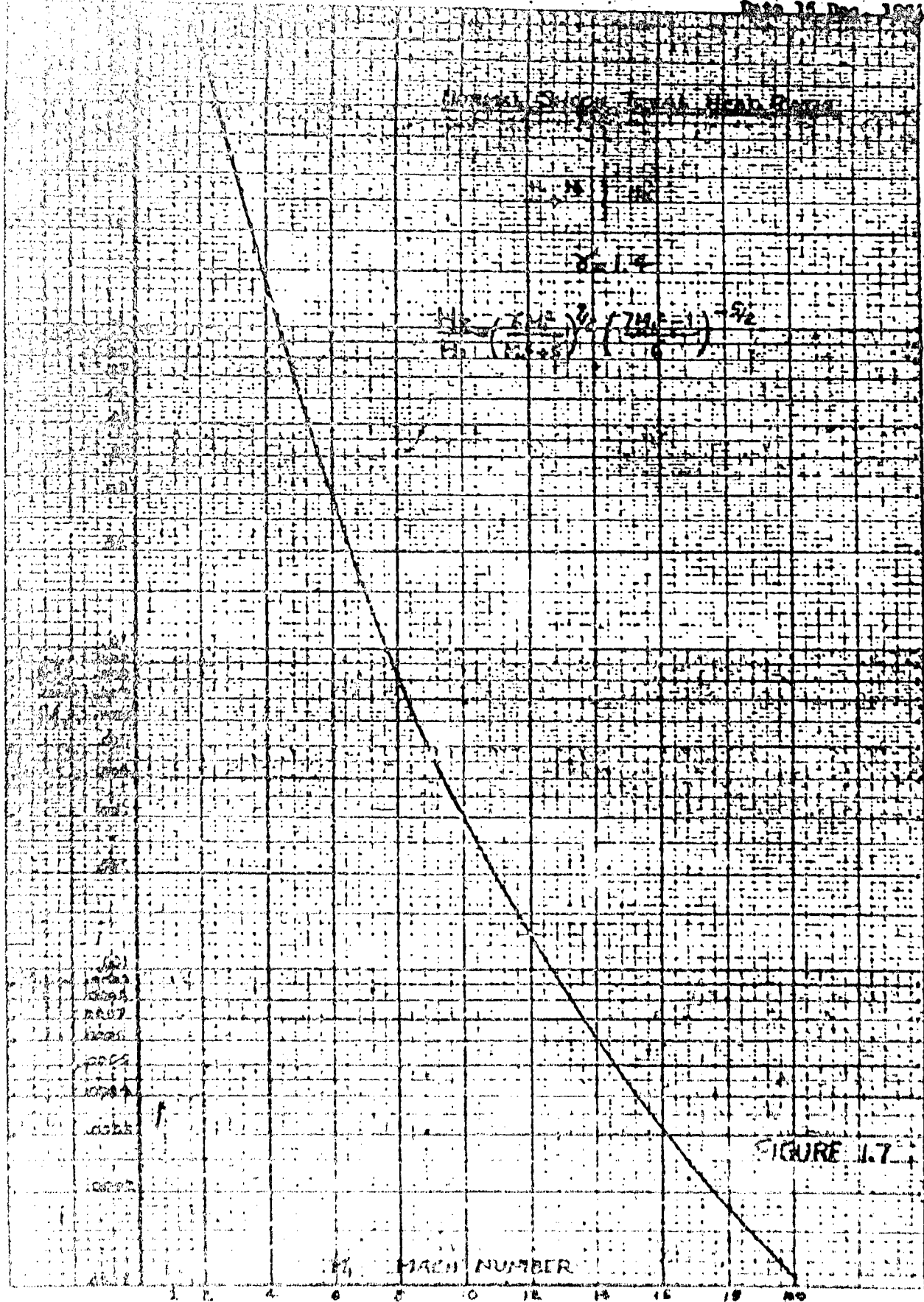
Date 25 Oct 1962



Page 25
Report No. A-1010-103
Date 15 Dec. 1958



Page 24
Report No. A-Atlas-103
Date 16 Dec 1964



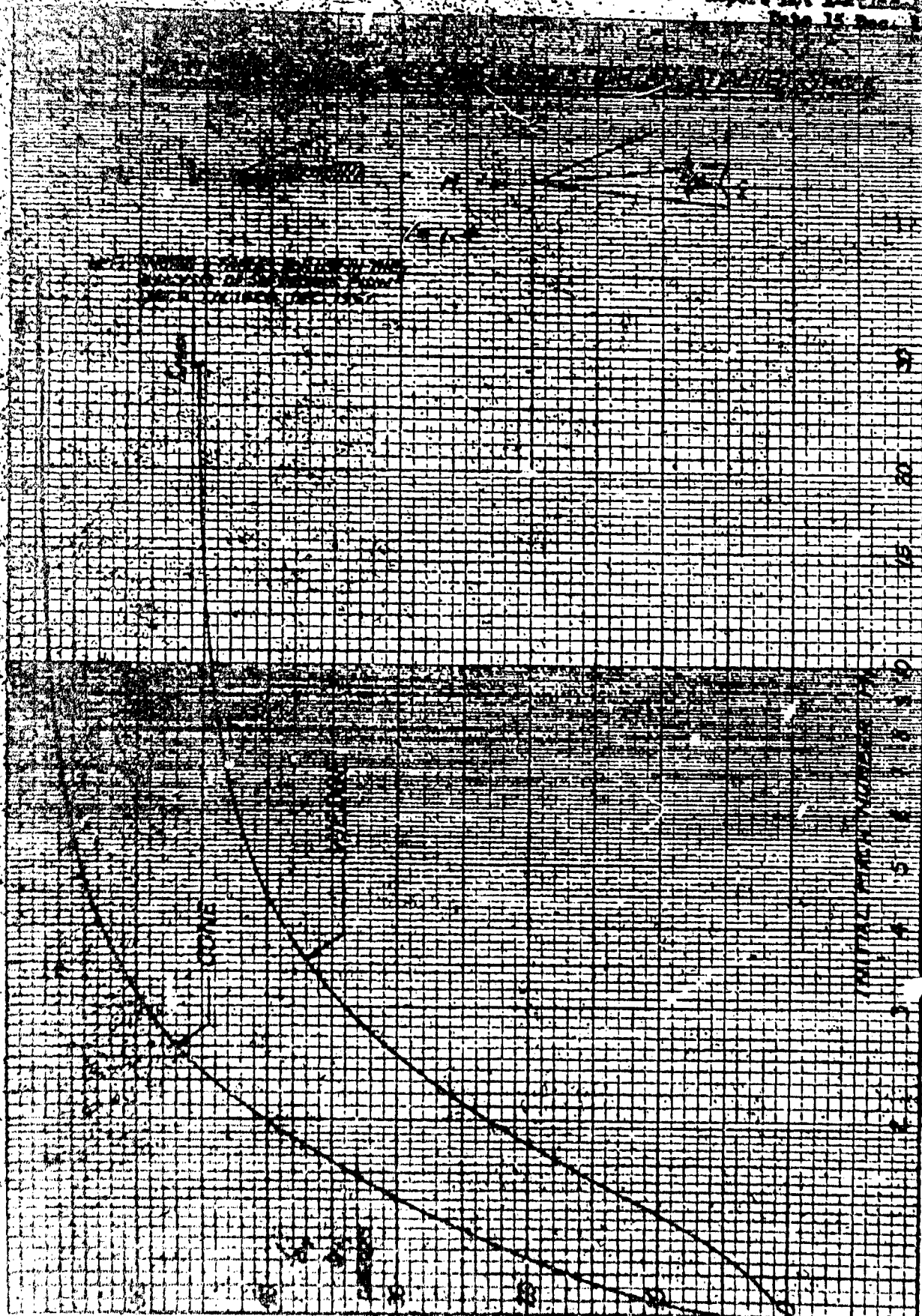
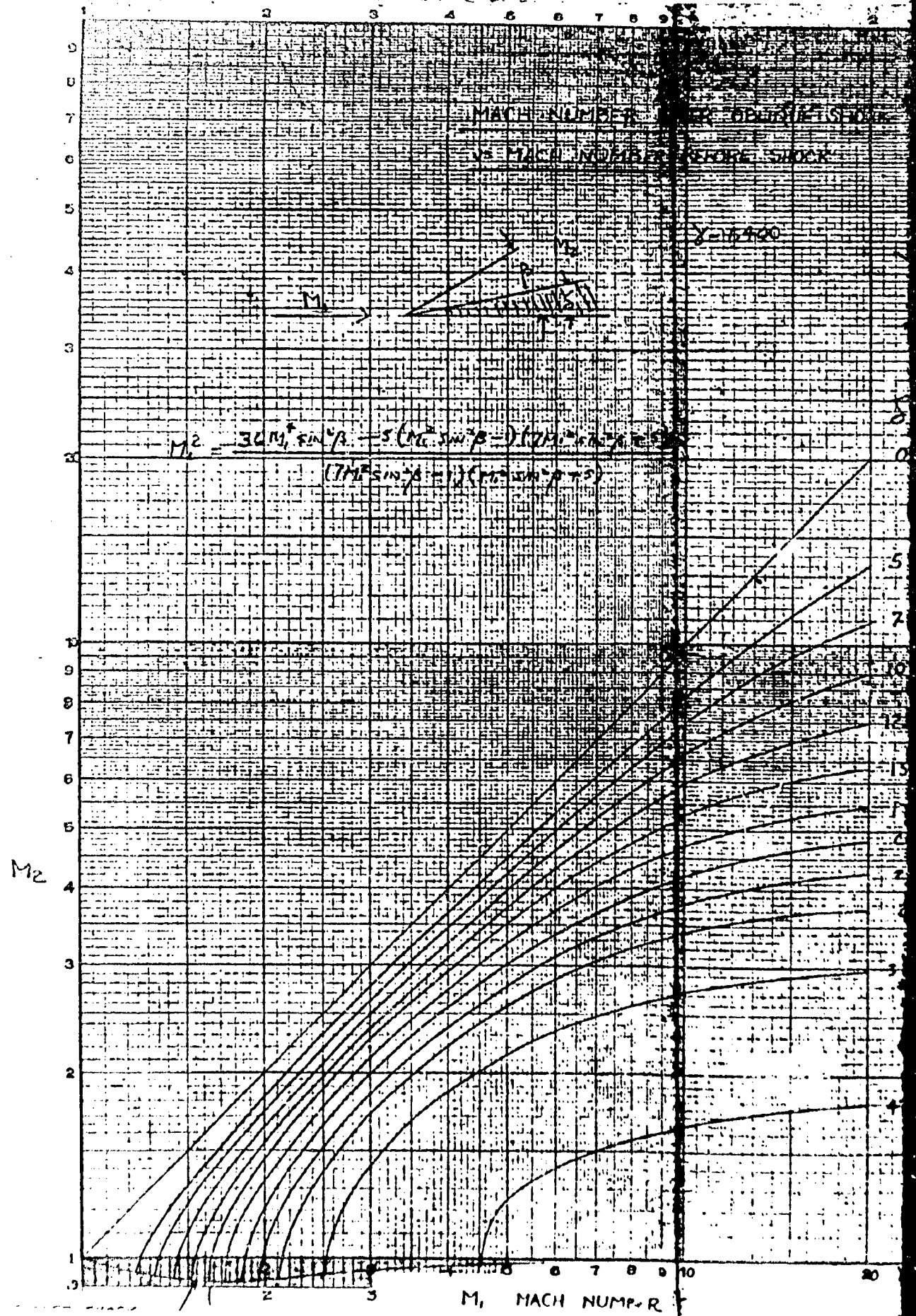


FIGURE 2.0



Page 29
Report No. A-At
Date
Date 15 D

M_2 vs M_1

B

FIGURE 2.

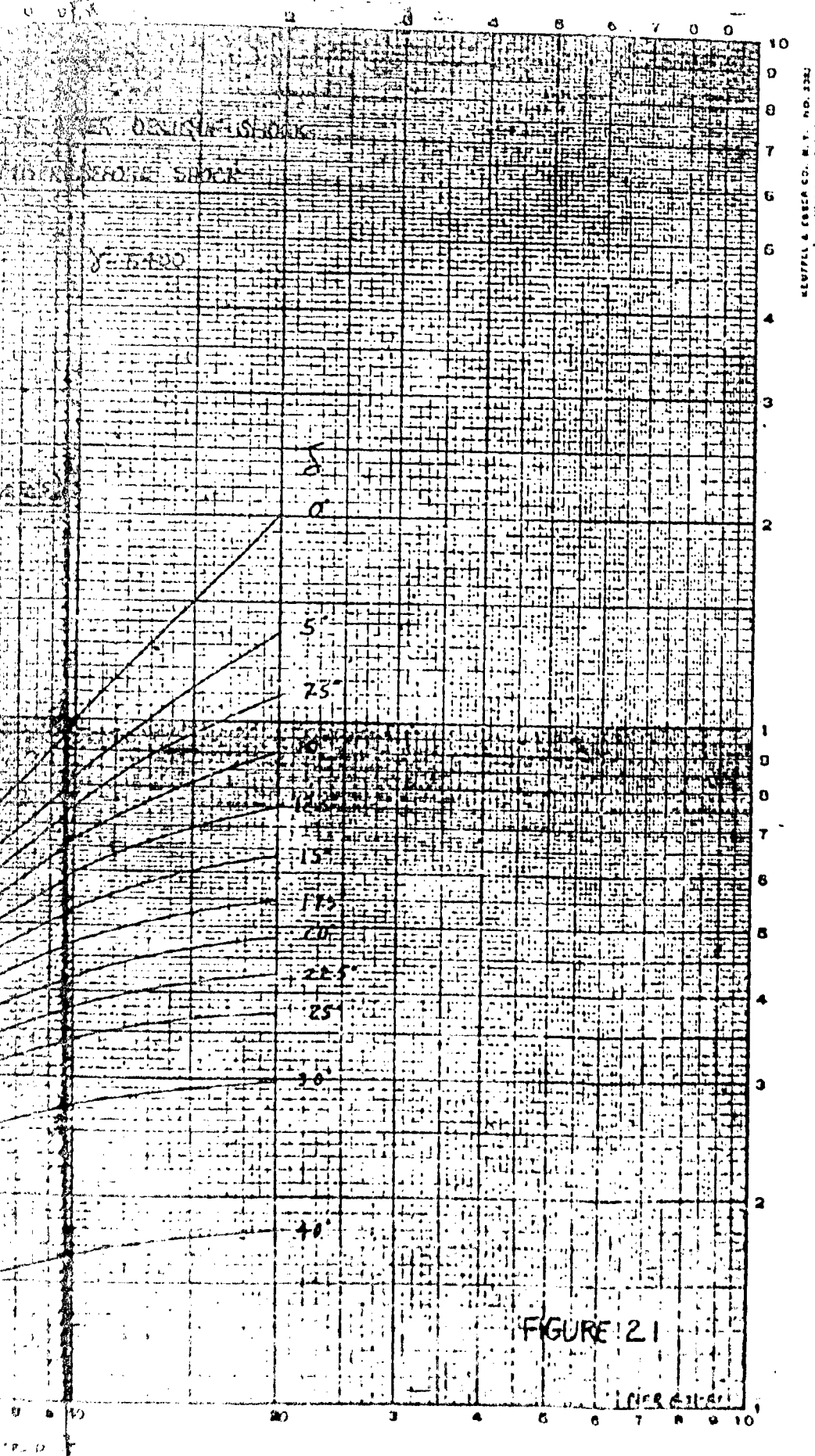
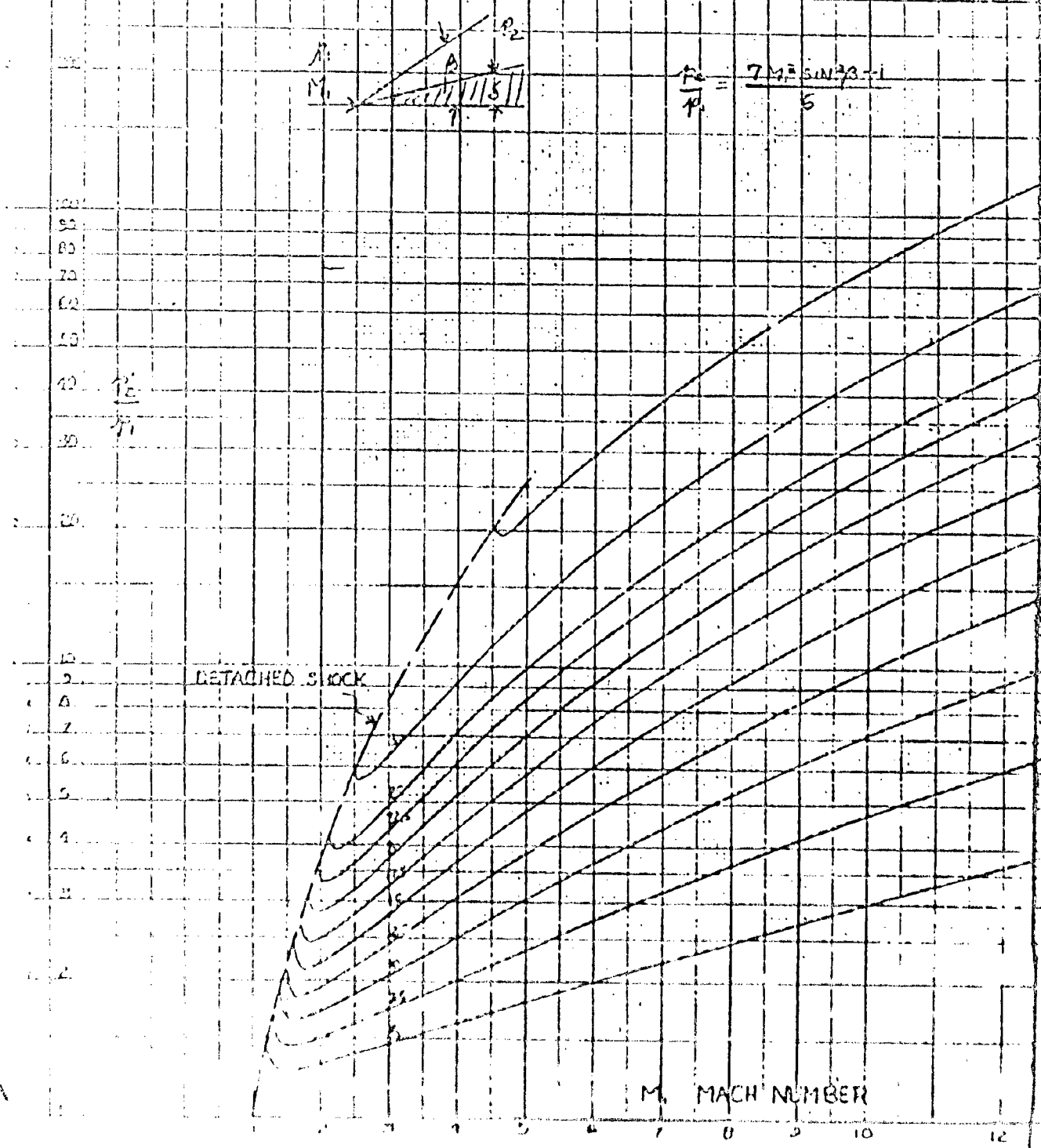


FIGURE 2.1

OBlique SHOCK STATIC PRESSURE P₂
VS MACH - NUMBER

M > 1.400

$$\frac{P_2}{P_1} = \frac{7M^2 \sin^2 \beta + 1}{5}$$



$\frac{P_2}{P_1}$ vs N_1

Page 30

Project No. A-A-103

103

Date 15 Dec.

1954

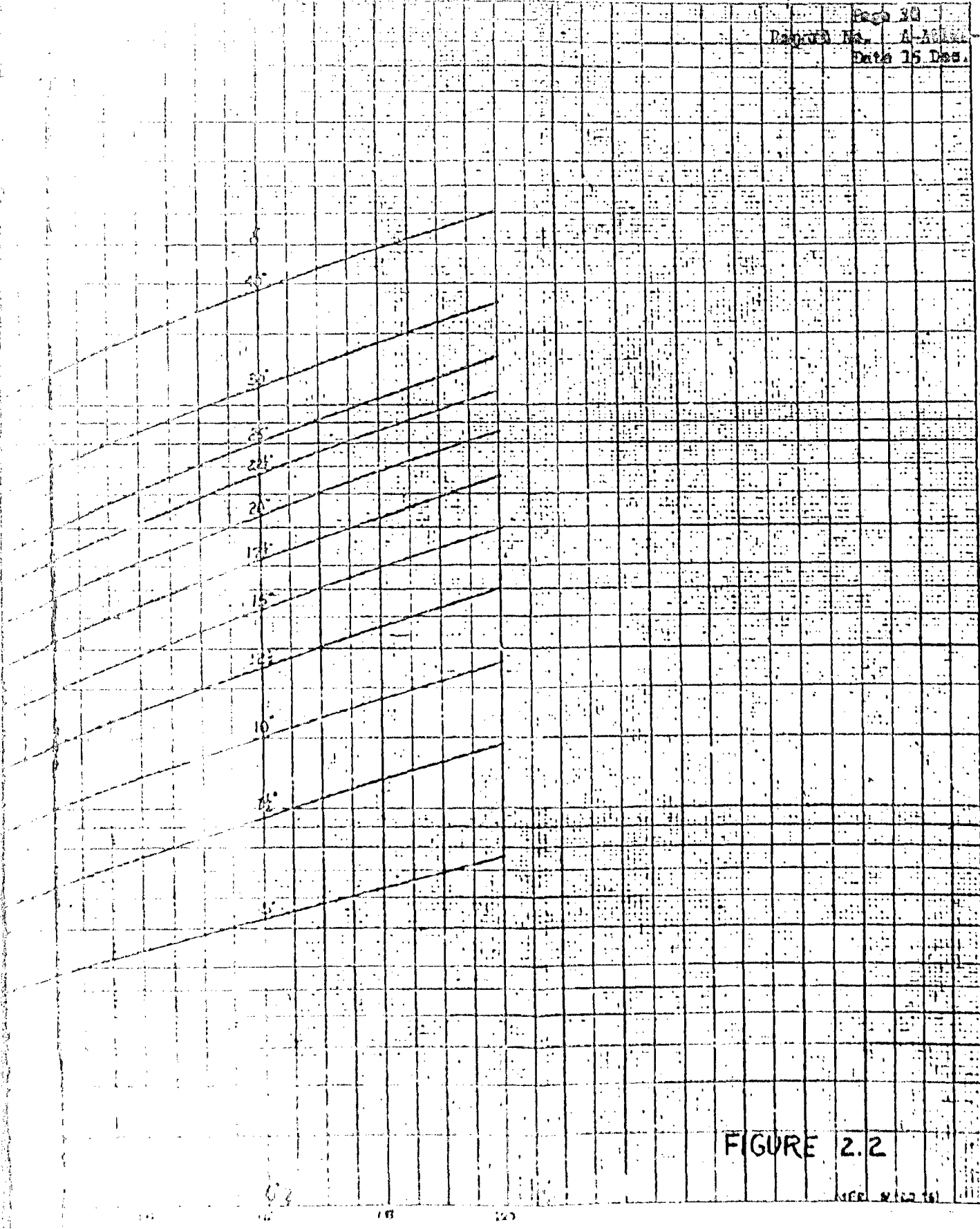
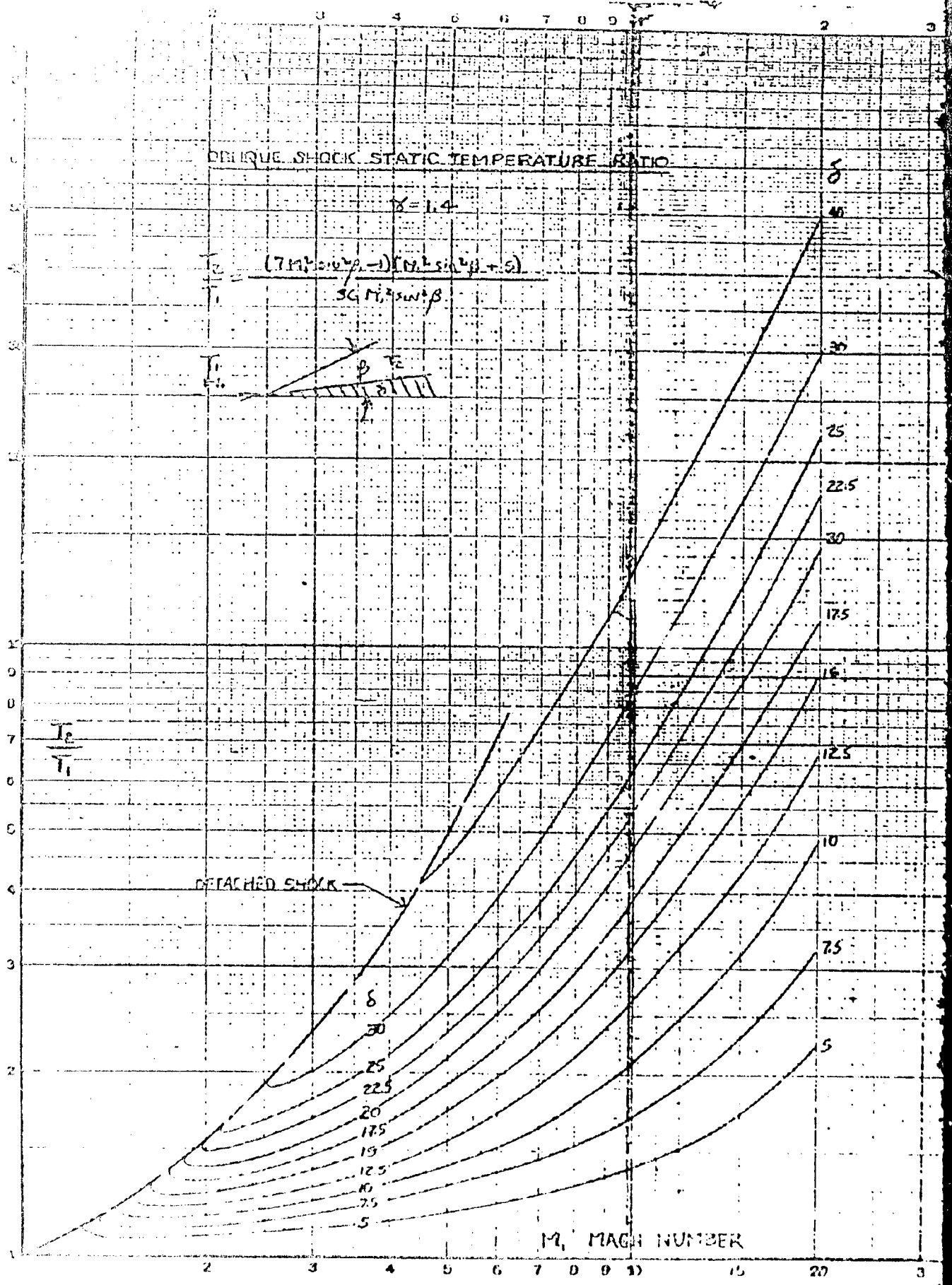


FIGURE 2.2

B



Page 21
Report No. A-4 Class-P
Date 15 Dec. 19

$$\frac{T_2}{T_1} \text{ vs } M_1$$

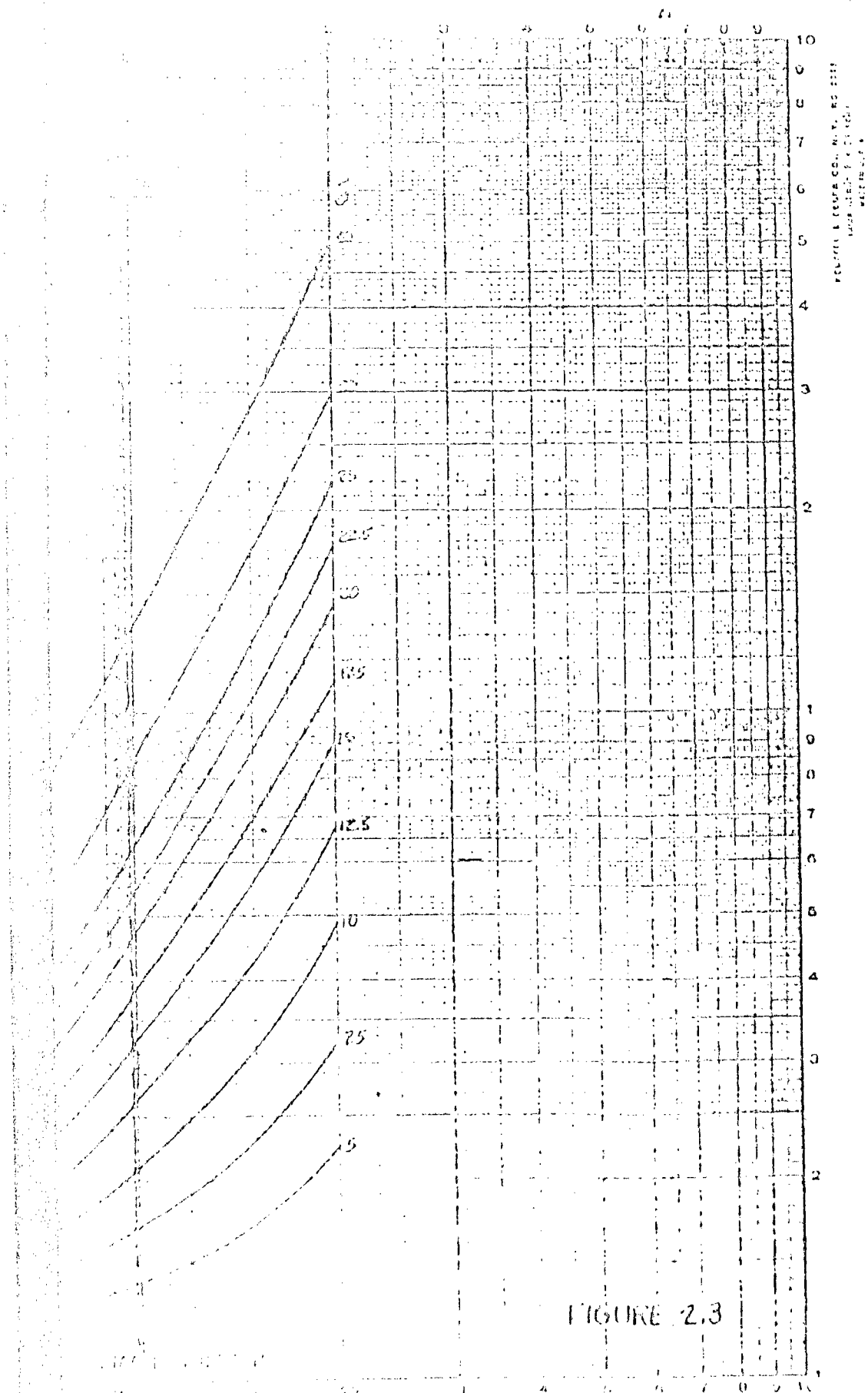
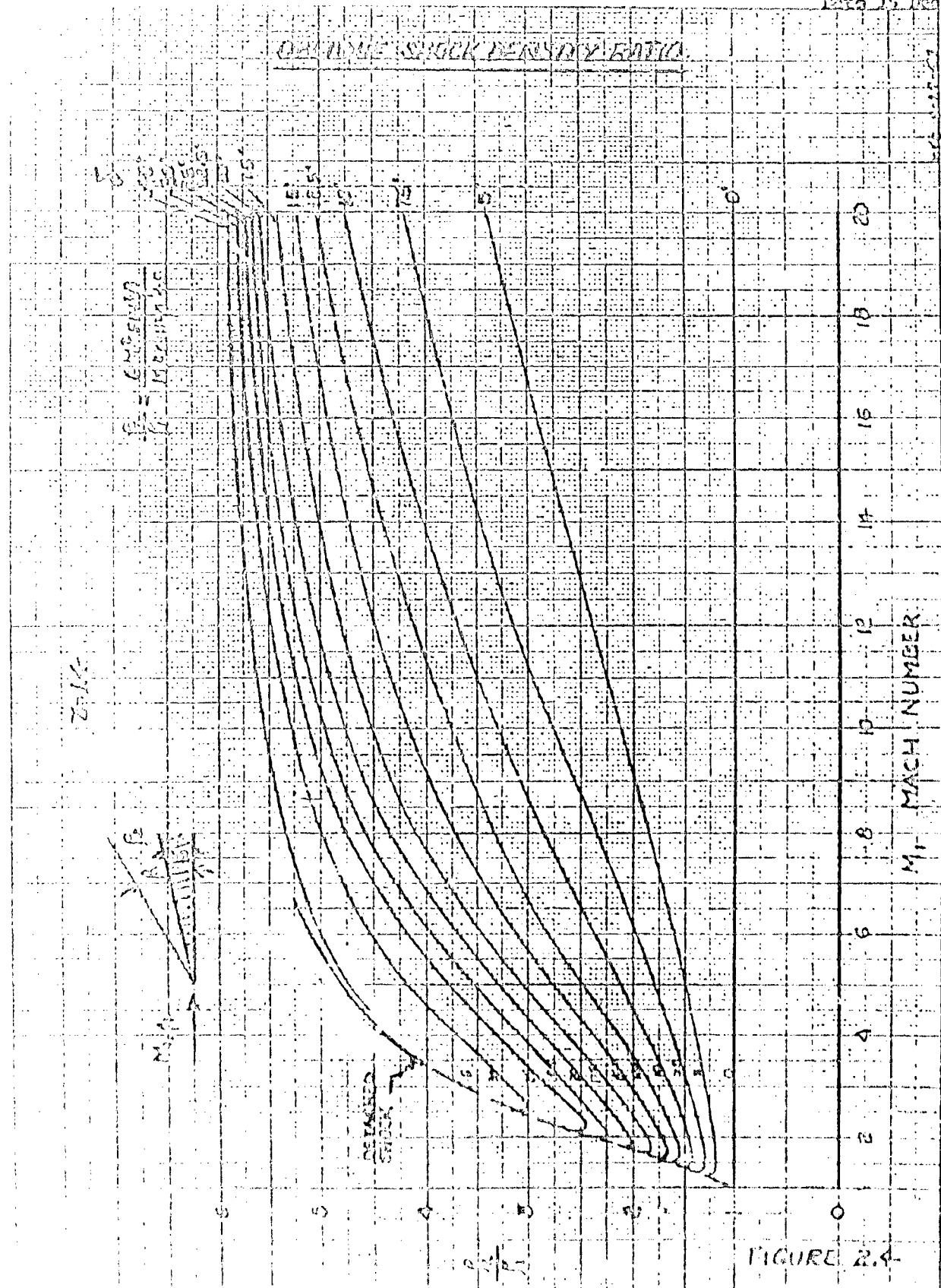


FIGURE 2.3

B

Page 32 of
Report No. A-Atlas-103
Date 15 Dec. 1954

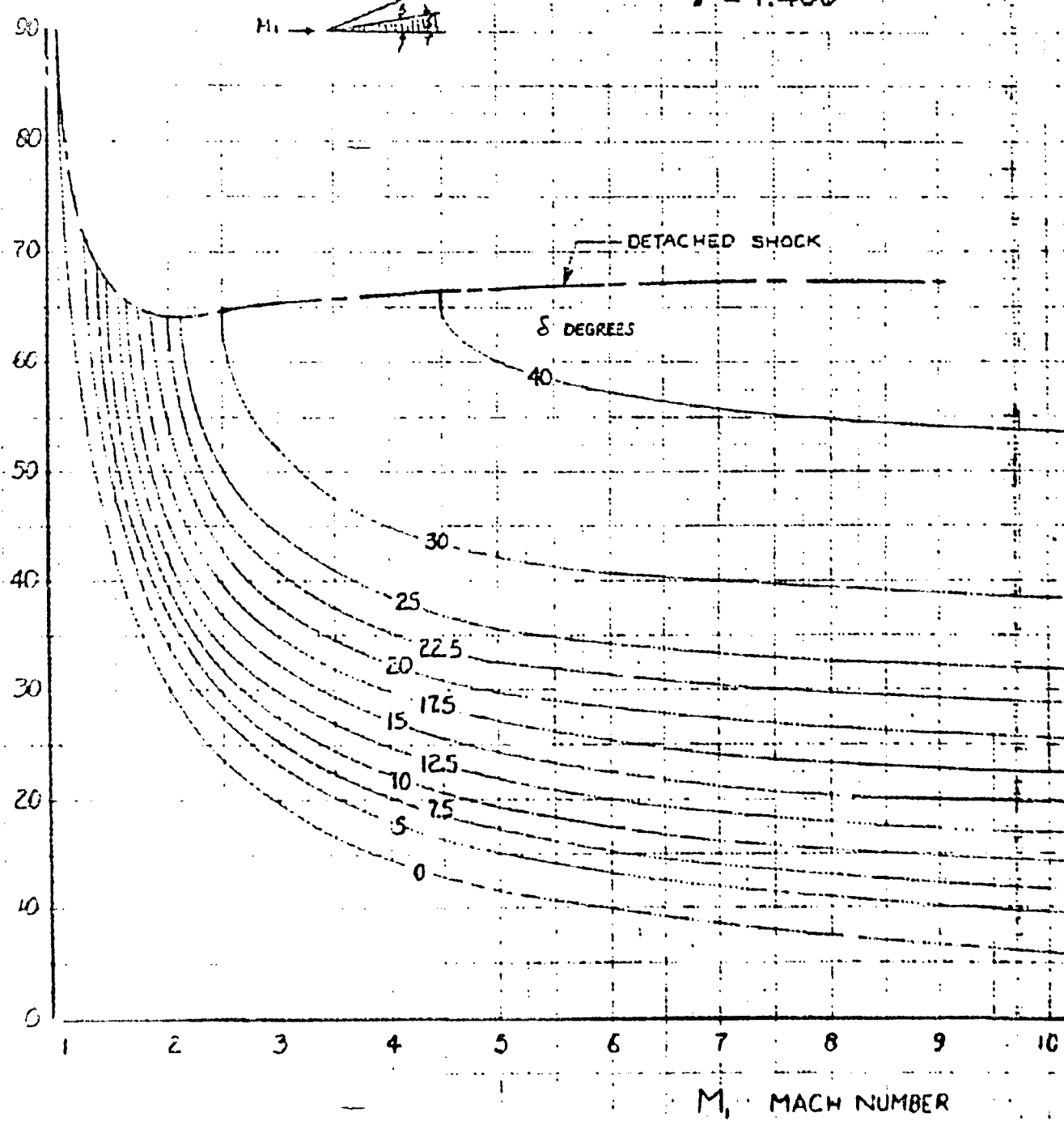


OBLIQUE SHOCK WAVE ANGLE

vs MACH NUMBER

β DEGREES

$\gamma = 1.400$



β vs M_1

Page 33

Report No. A-1100-103
Date 15 Dec. 1954

ANGLE

DATA FROM NACA TN 1373

AND $\tan \delta = \frac{M_1^2 \sin \beta - 2 \cot \alpha}{2 + M_1^2 (\gamma + \cos 2\beta)}$

5 DEGREES

10

20

25

22.5

20

17.5

15

12.5

10

7.5

5

0

10 11 12 13 14 15 16 17 18 19

FIGURE P.5

B

Bethel's Rec. 19

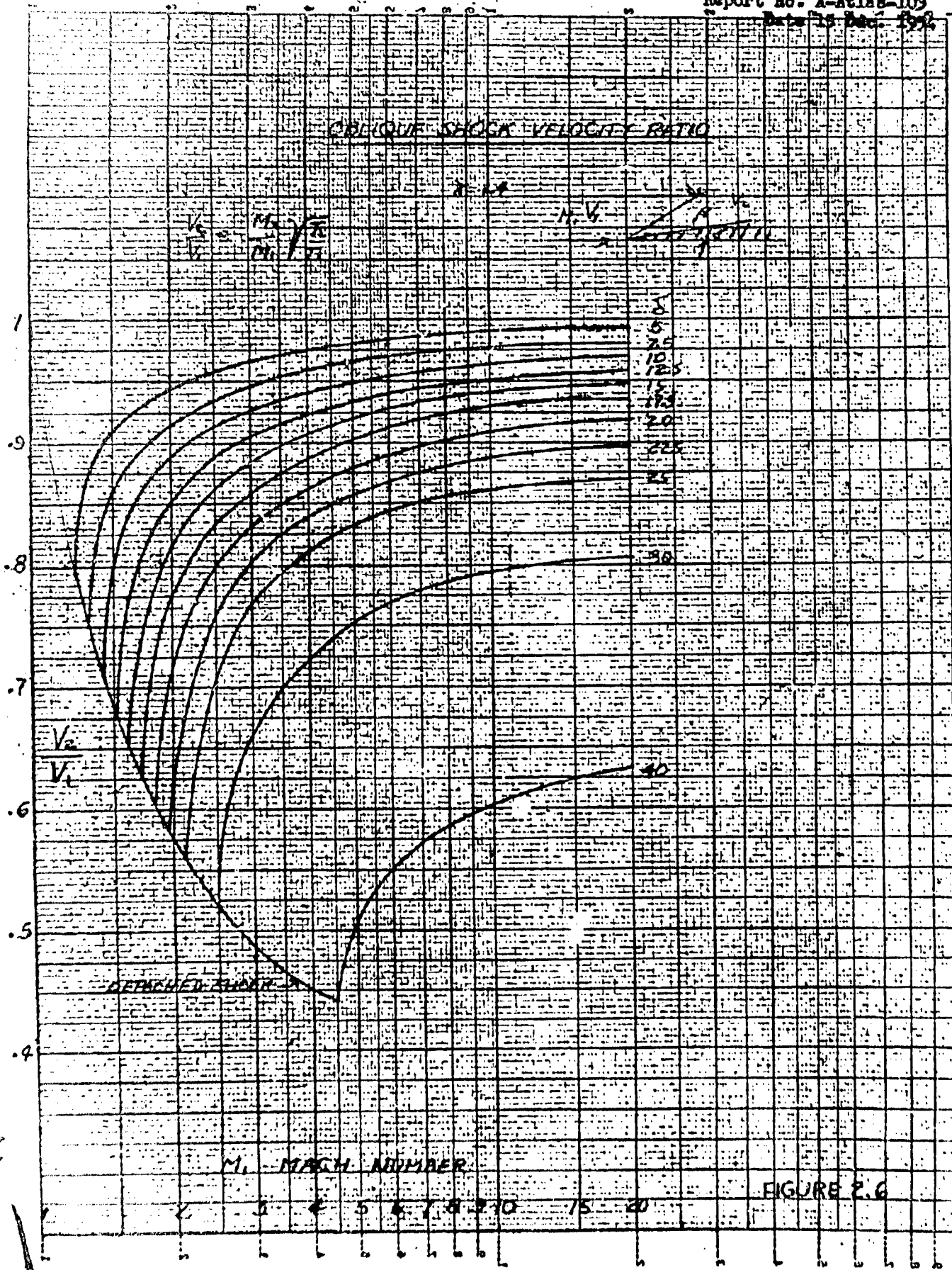
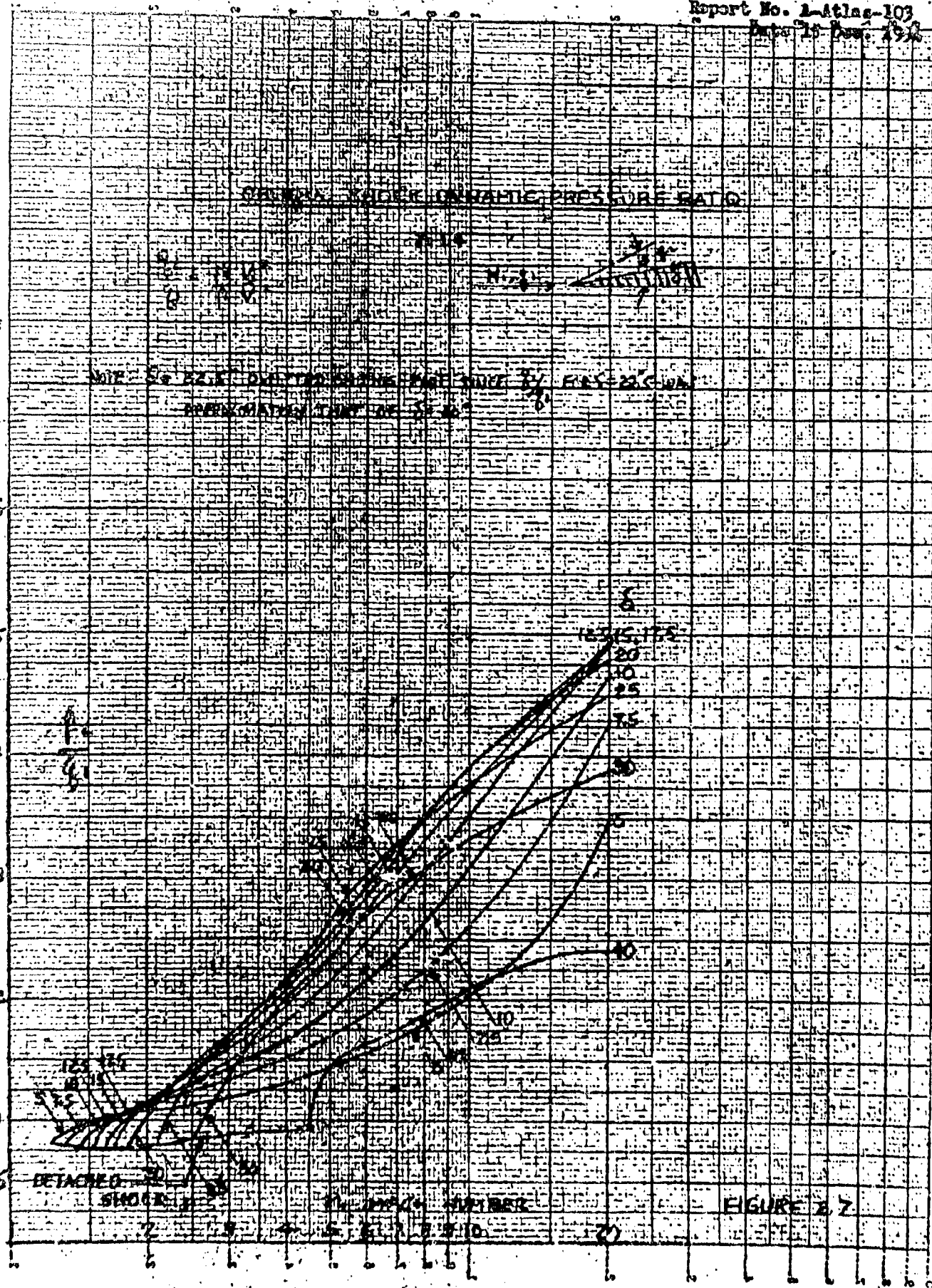
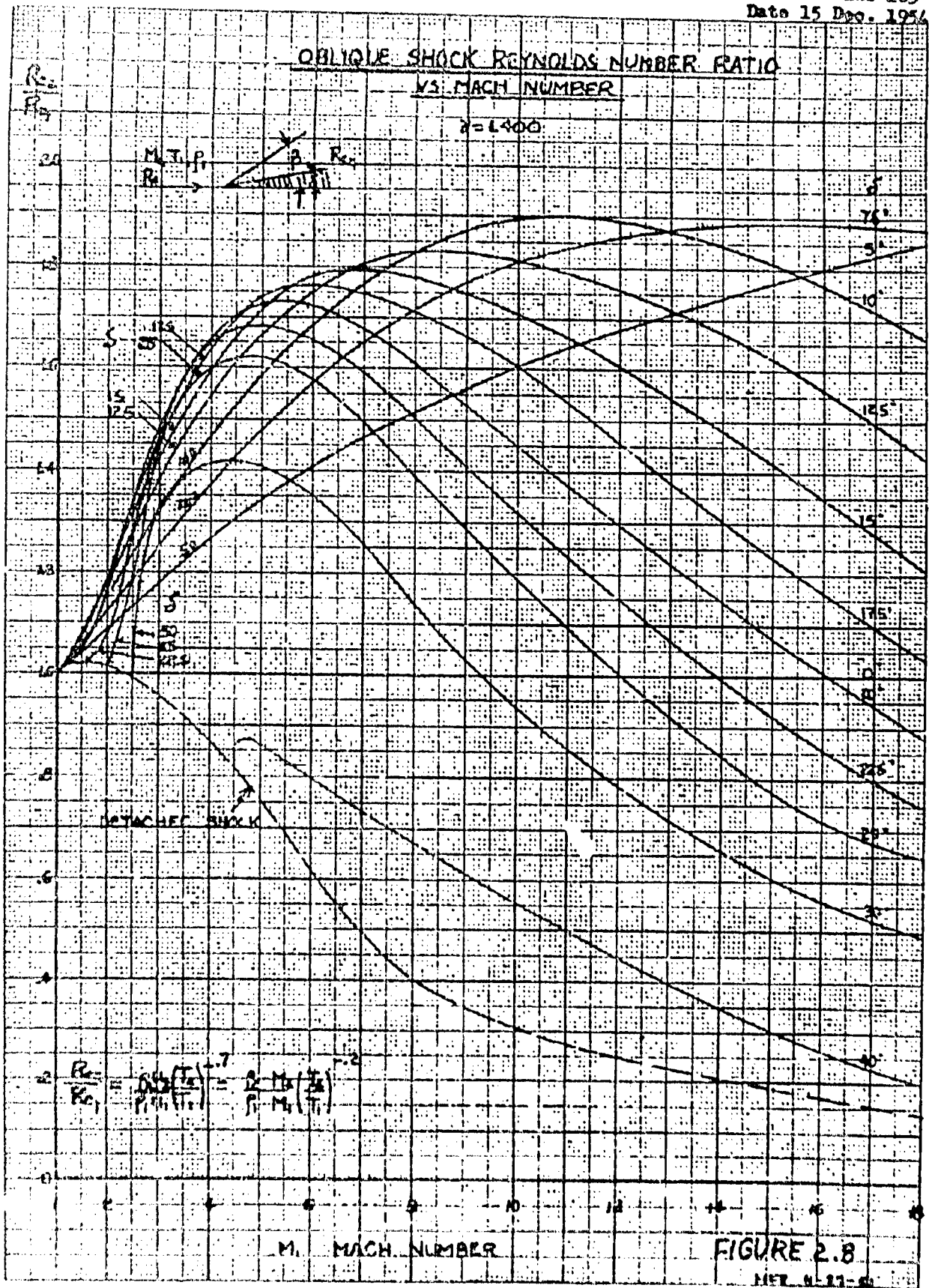
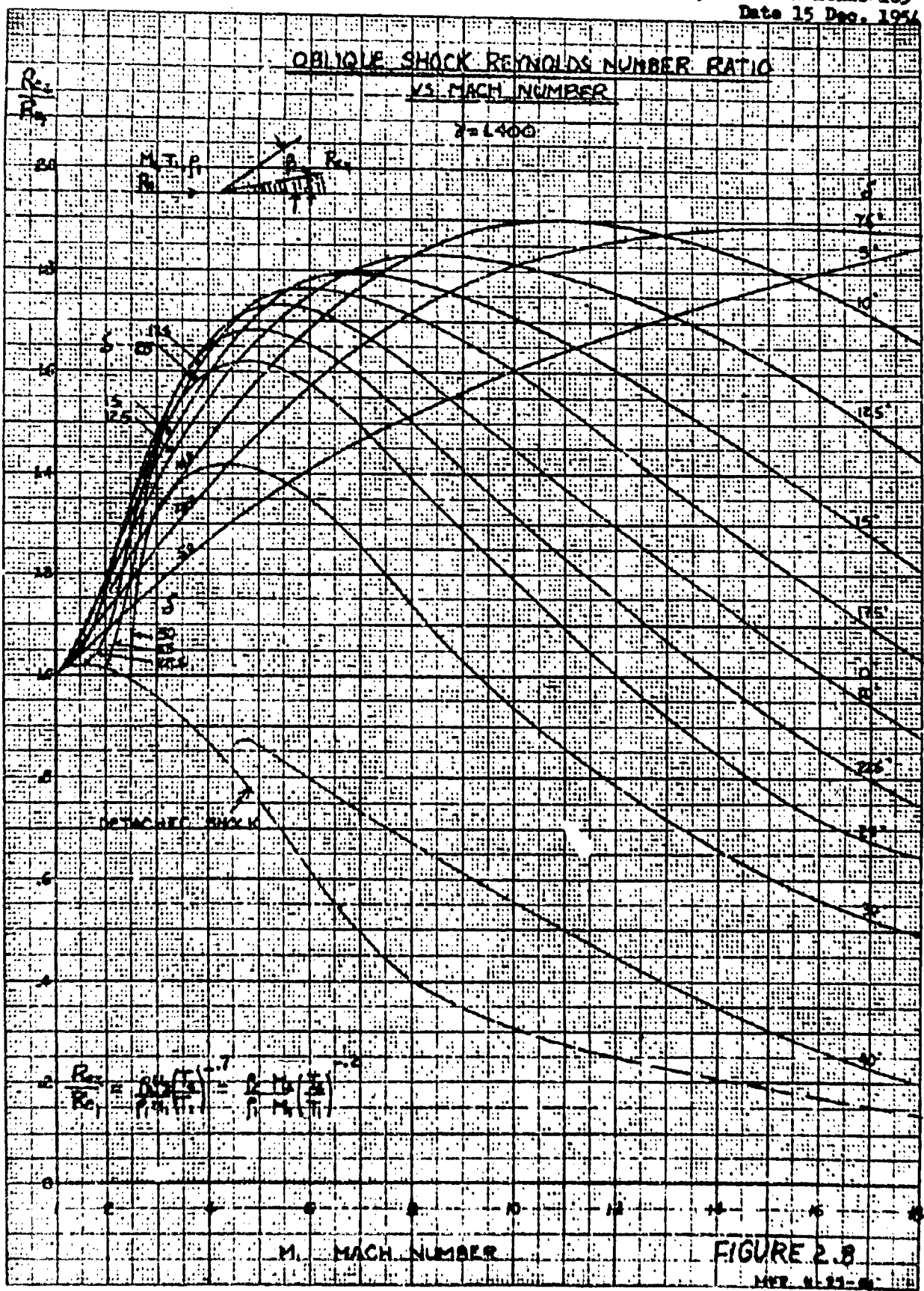
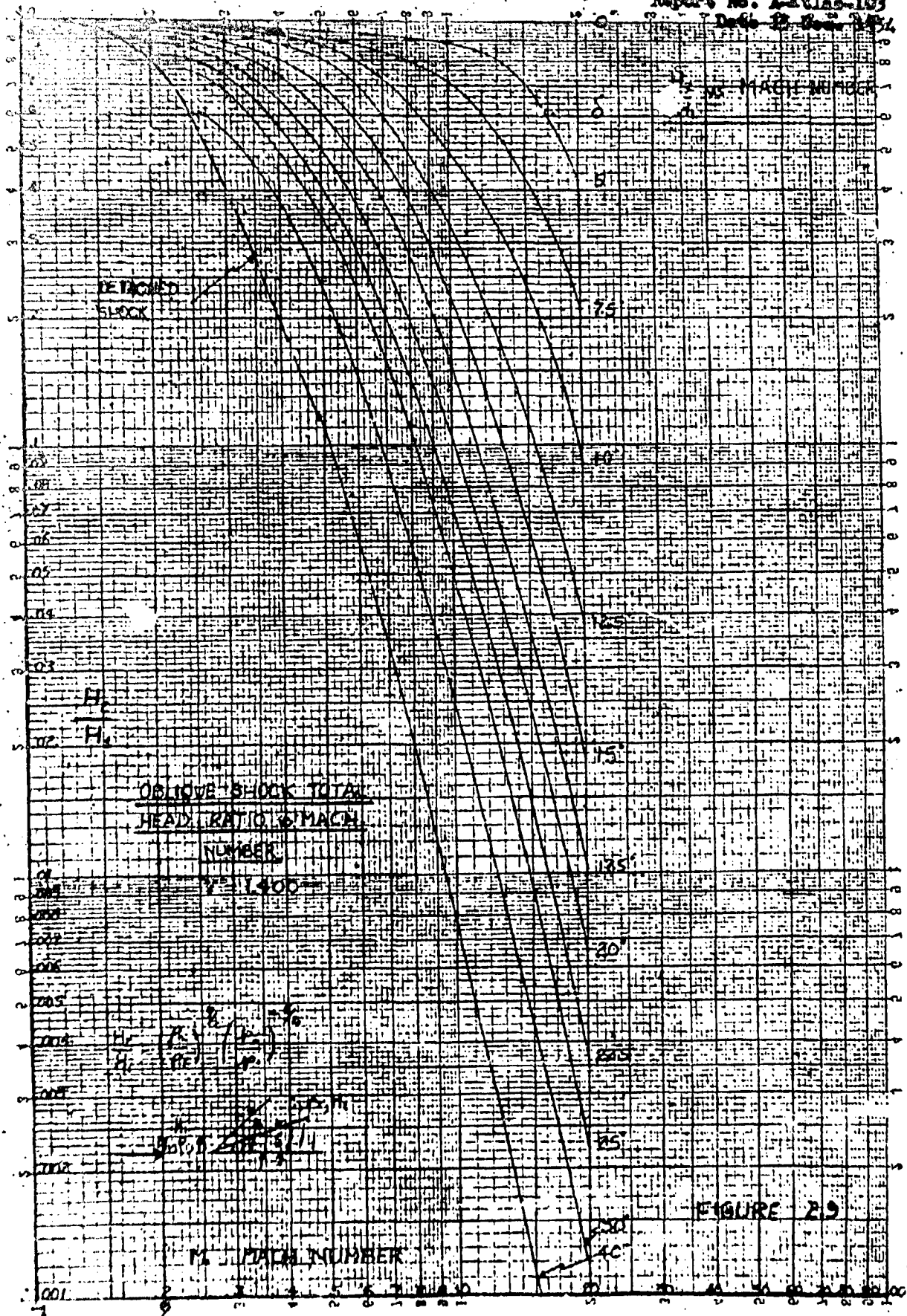


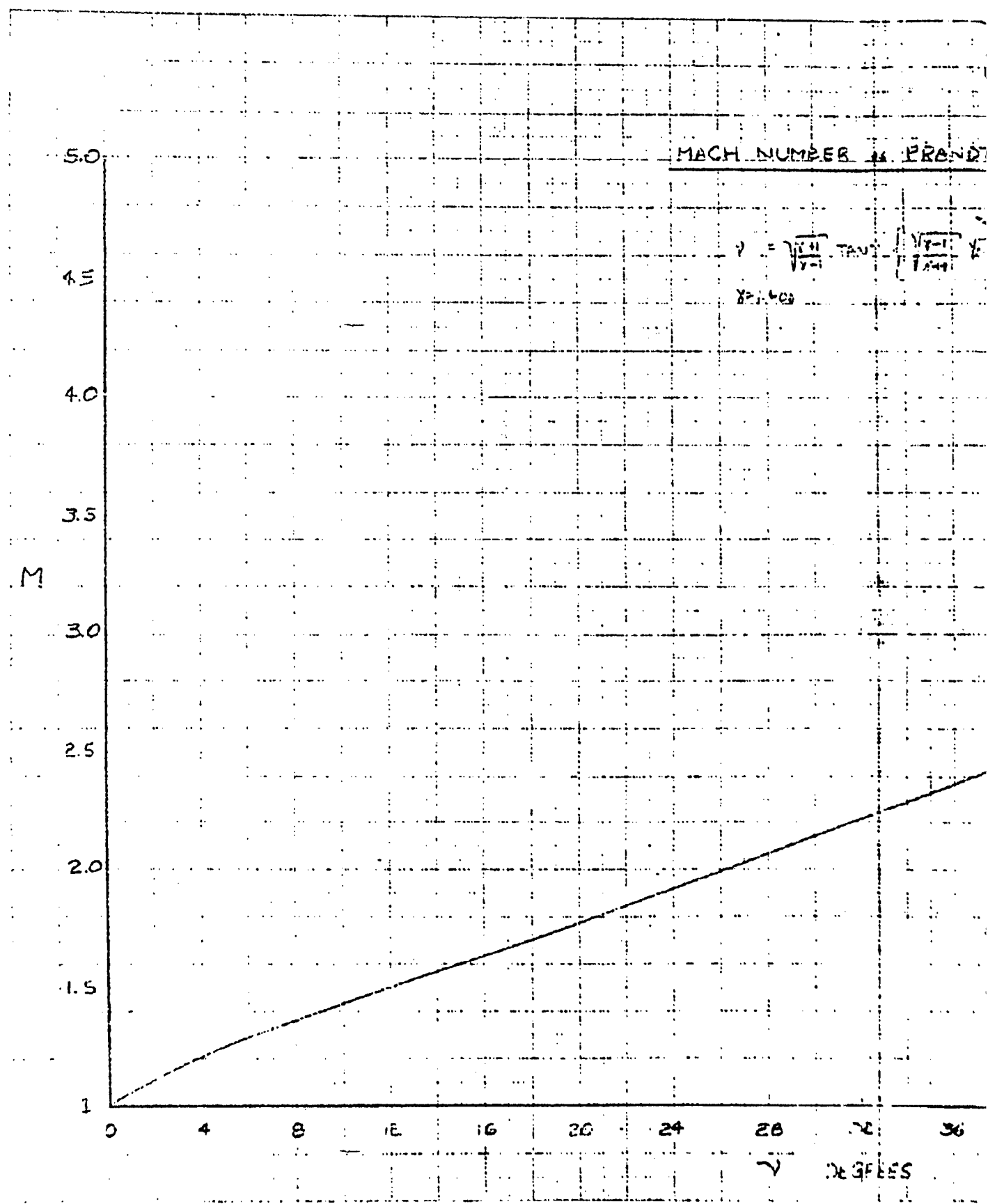
FIGURE 2.6





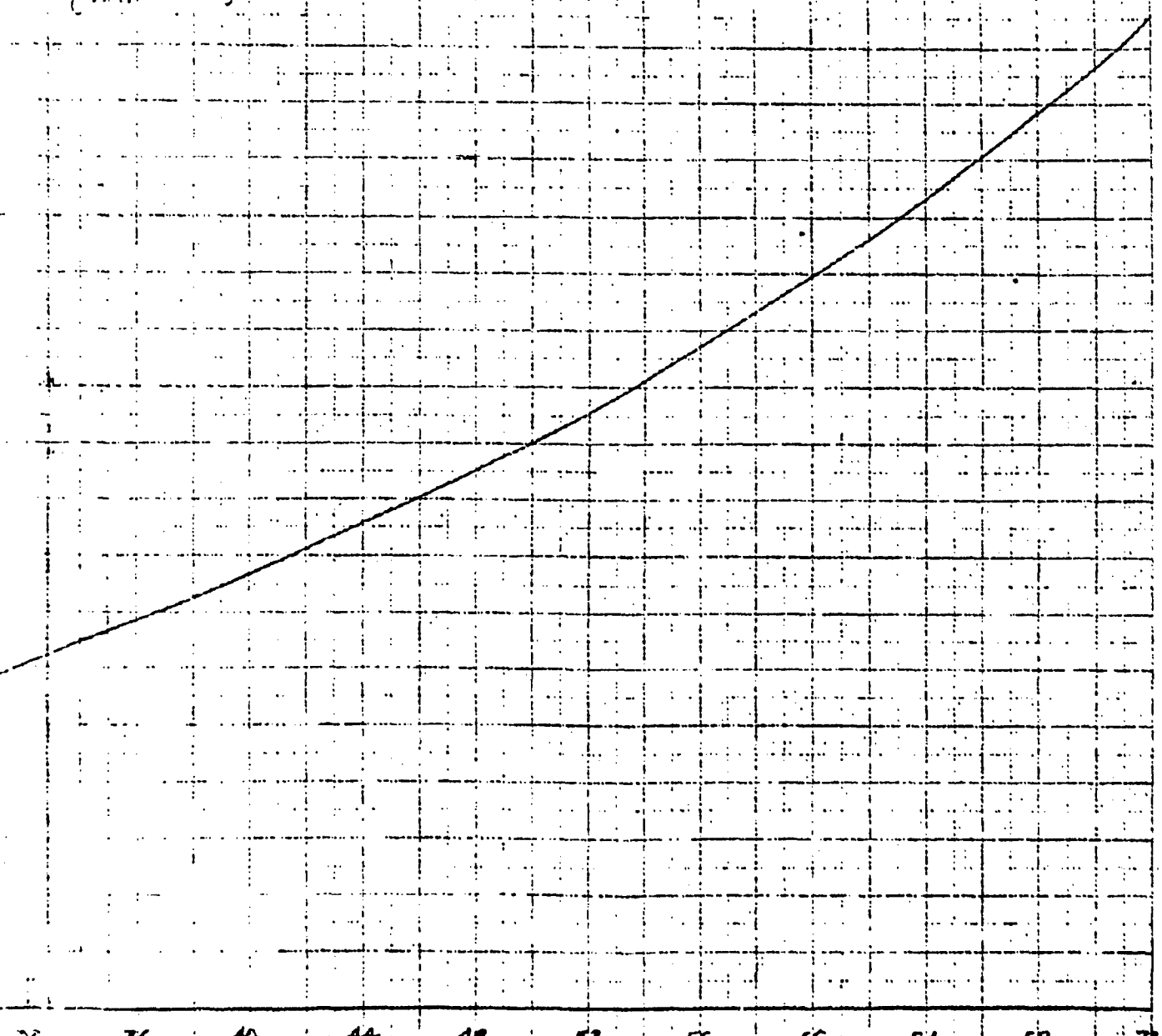






B. PRANDTL-MEYER ANGLE

$$\tan \{ \frac{V_1 - 1}{V_1 + 1} \} = 12.5 \quad Y_{M^2} = 1$$



DEGREES

FIGURE 2.10a

REF ID: A-Atlas-103

8

FIGURE 2.10P
PRANDTL-MEYER ANGLE

$$\left\{ \frac{V_0 - V}{V_0} = \sqrt{\frac{1 + \frac{1}{4} \tan^2 \gamma}{1 - \frac{1}{4} \tan^2 \gamma}} \right\} = \tan \gamma = M$$

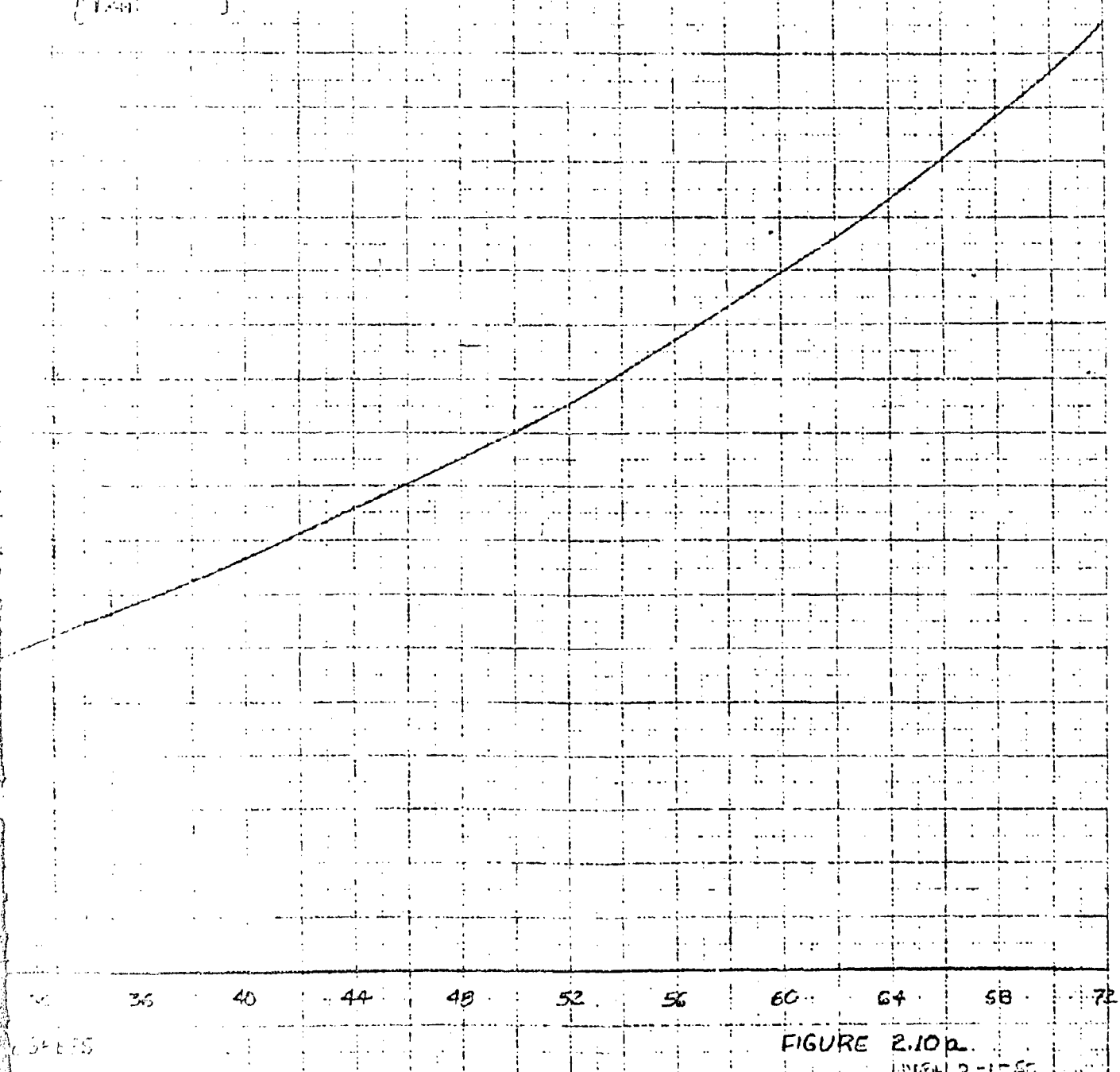


FIGURE 2.10P

16A 2-1-55

B

29

PIAGA NUMBER vs. PRANDTL-MEYER ANGLE.

$$\frac{dy}{dx} = \sqrt{\frac{2\gamma}{\gamma - 1}} \tan \left\{ \sqrt{\frac{\gamma + 1}{\gamma - 1}} \frac{dy}{dx} \right\} - \tan^{-1} \frac{dy}{dx}$$

$$y = f(x)$$

15

16

17

18

19

20

21

22

23

24

25

26



M vs γ Page 39
Report No. 4-1000-103
Date 15 Dec. 1952

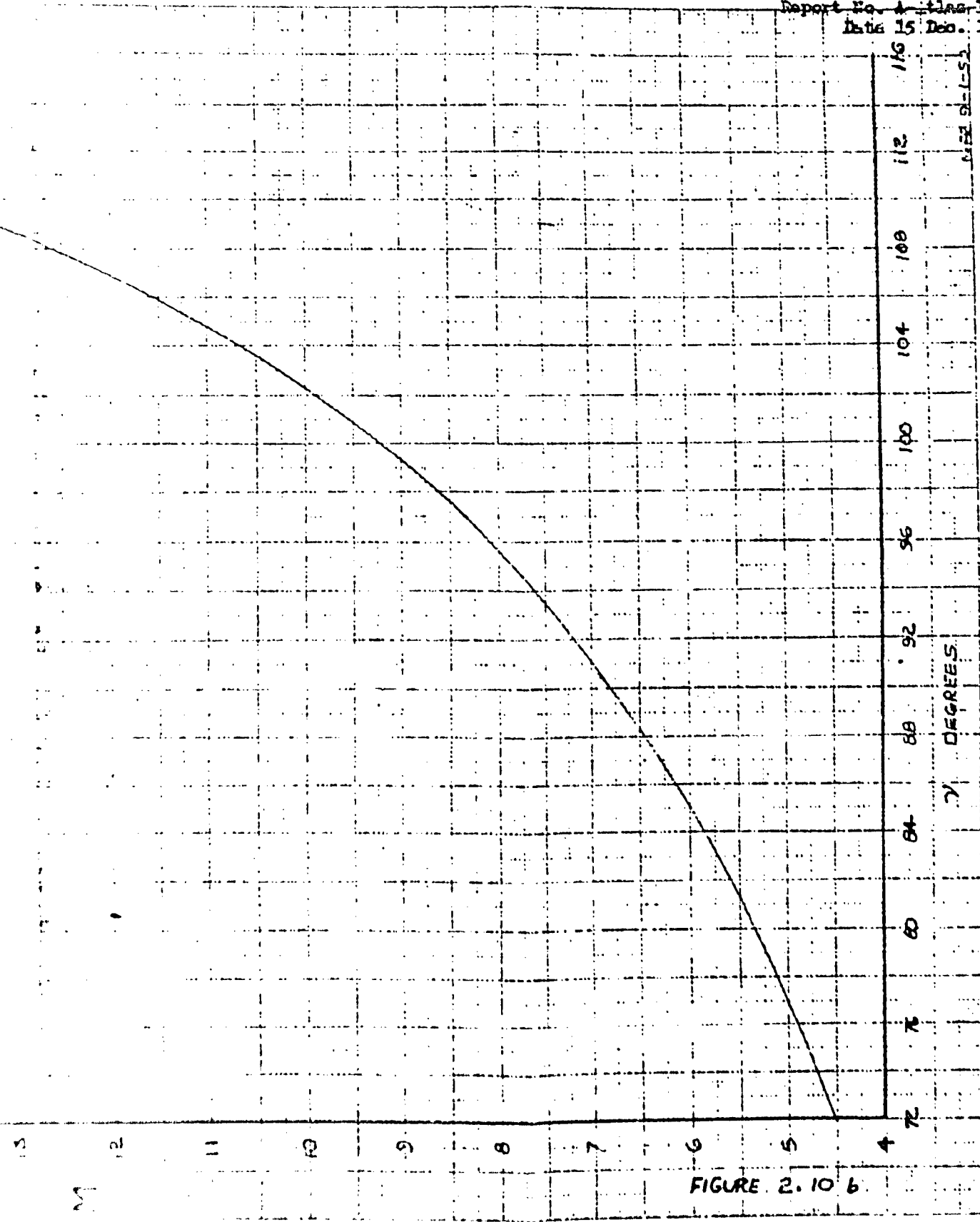


FIGURE 2.10.6

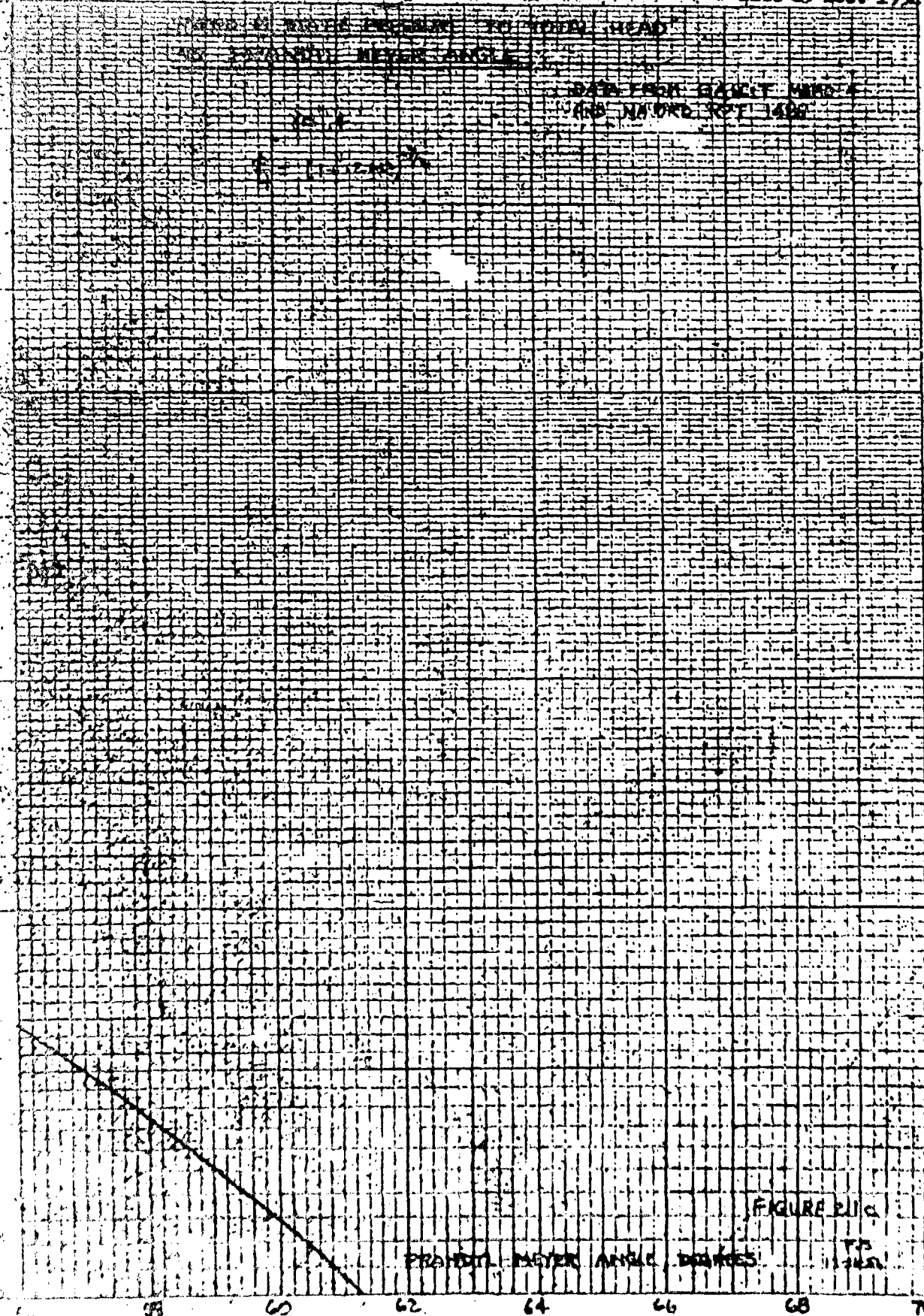
B

Page 2

Report No. Catline 102
Date 15 Dec. 1946

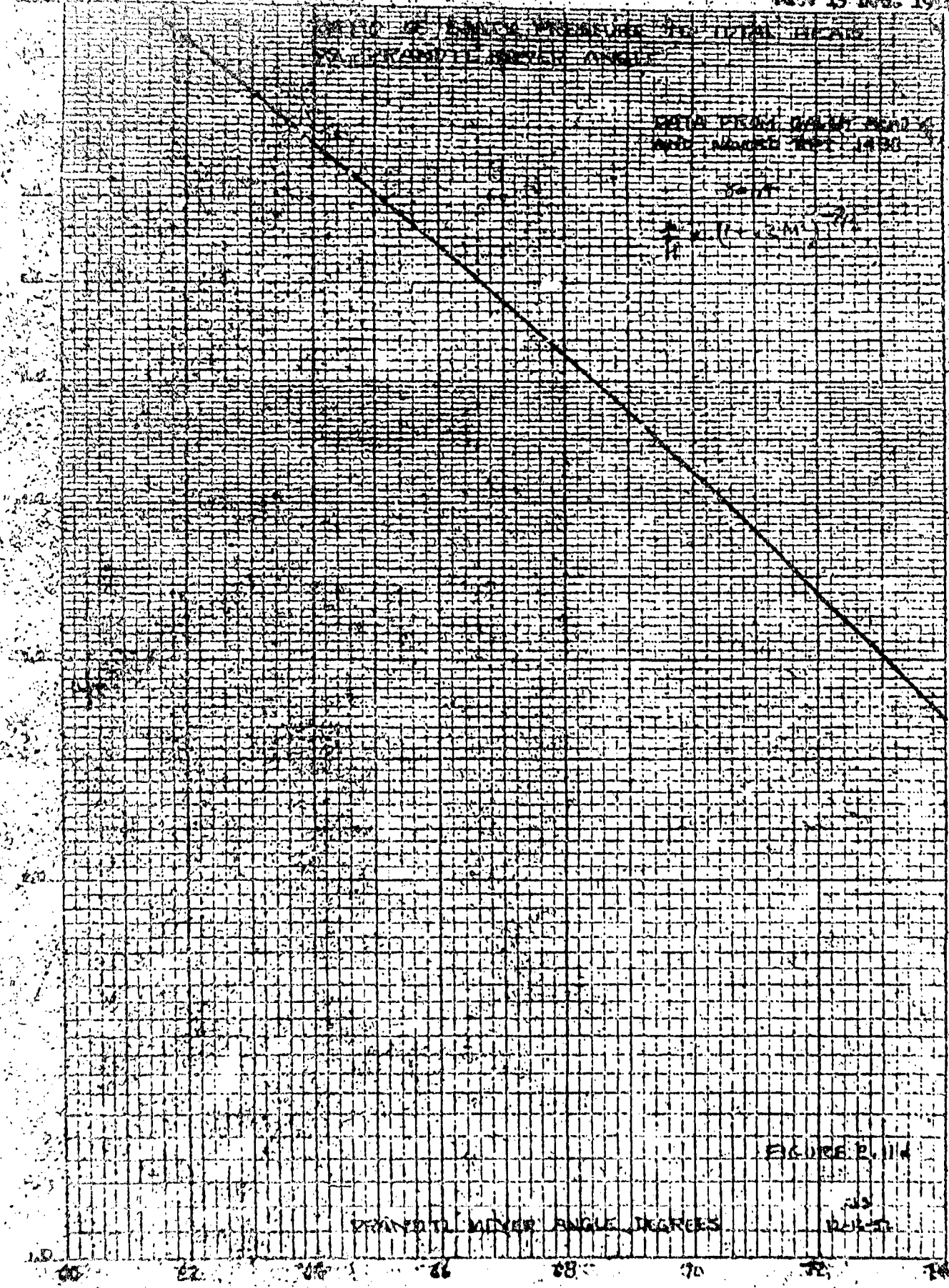


Page 1A
Report No. A-Atlan-103
Date 15 Dec. 1954



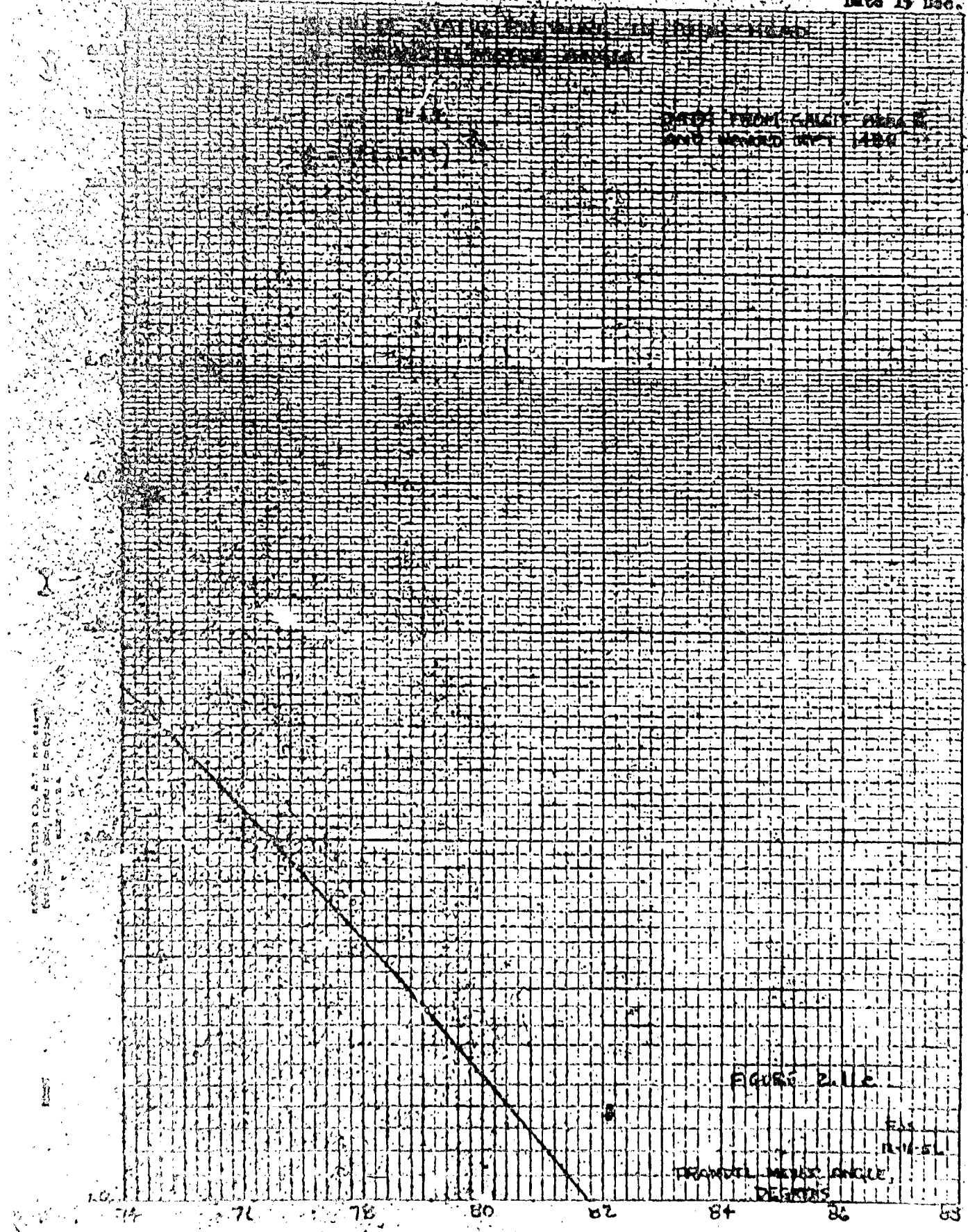
Project No. 1
Report No. 1
Date 15 Dec. 1943

Exhibit 1 - Location of the mine
Exhibit 2 - Map of the area



Report No. 4-A-118-253
Date 15 Dec. 1953

DETERMINED WIND VELOCITY AND DIRECTION
ON 15 DECEMBER 1953



1.000
15. Dec. 1967

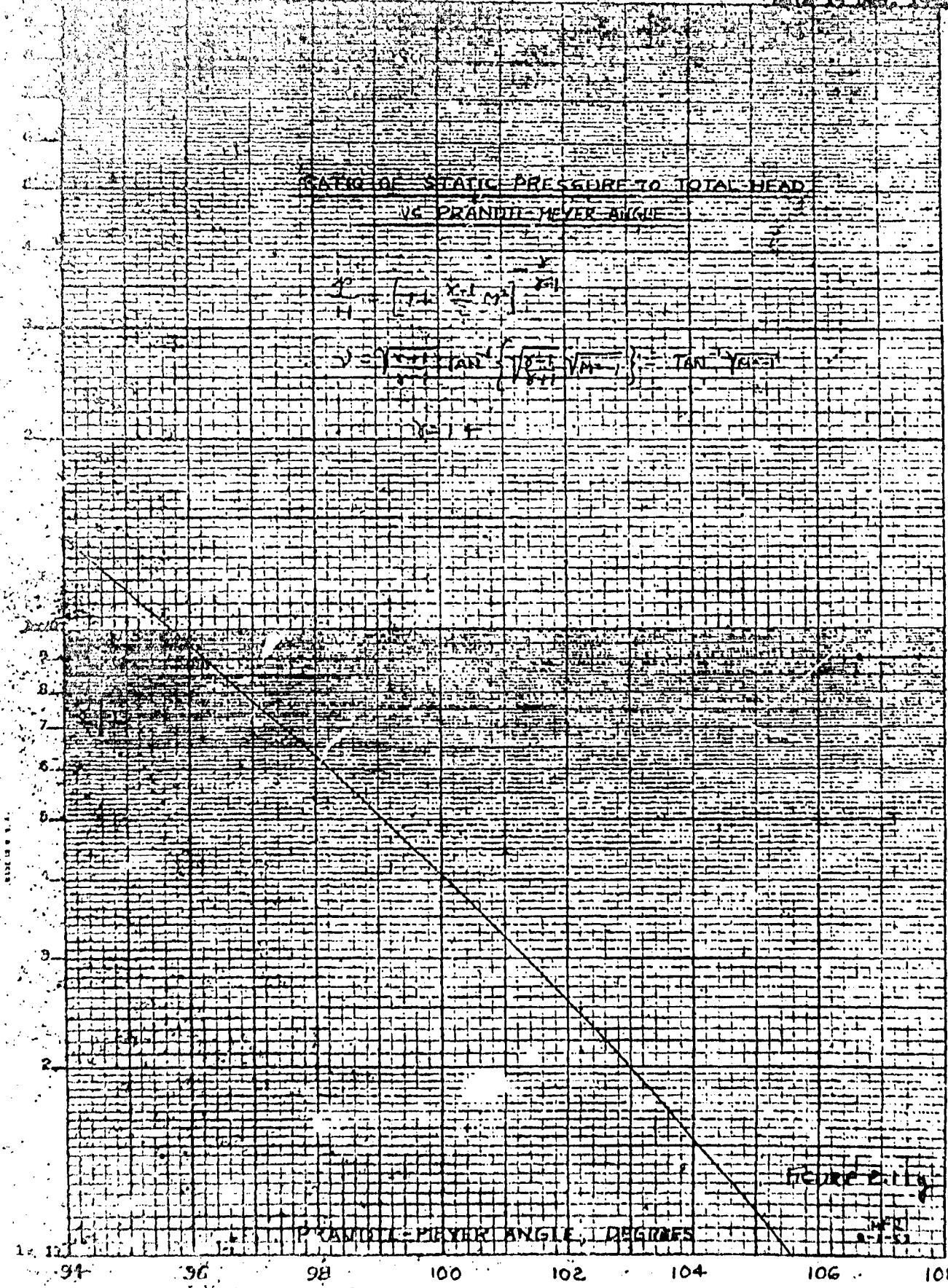
100' X 100'

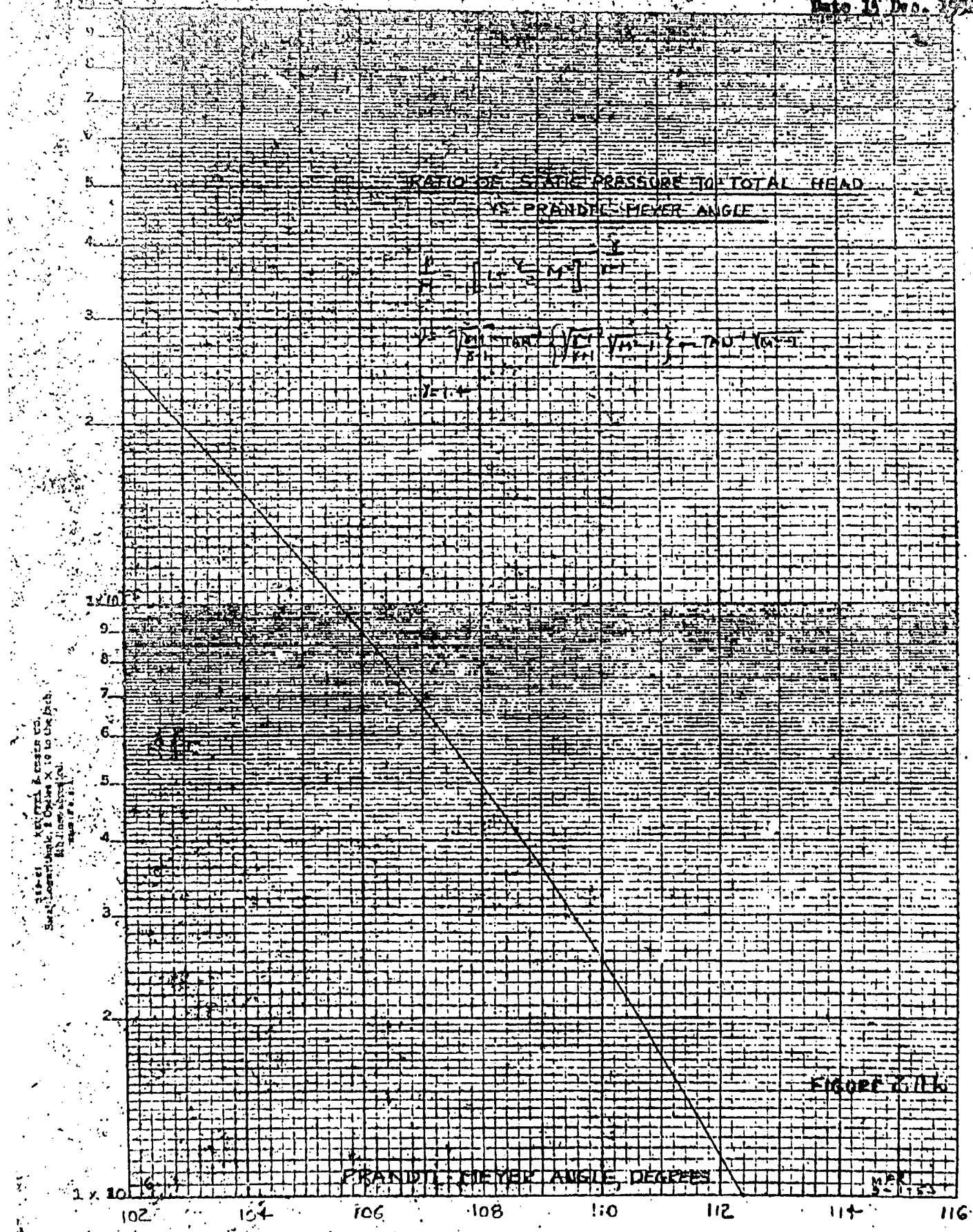
FIGURE 2.

GENERAL ELEVATION

120 110 100 90 80 70 60 50 40 30 20 10 0

Report No. 4-Atlas 103
Date 15 Dec. 1954





RATIO OF STATIC PRESSURE TO TOTAL HEAD
VS. PROBE METER ANGLE

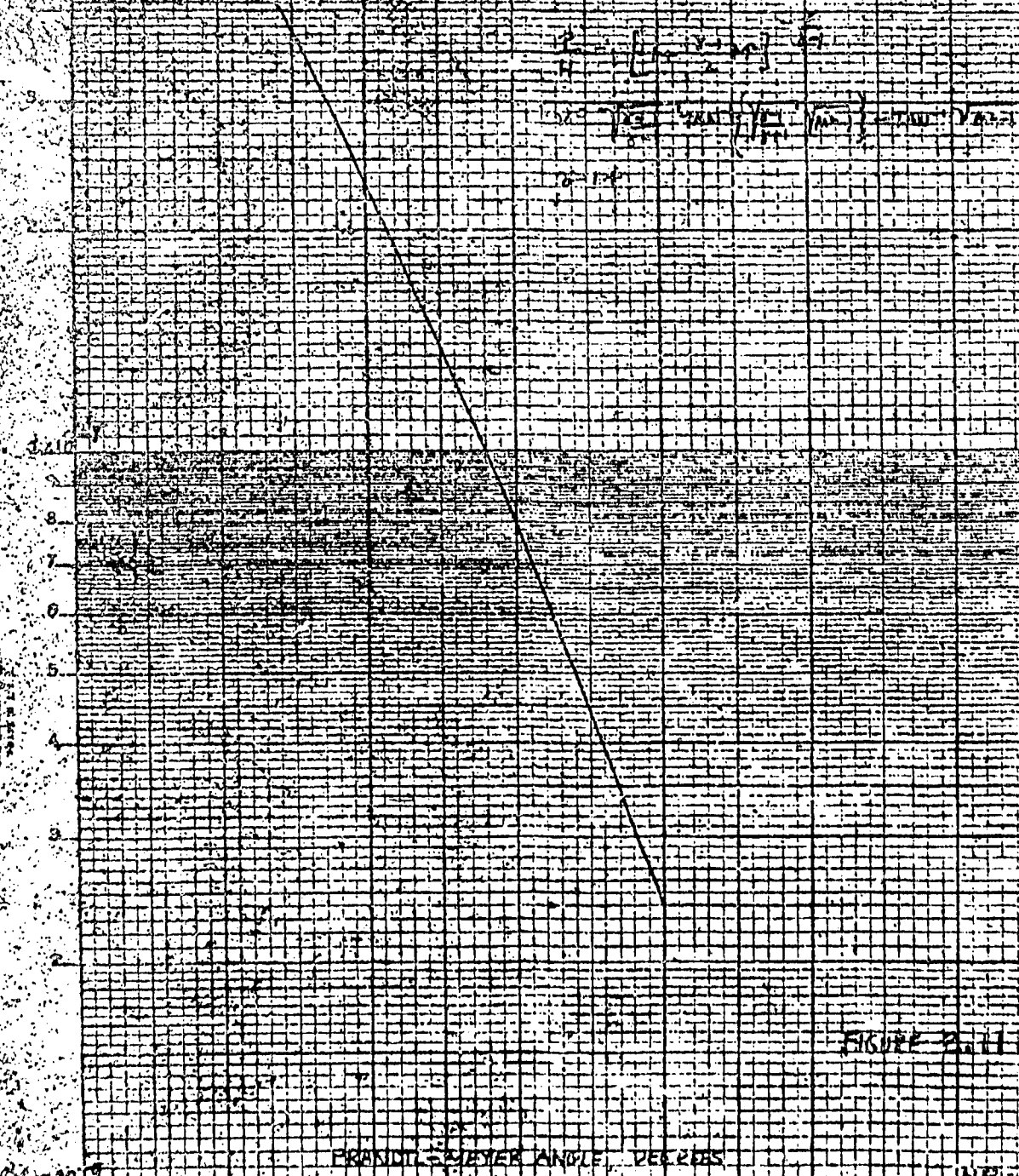
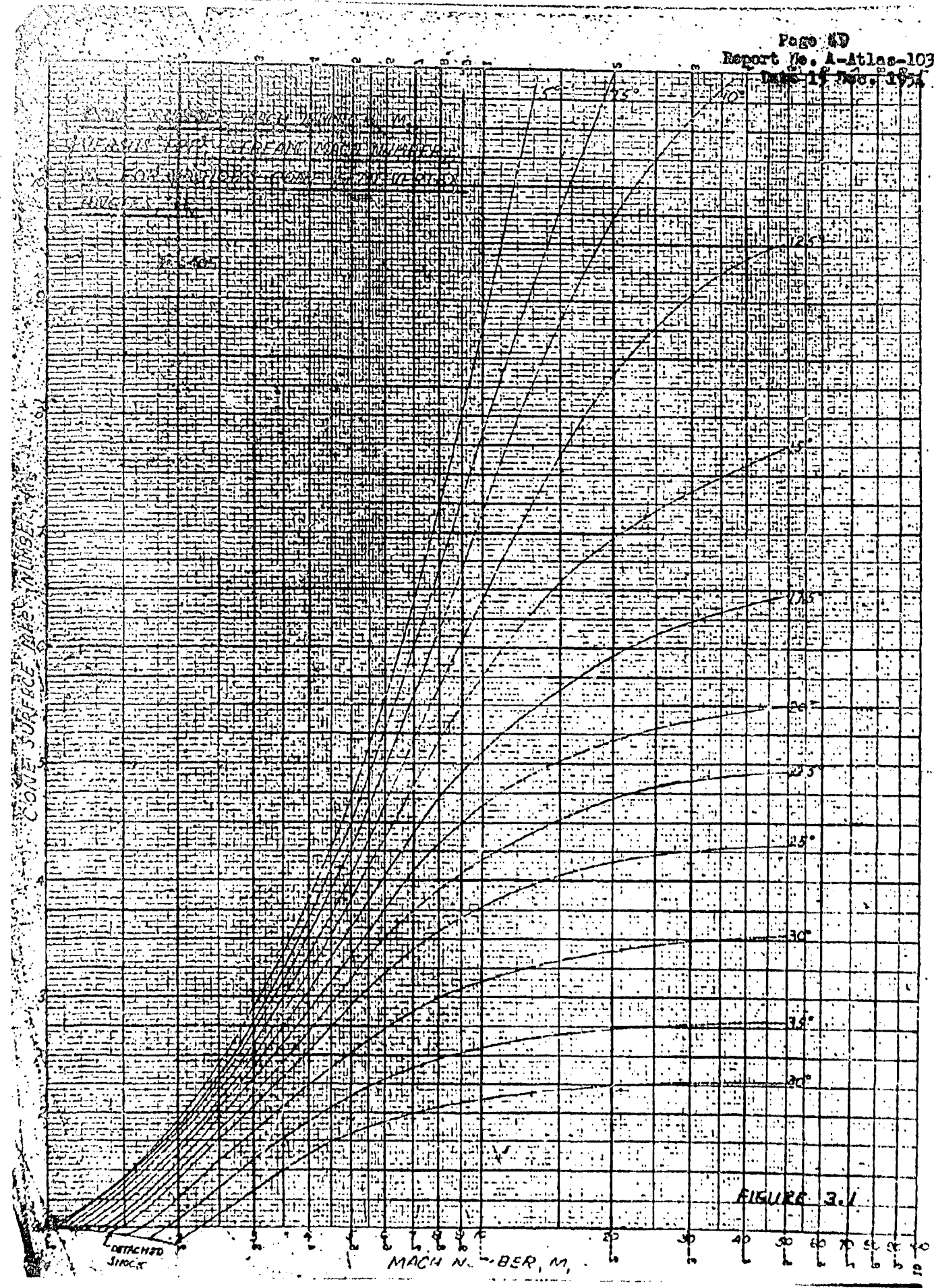
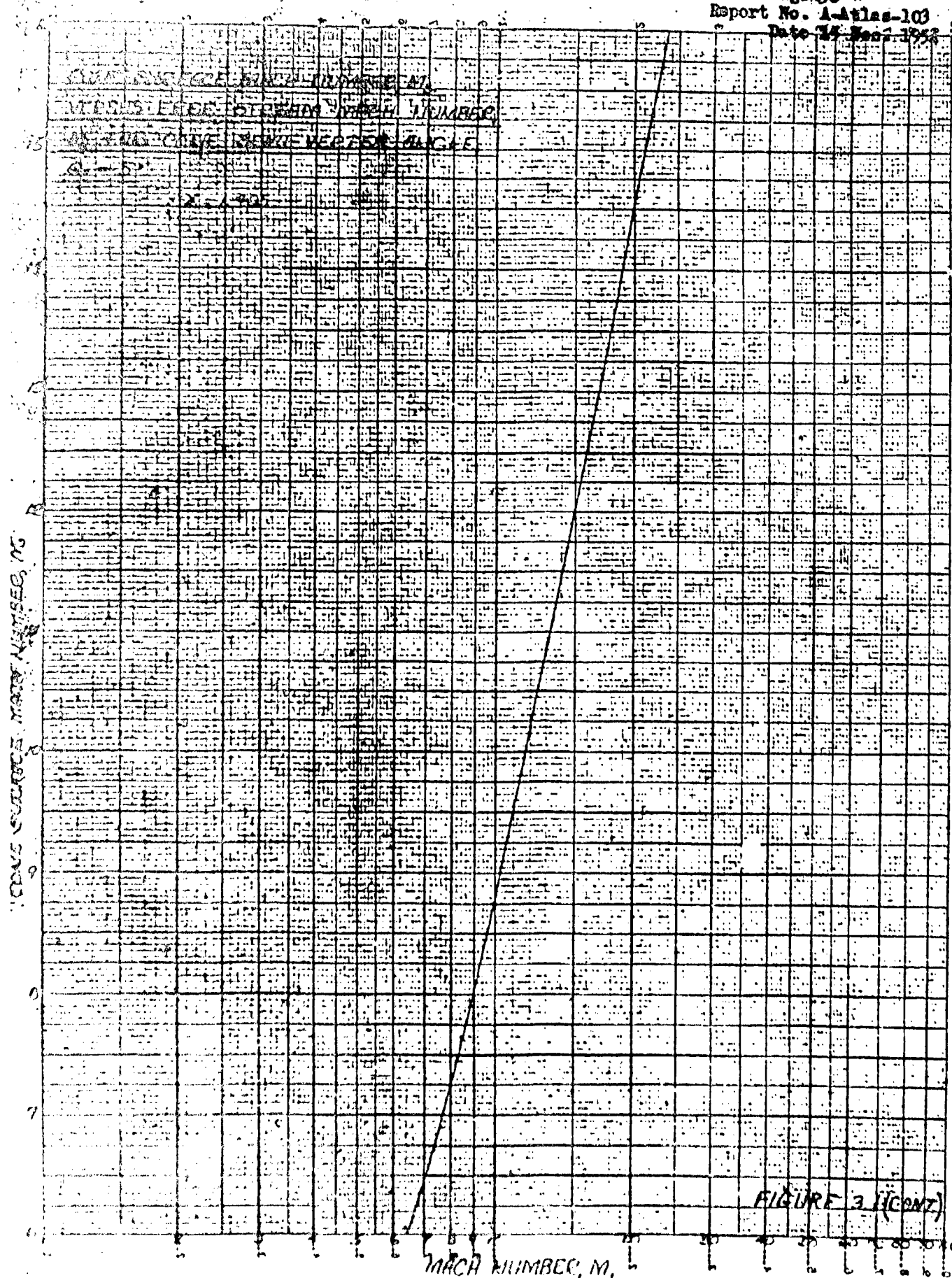


FIGURE 2.11

PROBE METER ANGLE, DEGREES

112 114 116 118 120 122





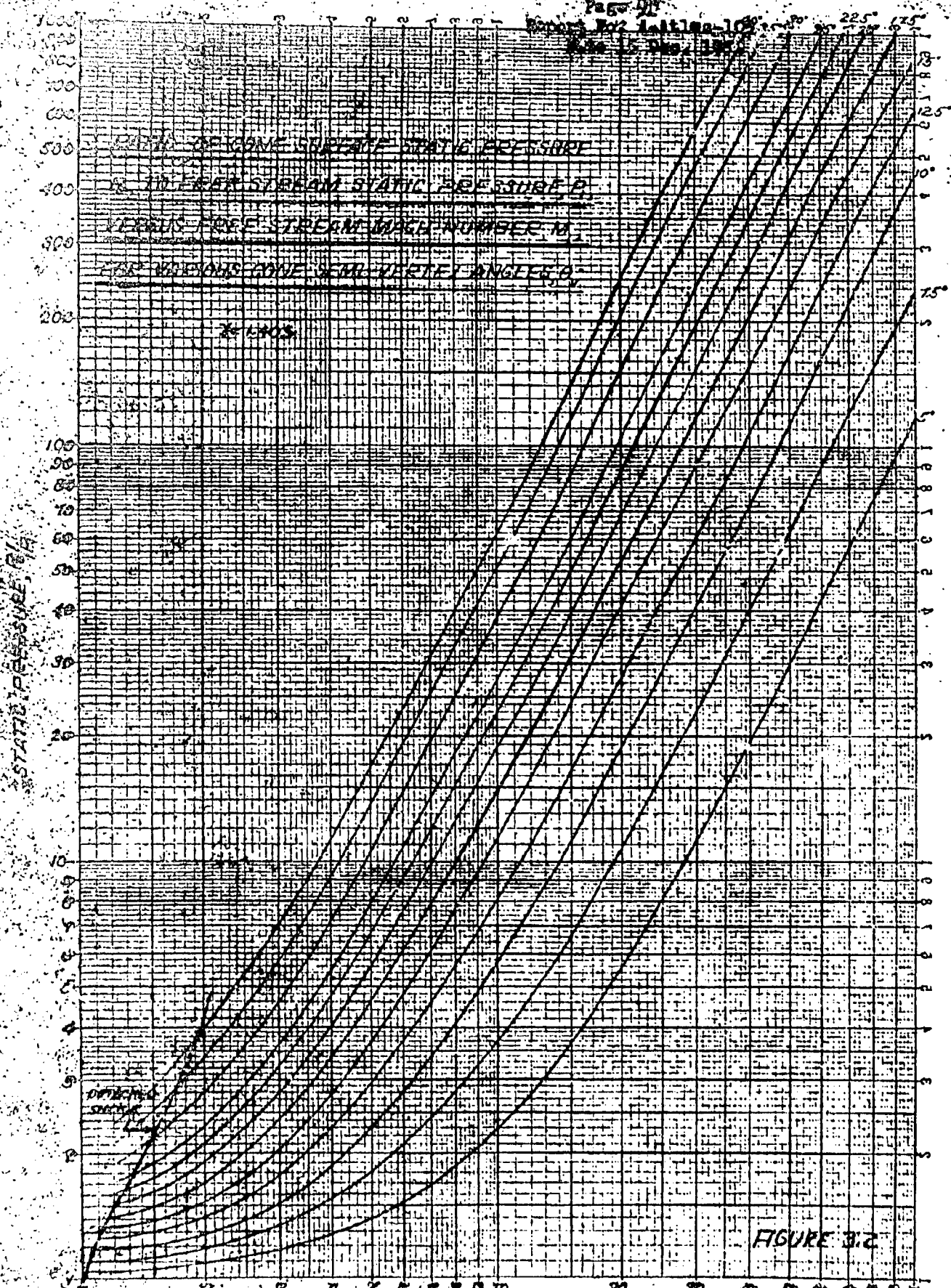


FIGURE 3.C

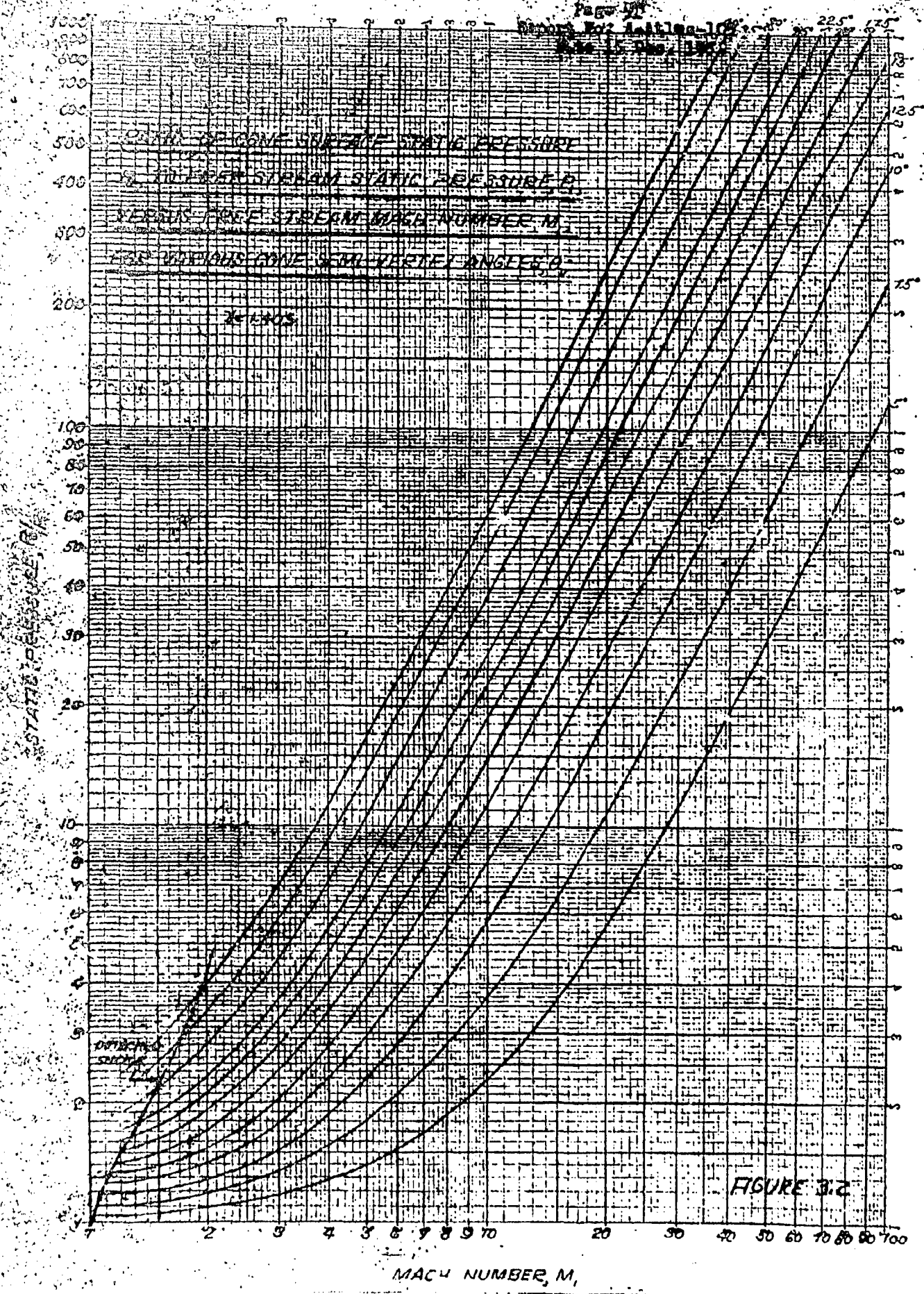


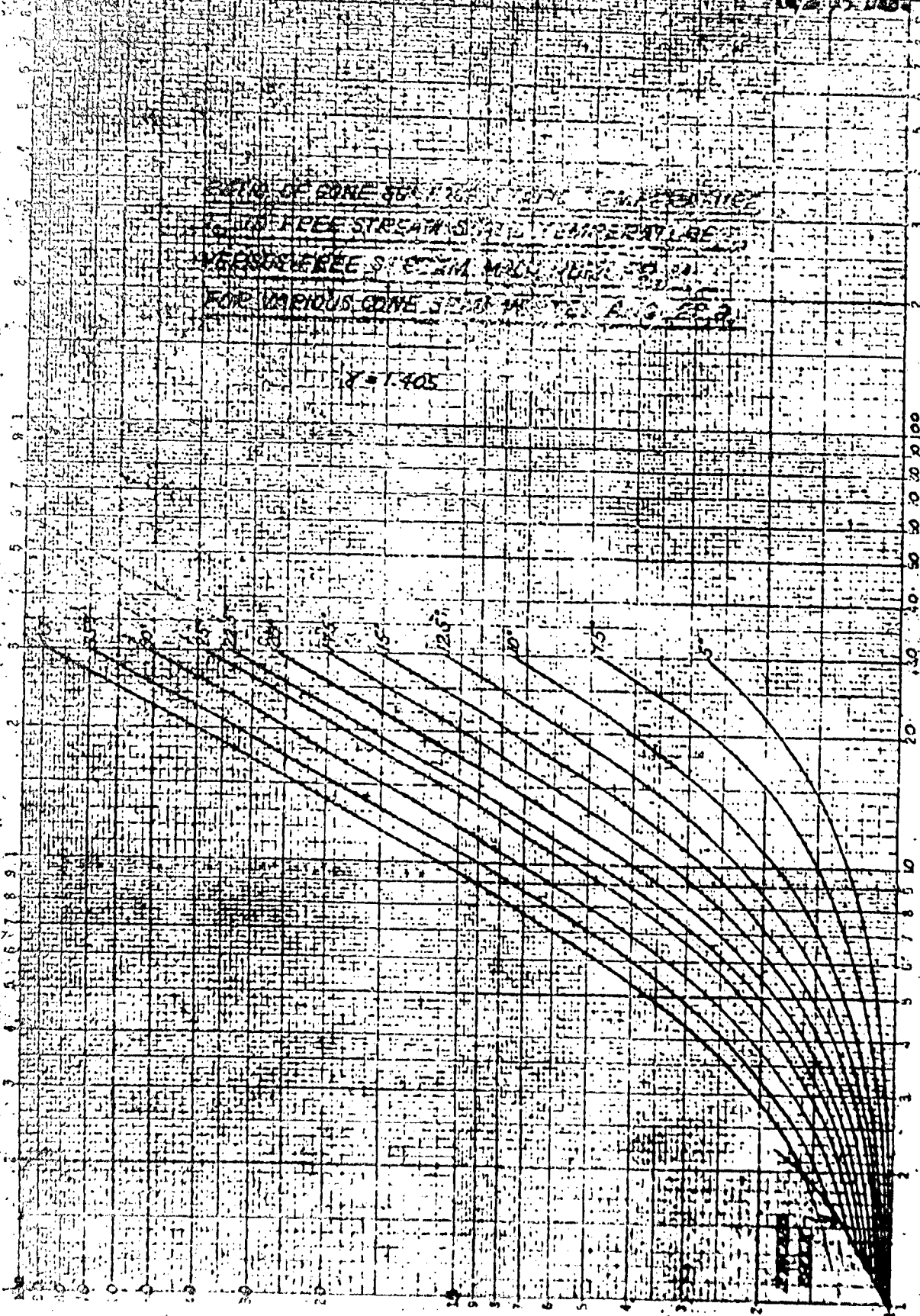
FIGURE 3.2

MACH NUMBER, M,

Pa. 52
Report No. A-Atlas-103
147-29 Dec 1976

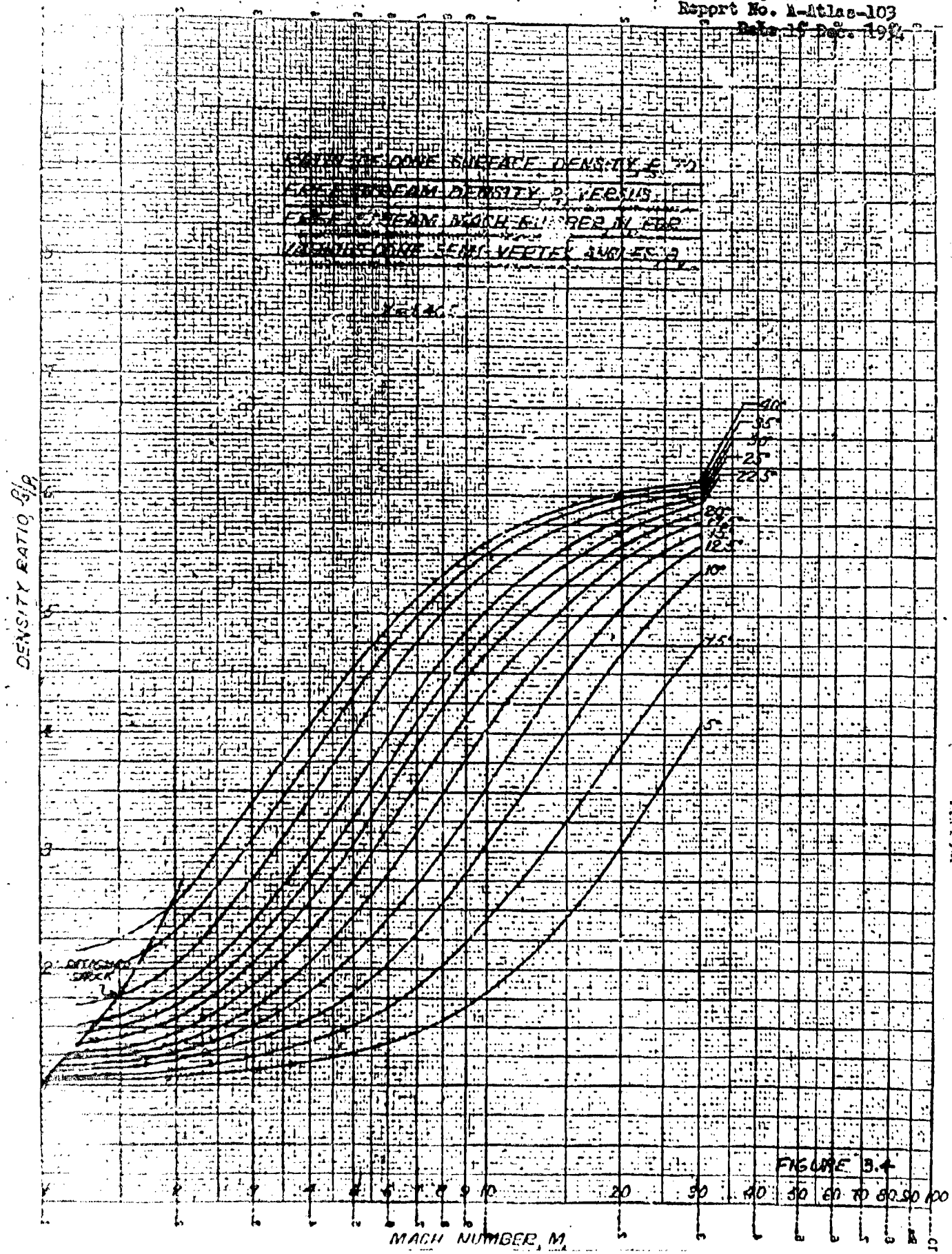
TABLE OF DOME 361126 FOR 100% EXPANSION
IN FREE STREAM IS 100% EXPANSION
HYDROGEN FREE STREAM MACH NUMBER
FOR VARIOUS DOME SPACING AND AREA RATIO

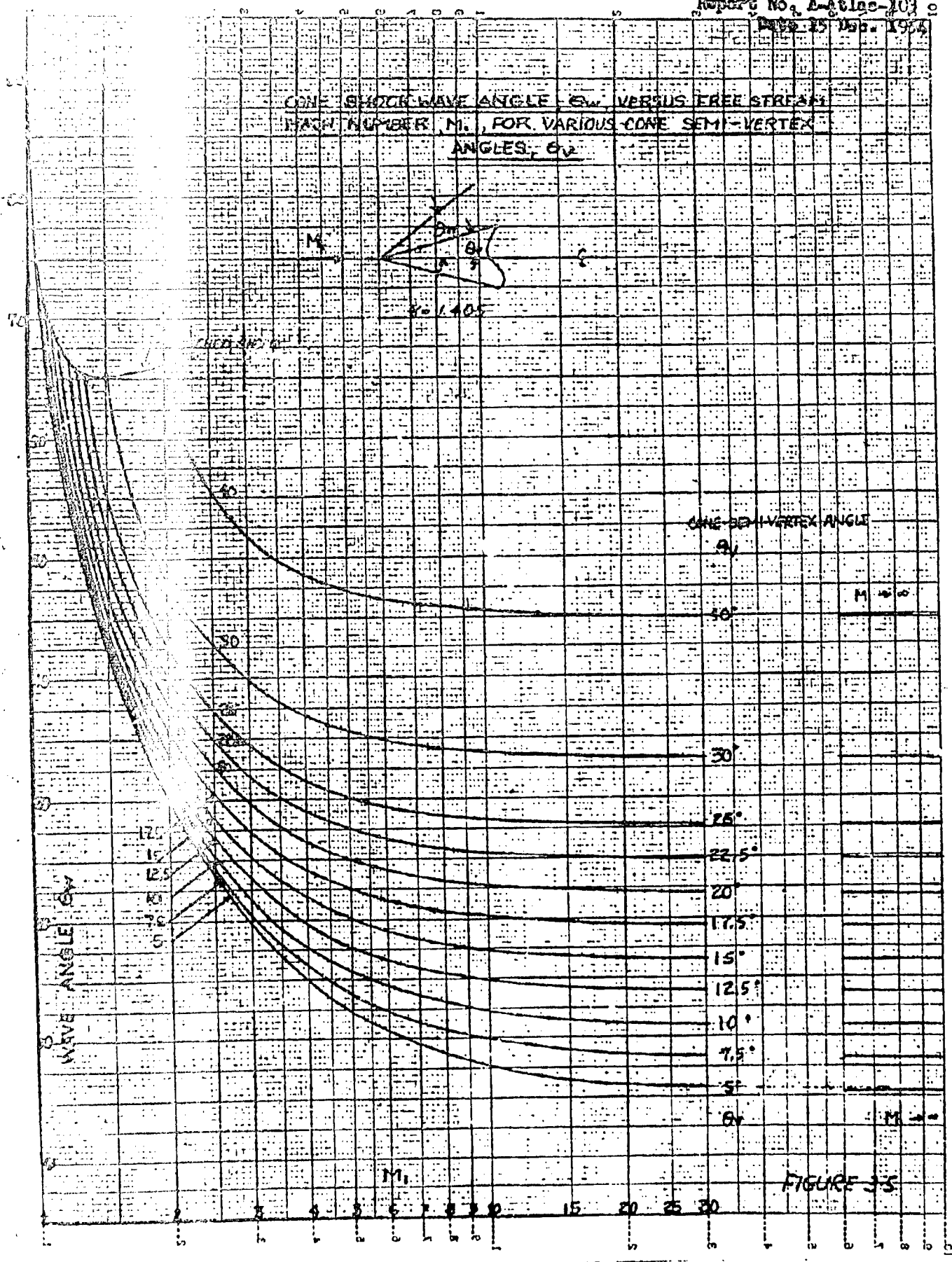
$$A = 1.405$$



STATIC TEMPERATURE RATIO, T_2/T_1

FIGURE 33





RATIO OF CONE SURFACE VELOCITY, U_s , TO
FREE STREAM VELOCITY, U_1 , VERSUS AREA
STREAM MACH NUMBER, M_1 , FOR VARIOUS
CONE SEMI-VERTEX ANGLES, θ

X2795

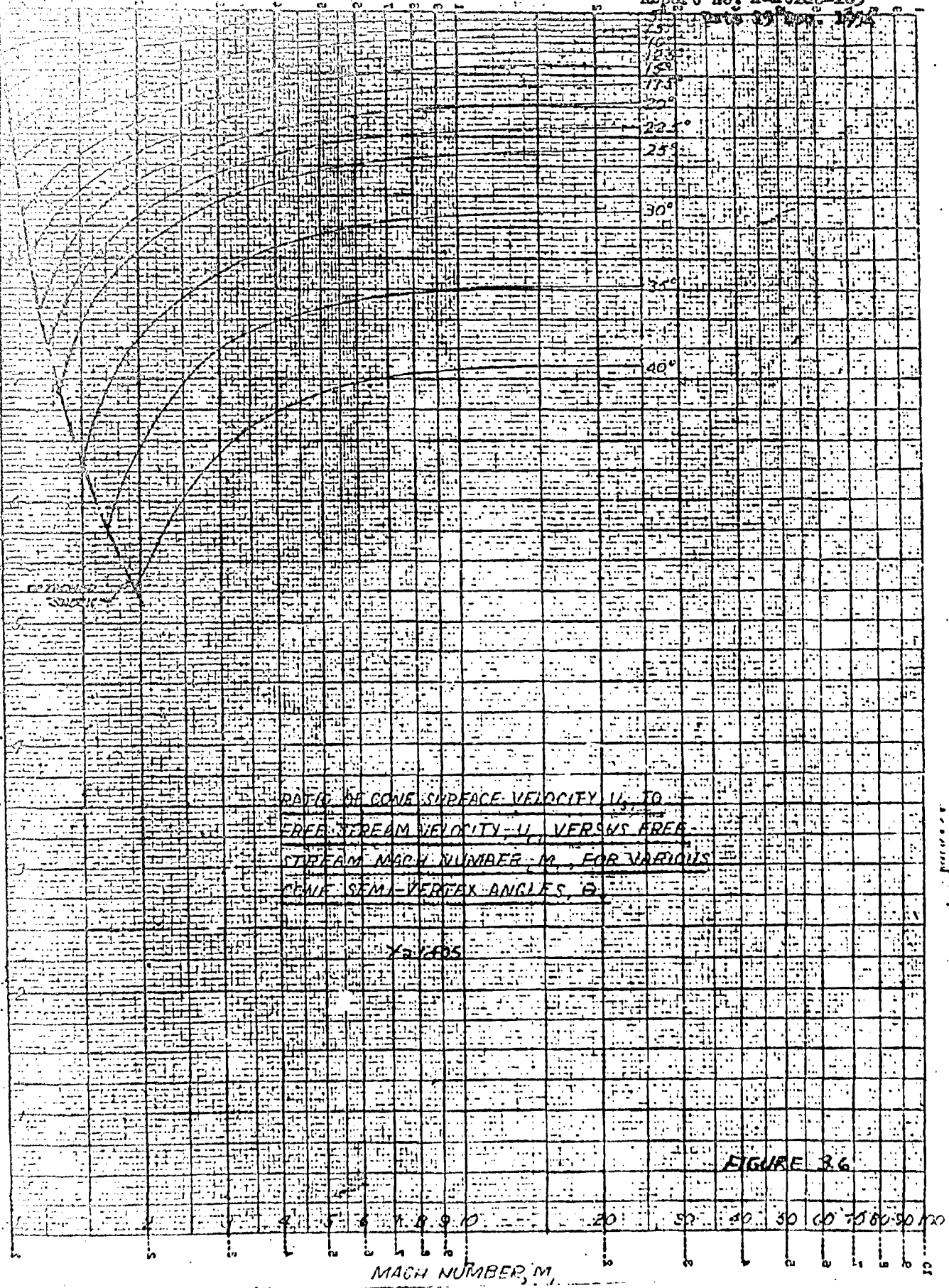
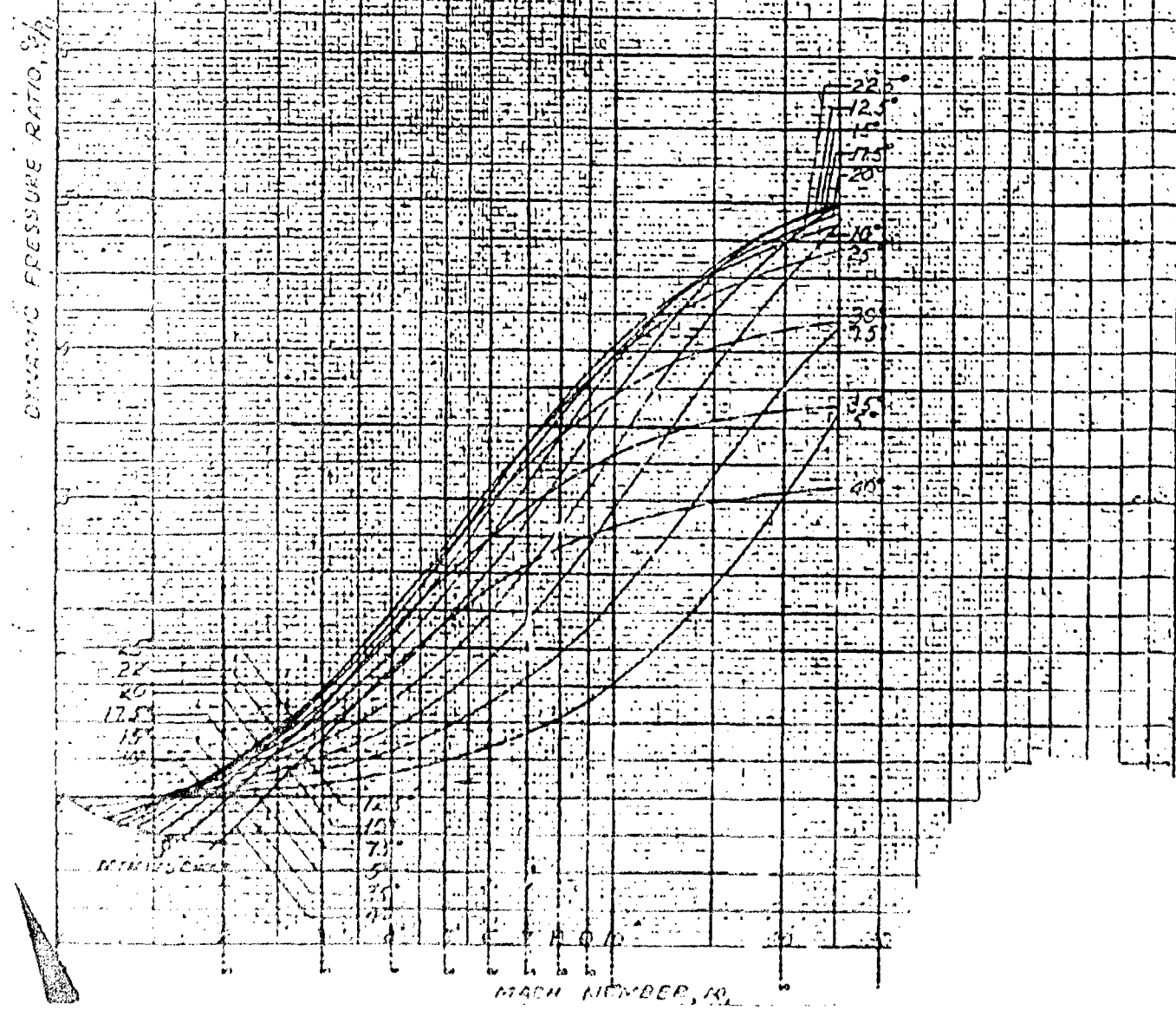
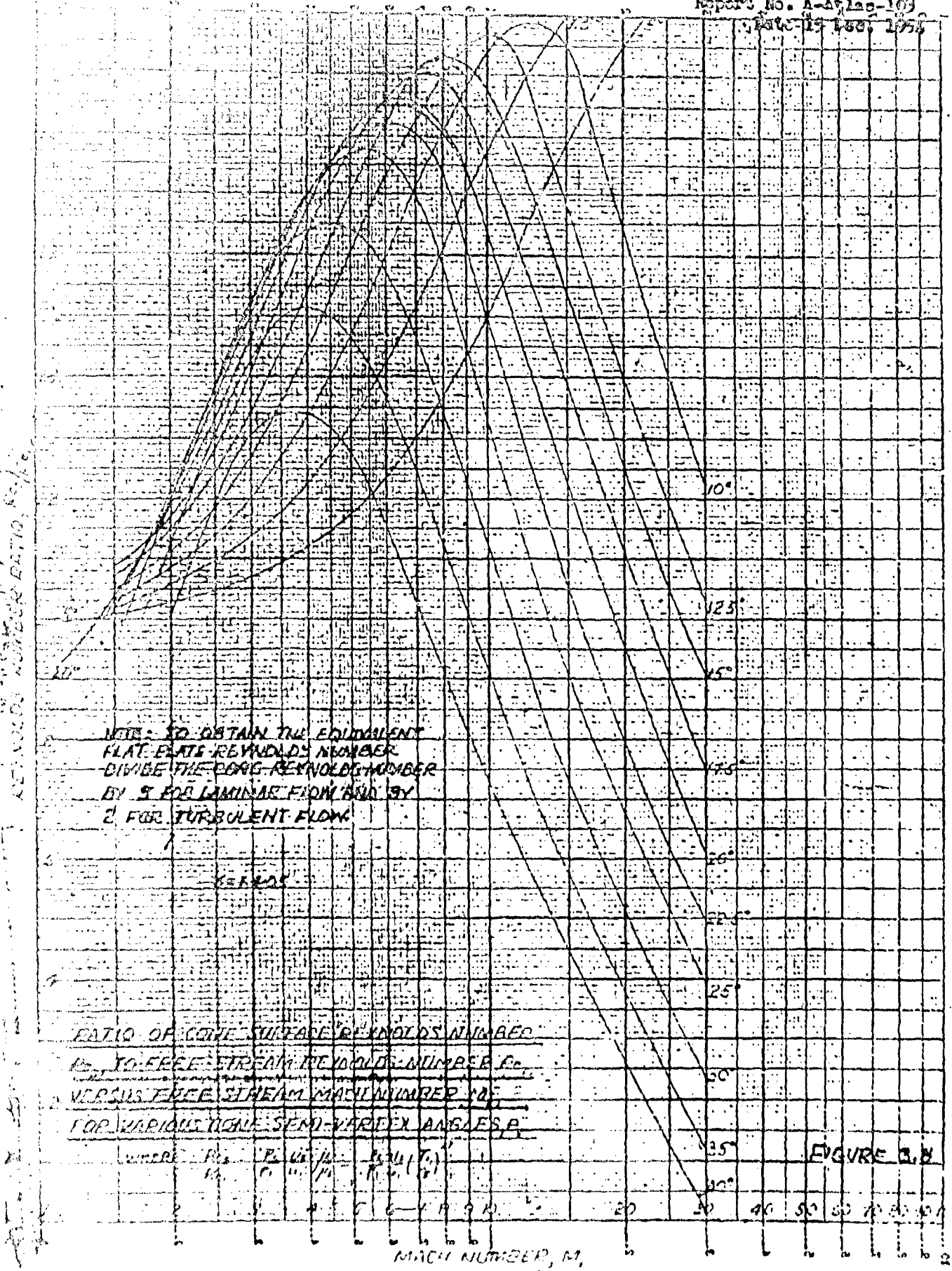
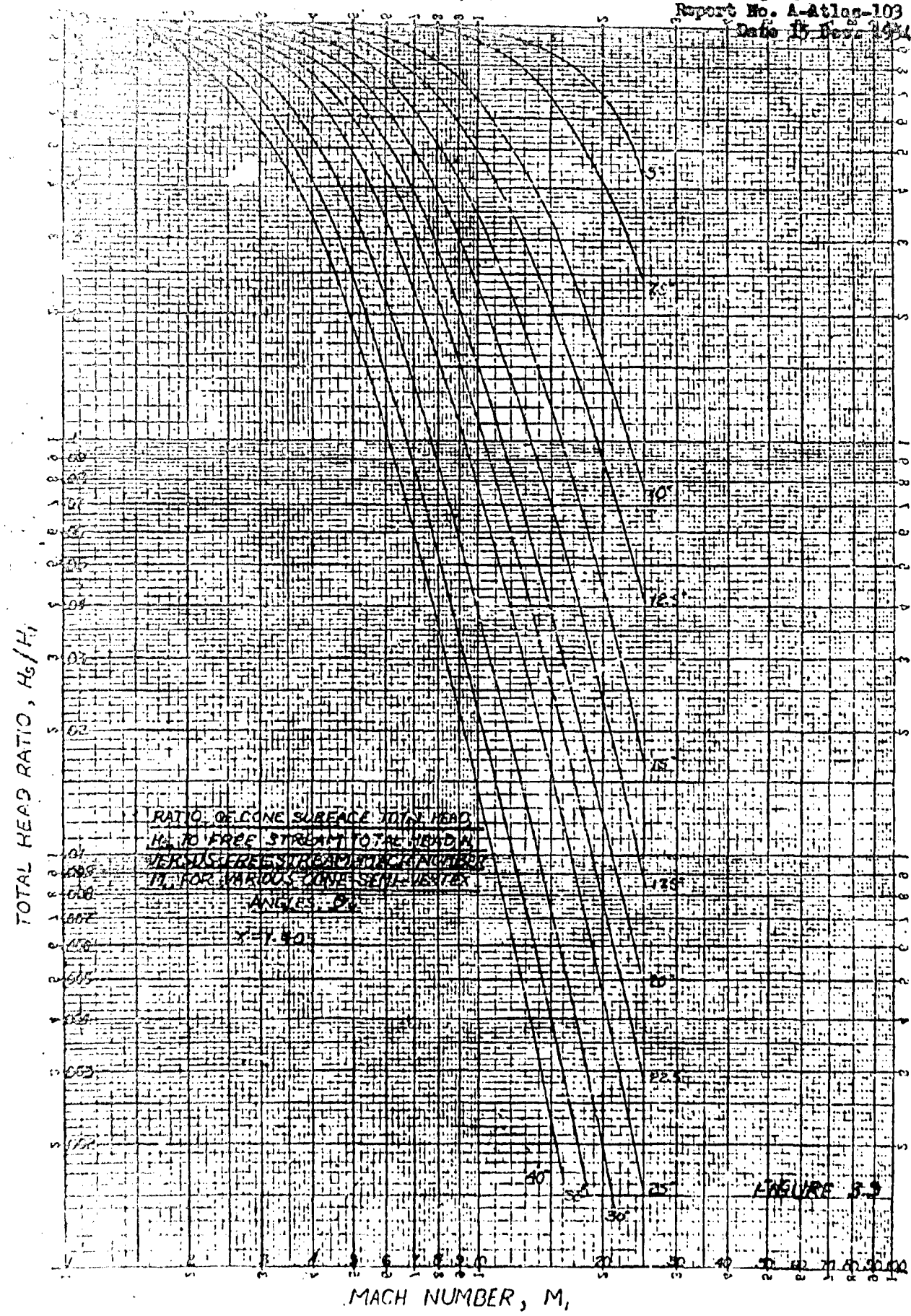


FIGURE 26

RATIO OF WING SURFACE DYNAMIC PRESSURE,
TO FREE STREAM DYNAMIC PRESSURES,
VERSUS FREE STREAM ATTACH NUMBER M,
FOR VARIOUS POINT SEMI-VERTEX ANGLES θ_v .





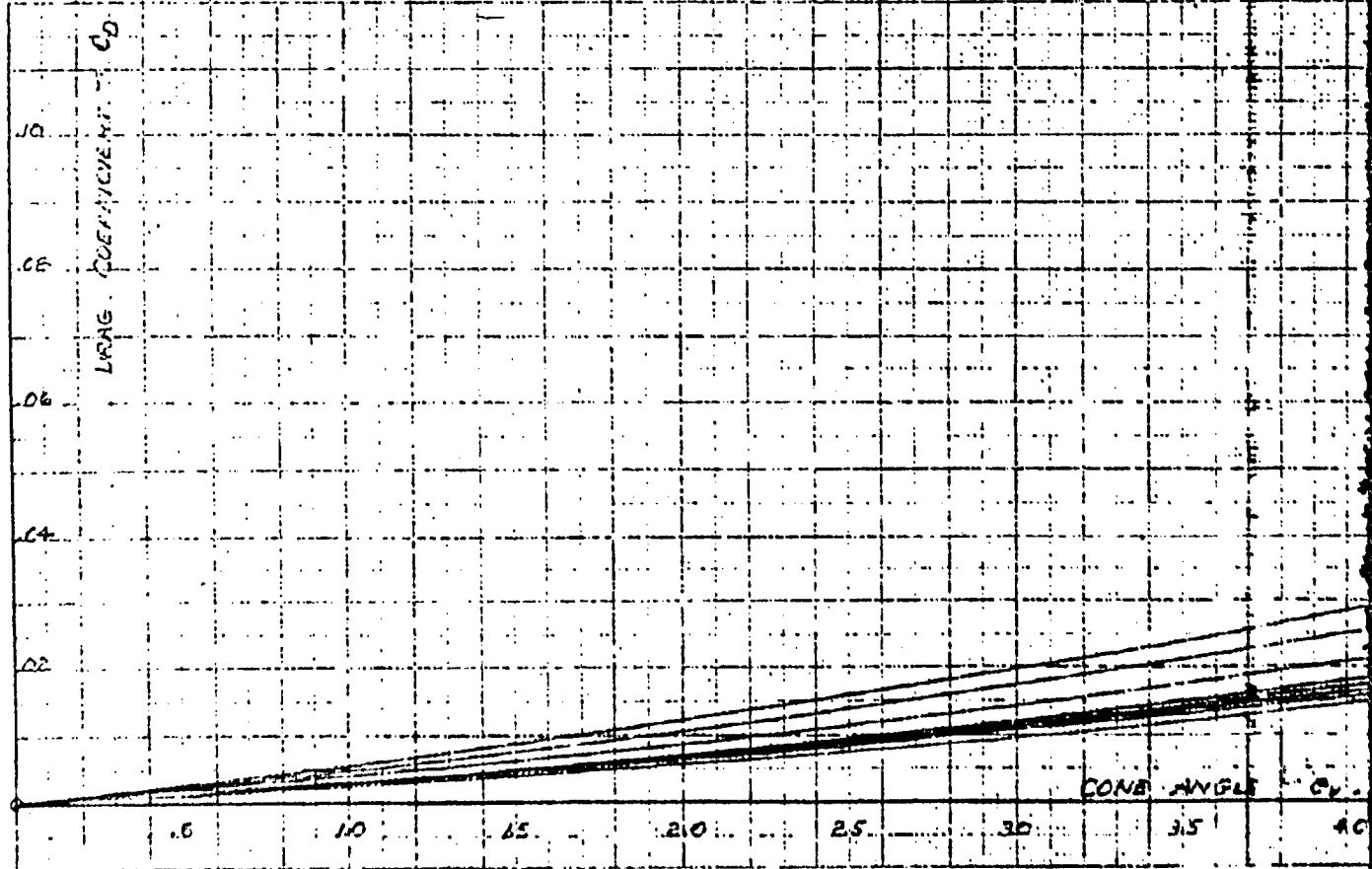


WAVE DRAG COEFFICIENT OF A CONE
VS. CONE HALF ANGLE

TAN DUE = MAX COEFFICIENT
AREA = FREE AREA OF CONE

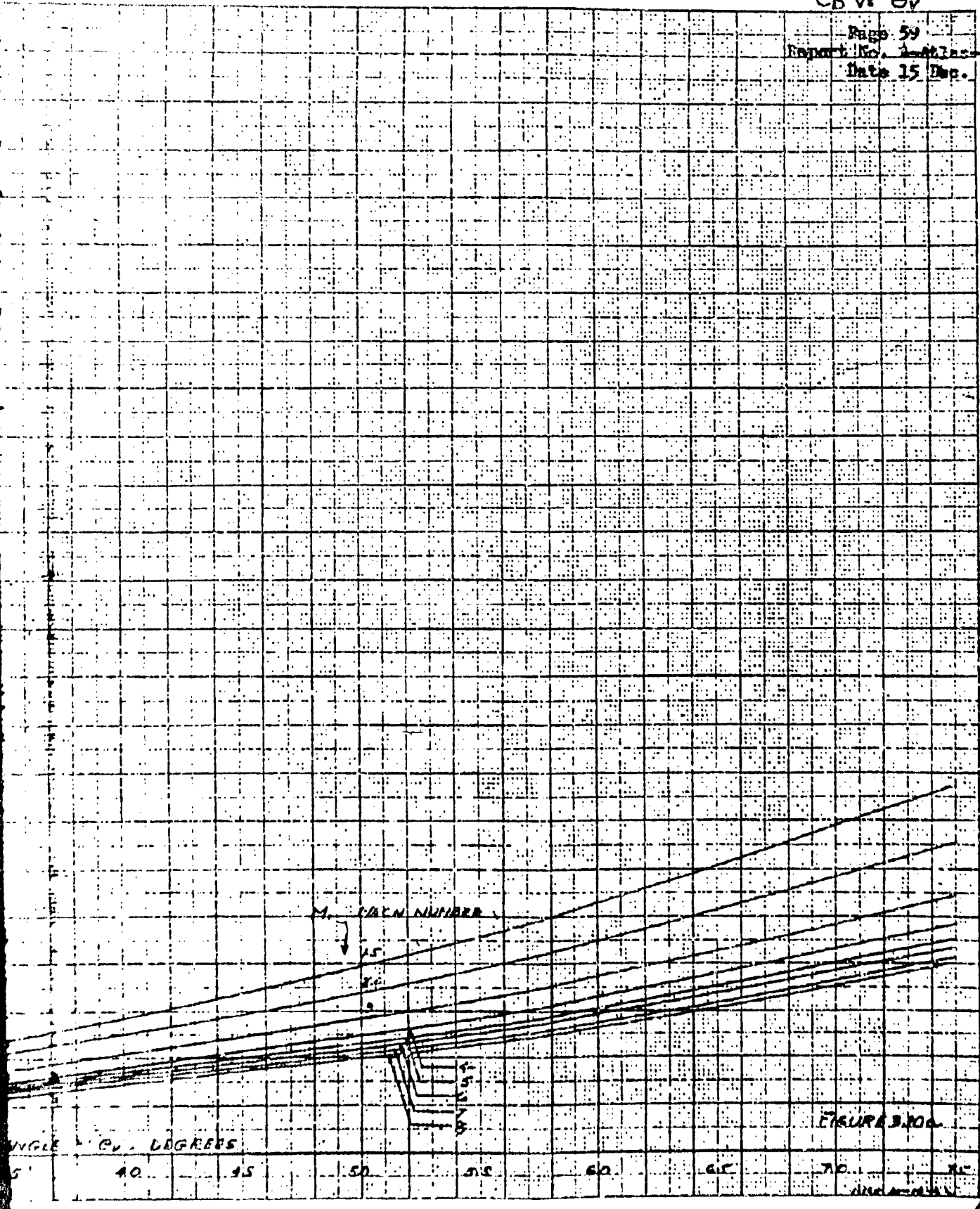
FOR MACH. NUMBERS 1.5-E.O.
 $C_D = 0 - 2.5^{\circ}$

$$\chi = 1.405$$



C_D vs θ_V

Page 59
Report No. 1-Miss-103
Date 15 Sep. 1954



B

C_D vs Θ_V

Page 59
Report No. A-627-103
Date 15 Sep. 1954

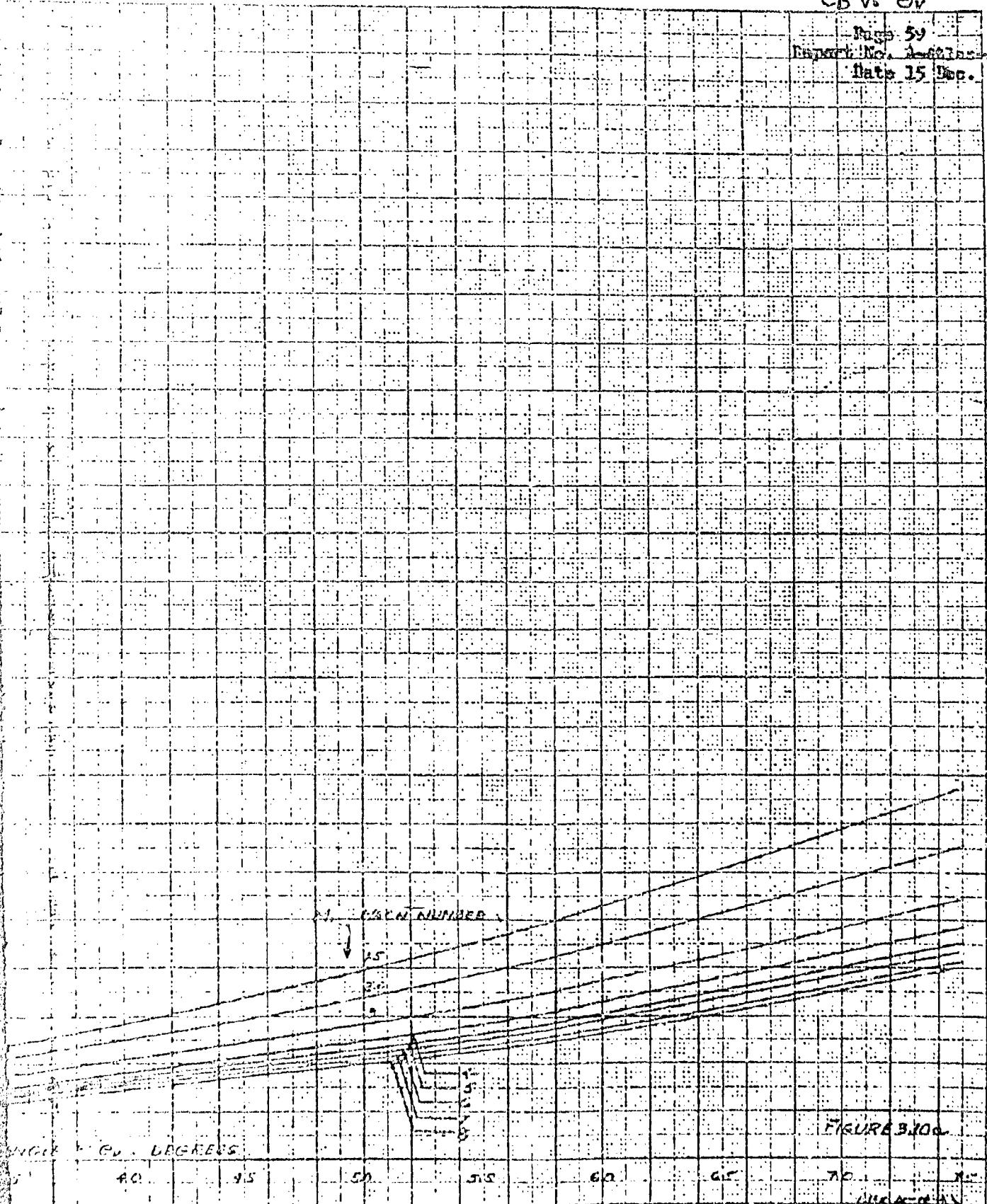


FIGURE 3.10a

B

WAVE DRAG COEFFICIENT OF A CONE
vs CONE HALF-ANGLE

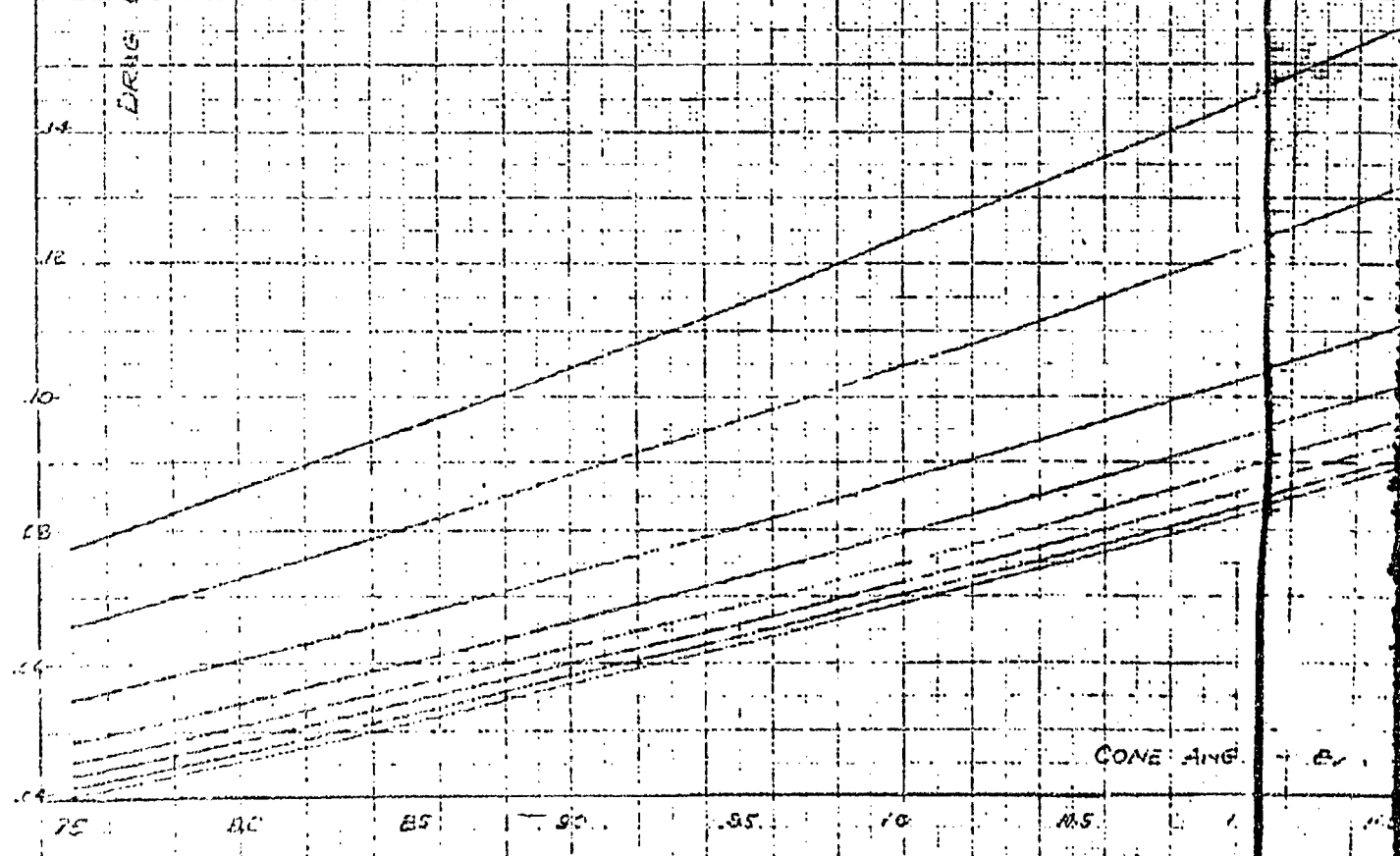
TURBULENT VALUES
BASE MACH = 1.0

FOR MACH NUMBERS 1.0-2.1

$$M_2 = 2.5^{\circ} - 1.5^{\circ}$$

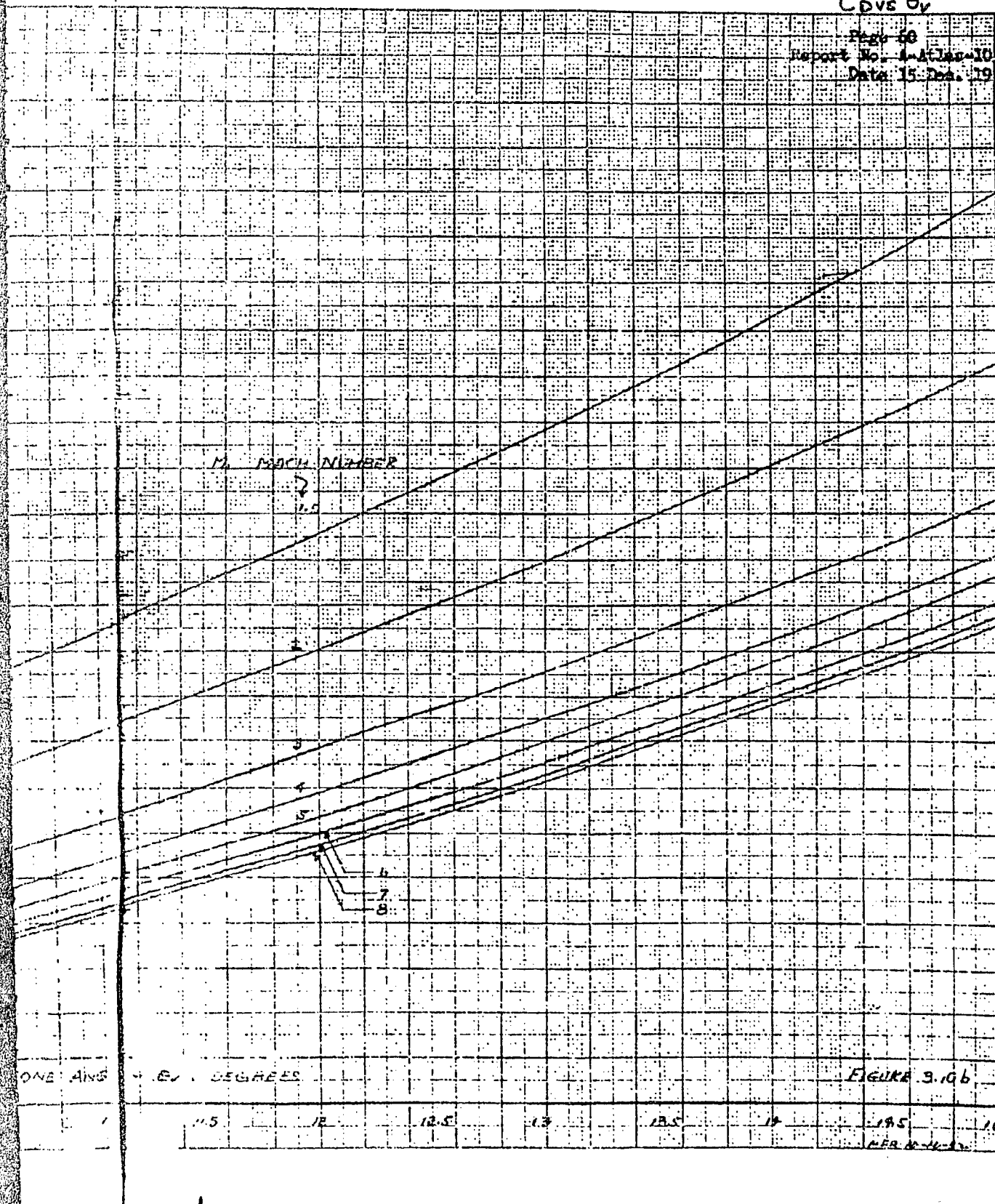
$$\delta = 1.405$$

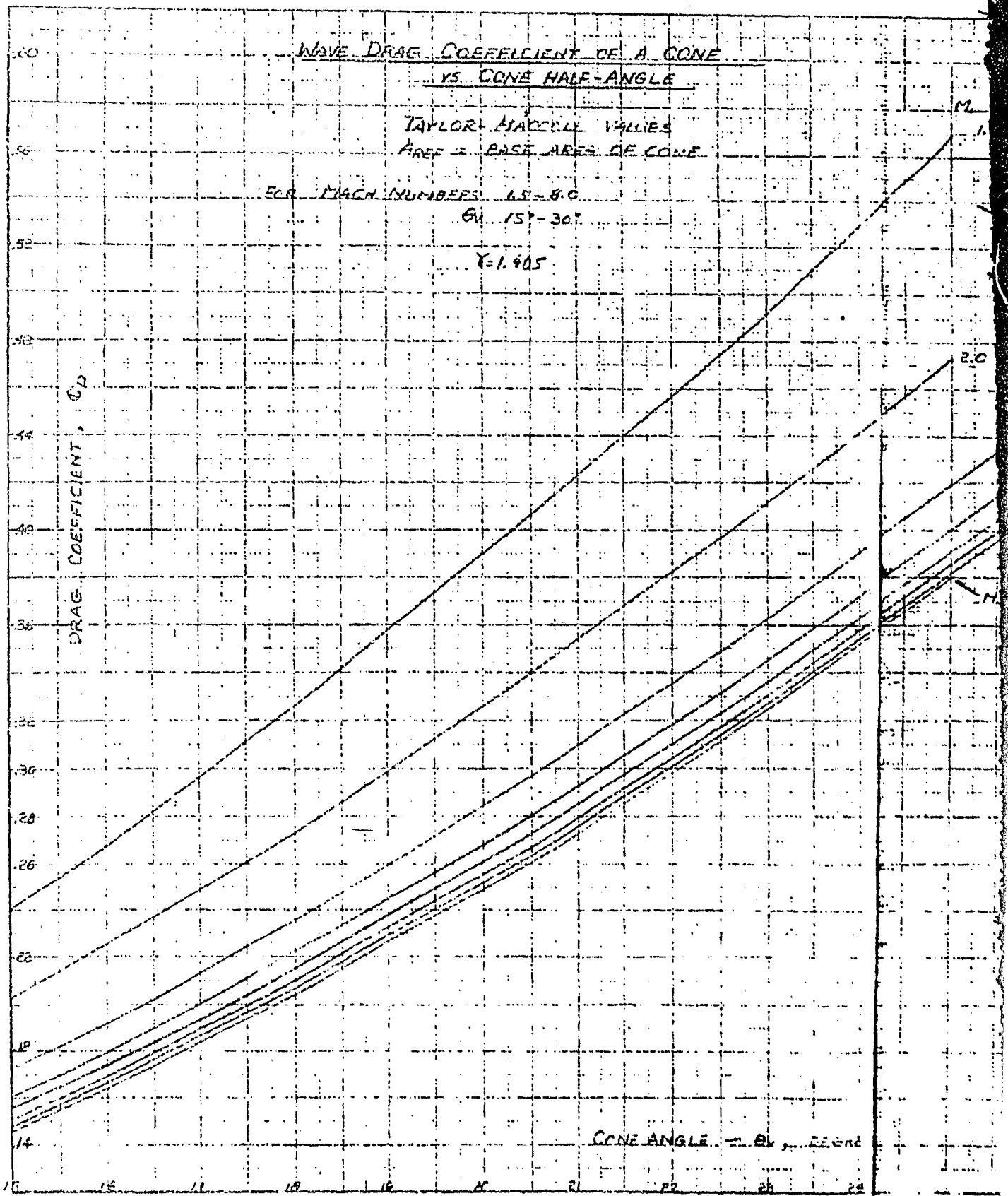
DRAG COEFFICIENT = C_D



C_D vs θ_V

Plot No. 63
Report No. A-5740-103
Date: 15 Dec. 1954





C_D vs θ_v

Page 61

Report No. A-Atlas-103
Date 15 Dec. 1954

MACH NUMBER

1.8

M →

M = 3.0

2.0

M = 3.0

FIGURE 3.10

REF - 10-20-51

B

Wave Drag Coefficient of a Cone
vs. CONE HALF-ANGLE

TAYLOR + MACCOLL VALUES.

$A_{\text{ref}} = \text{BASE AREA OF CONE}$

FR. MACH NUMBERS 10, 12.5, 15

$B_r = 0 - 2^{\circ}$

$\delta = 1.405$

WAVE COEFFICIENT OF CONE

.16

.14

.12

.10

.08

.06

.04

.02

0

0 1 2 3 4 5 6 7 8 9 10

✓

$C_D = \theta$

Page 62

Report No. 4-M-103

Date 15 Dec. 1954

AT CRITICAL NUMBER

10
12.5
15

$M = \infty$

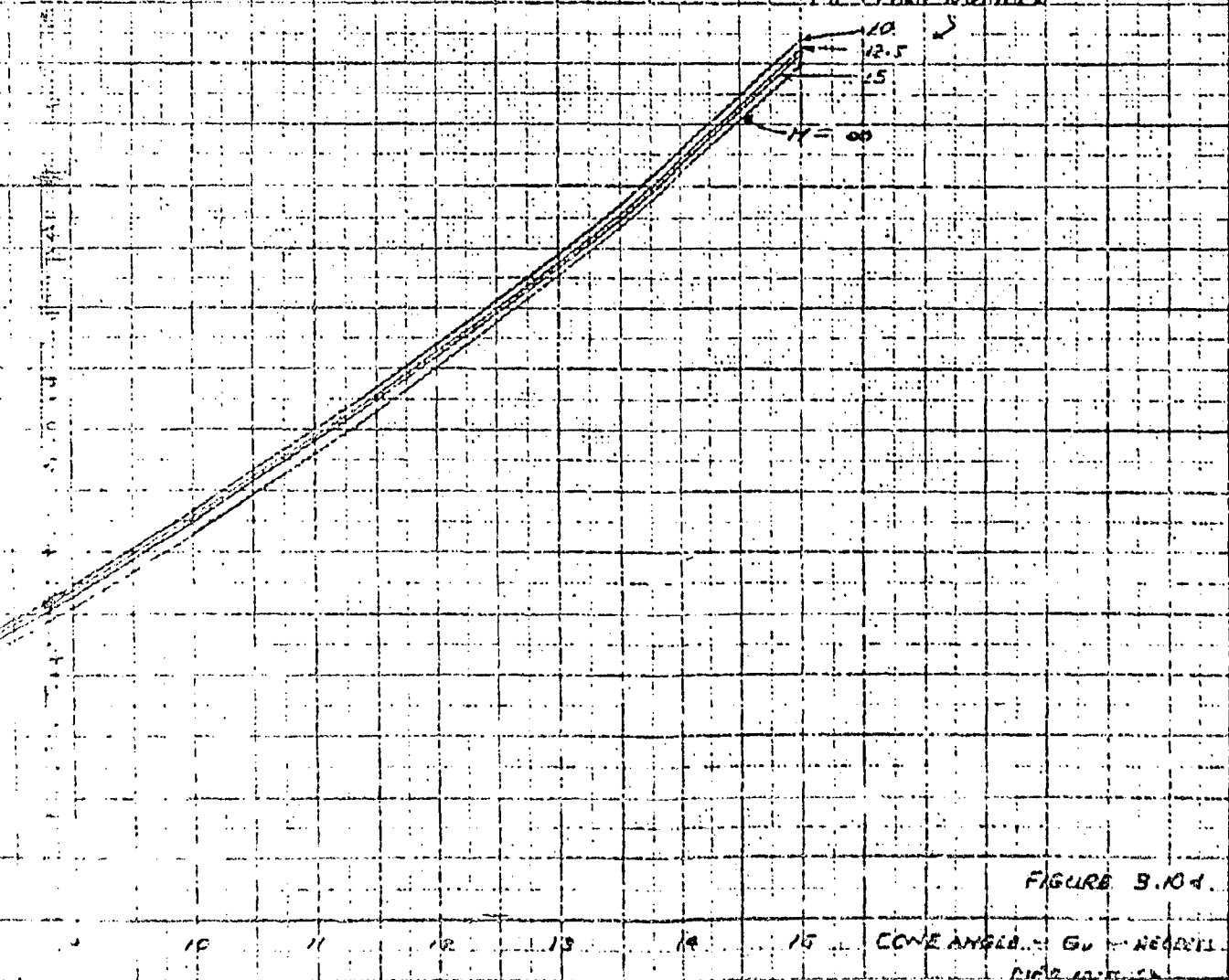


FIGURE B.10d.

cone angle - Gu - Nederl.
crit. number

B

INITIAL AXIAL FORCE COEFFICIENT / SIN FOR CONES

C_x = AXIAL FORCE COEFFICIENT (CONE BASE AREA =

θ_v = CONE SEMI-VERTEX ANGLE (DEGREES)

α = ANGLE OF ATTACK (RADIAN)

$$\alpha = 1.405$$

INITIAL AXIAL FORCE COEFFICIENT / SIN θ_v

5

4

3

2

1

θ_v :
5°

7.5°

10°

12.5°

15°

20°

25°

30°

35°

40°

1 2 3 4 5 6 7 8 9 10

MACH NUMBER

C_x vs M_1

Page 63
Report No. A-Milan-03
Date 15 Dec. 1954

ELEMENT SIN²θ VS MACH NUMBER

(REFERENCE AREA)

(DEGREES)

VS

NOTE: $C_{x_{\alpha=0}} / \sin^2 \theta = 2.0$ FOR NEWTONIAN
FLOW

$C_{x_{\alpha=0}} / \sin^2 \theta = 2.091$
 $M_1 = 0$

9 10 11 12 13 14 15 16 17 18 19

NUMBER

FIGURE 3.11

FJD
5-22-55

R

INITIAL NORMAL FORCE COEFFICIENT SLOPE / COS²θ

FOR CONES

2.1

C_N = NORMAL FORCE COEFFICIENT (CONE BASE AREA = R^2)

θ_v = CONE SEMI-VERTEX ANGLE (DEGREES)

α = ANGLE OF ATTACK (RADIAN)

$$\alpha = 1.405$$

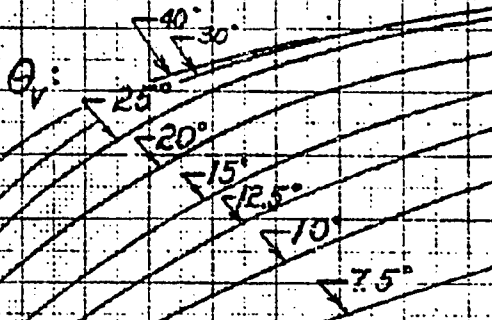
INITIAL NORMAL FORCE COEFFICIENT SLOPE / COS²θ

2.0

1.9

1.8

1.7



MACH NUMBER

$$\left(\frac{dC_n}{dx}\right)_{x=0} / \cos^2 \theta_v \text{ vs } M_1$$

$\sqrt{\cos \theta_v}$ vs MACH NUMBER

Page 4
Report No. A-3100-1
Date 15 Feb. 1958

PASE AREA = REFERENCE AREA)

(ES)

$$\left[\left(\frac{dC_n}{dx}\right)_{x=0}\right] / \cos^2 \theta_v = 2.037 \quad M=0$$

$$\text{NOTE: } \left(\frac{dC_n}{dx}\right)_{x=0} / \cos^2 \theta_v = 2.0$$

FOR NEWTONIAN FLOW



FIGURE 3.12

FID
53355

B

ADDITIONAL AXIAL FORCE COEFFICIENT DUE TO ANGLE OF
FOR CONES FOR $\alpha \leq 90^\circ$

C_x = AXIAL FORCE COEFFICIENT (CONE BASE AREA = REFERENCE AREA)

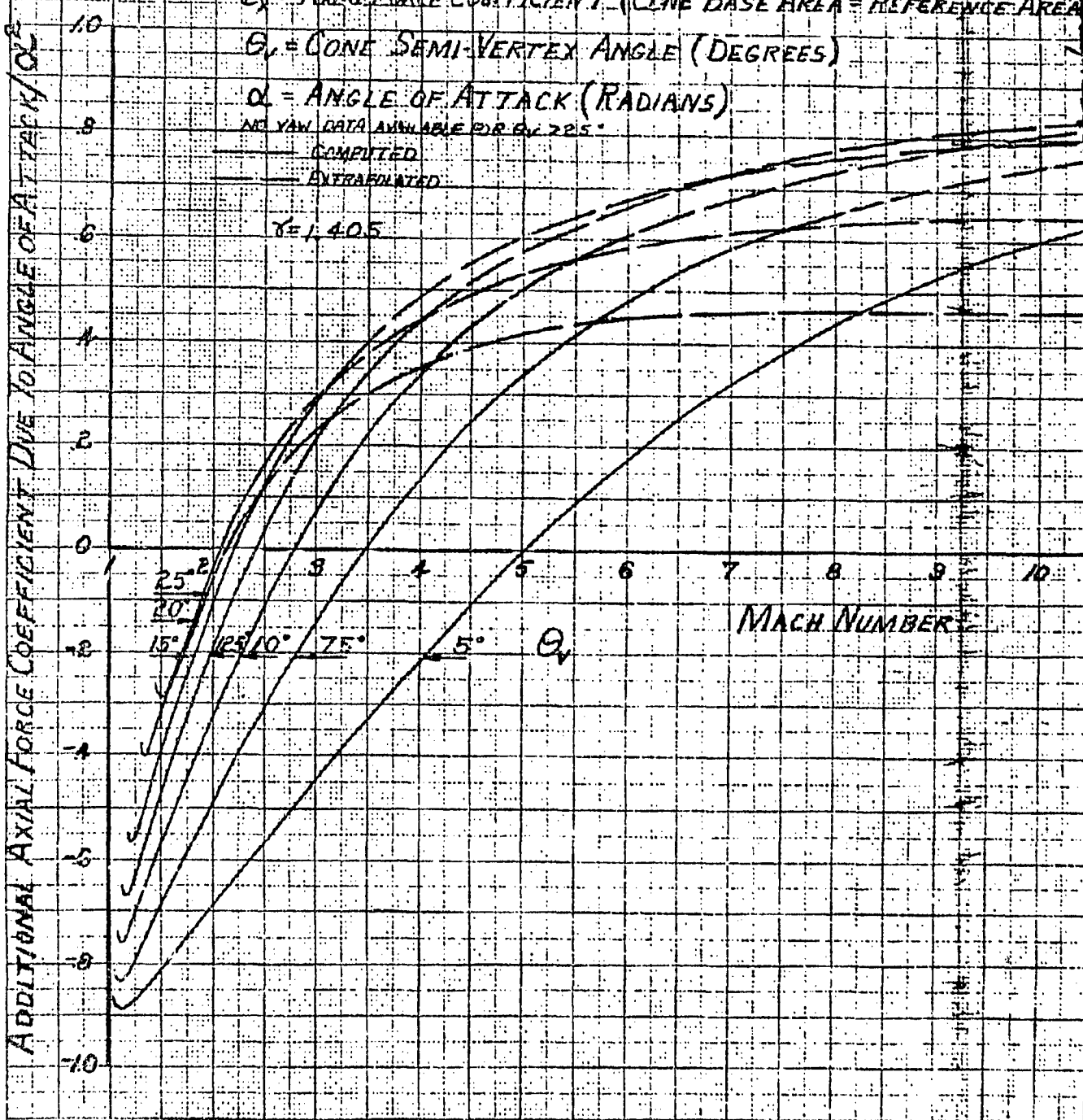
Θ_v = CONE SEMI-VERTEX ANGLE (DEGREES)

α = ANGLE OF ATTACK (RADIAN)

ALL YAN DATA AVAILABLE P.R.E. 225

~~COMPILED~~

~~AMERICANIZED~~



$\Delta C_x / \alpha^2$ vs M_1

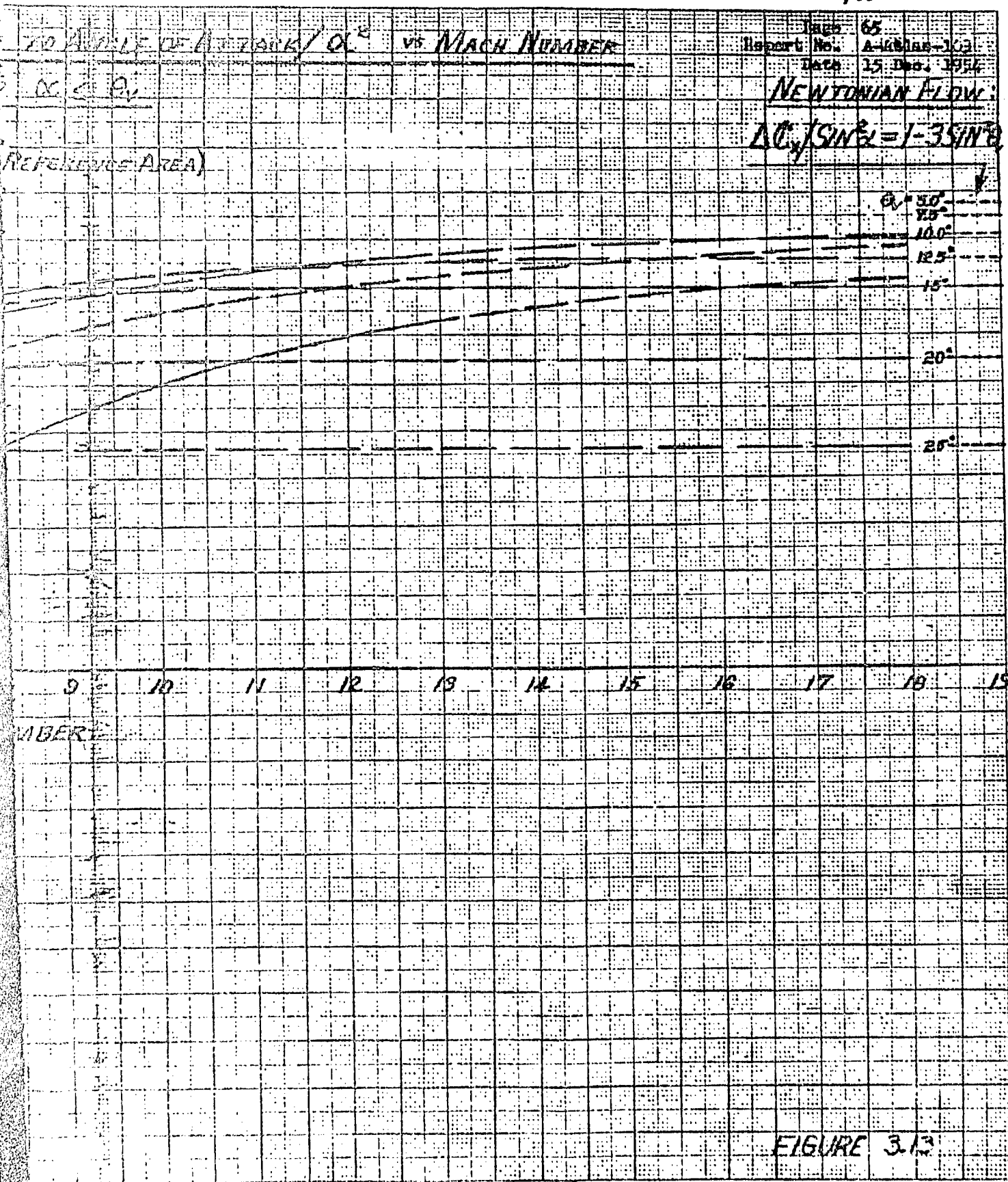


FIGURE 3.13

B

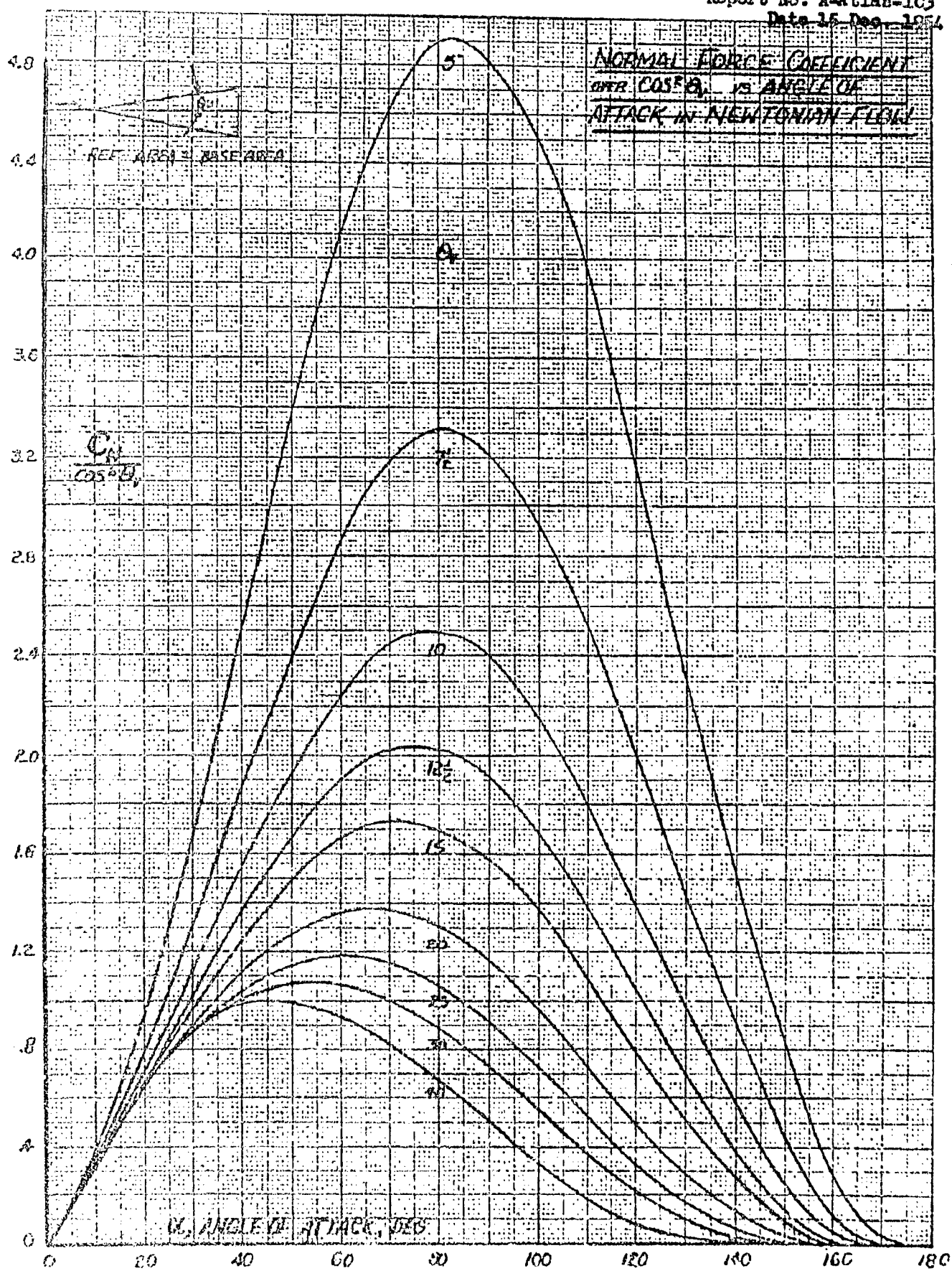


FIGURE 3.14

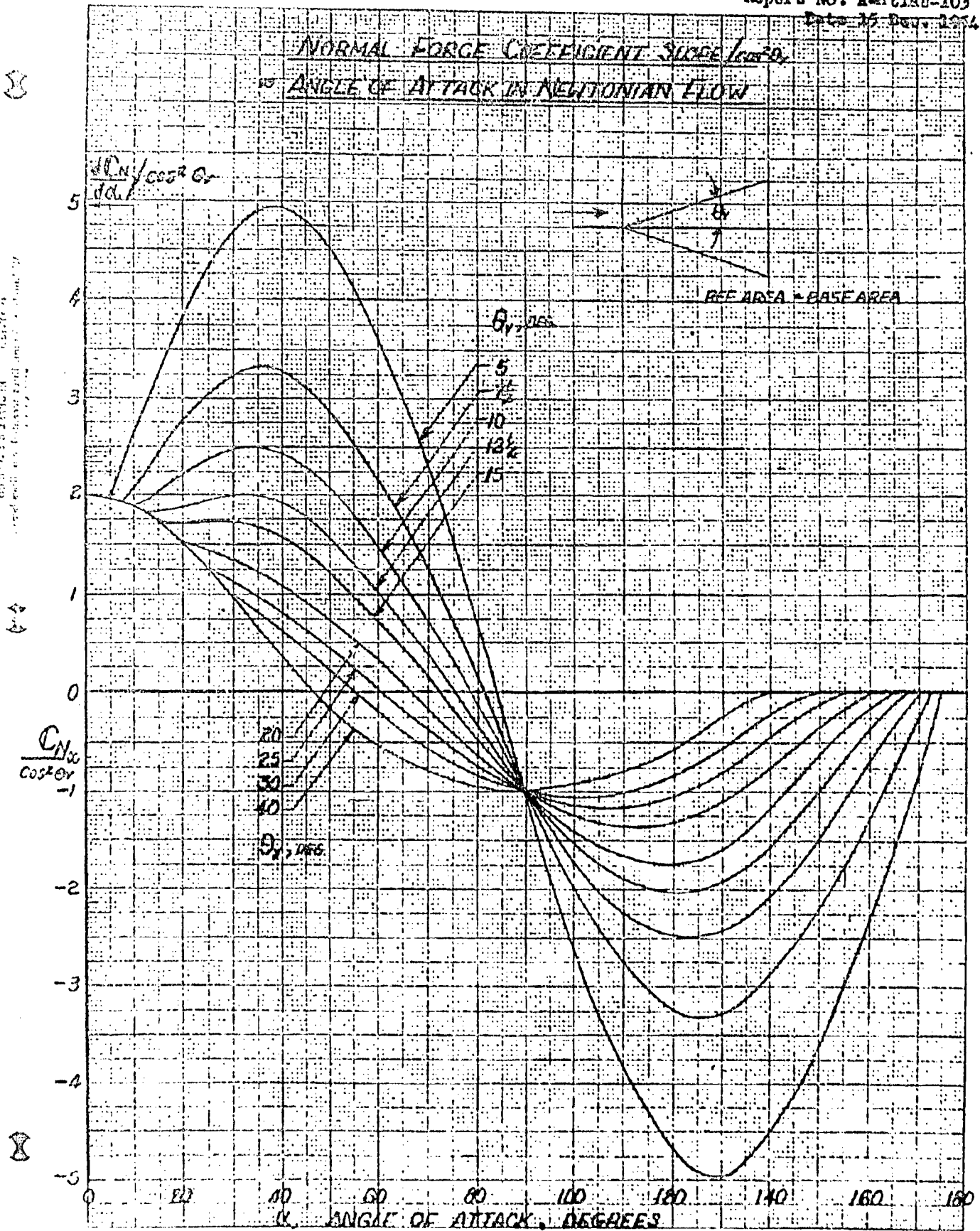


FIGURE 3.15

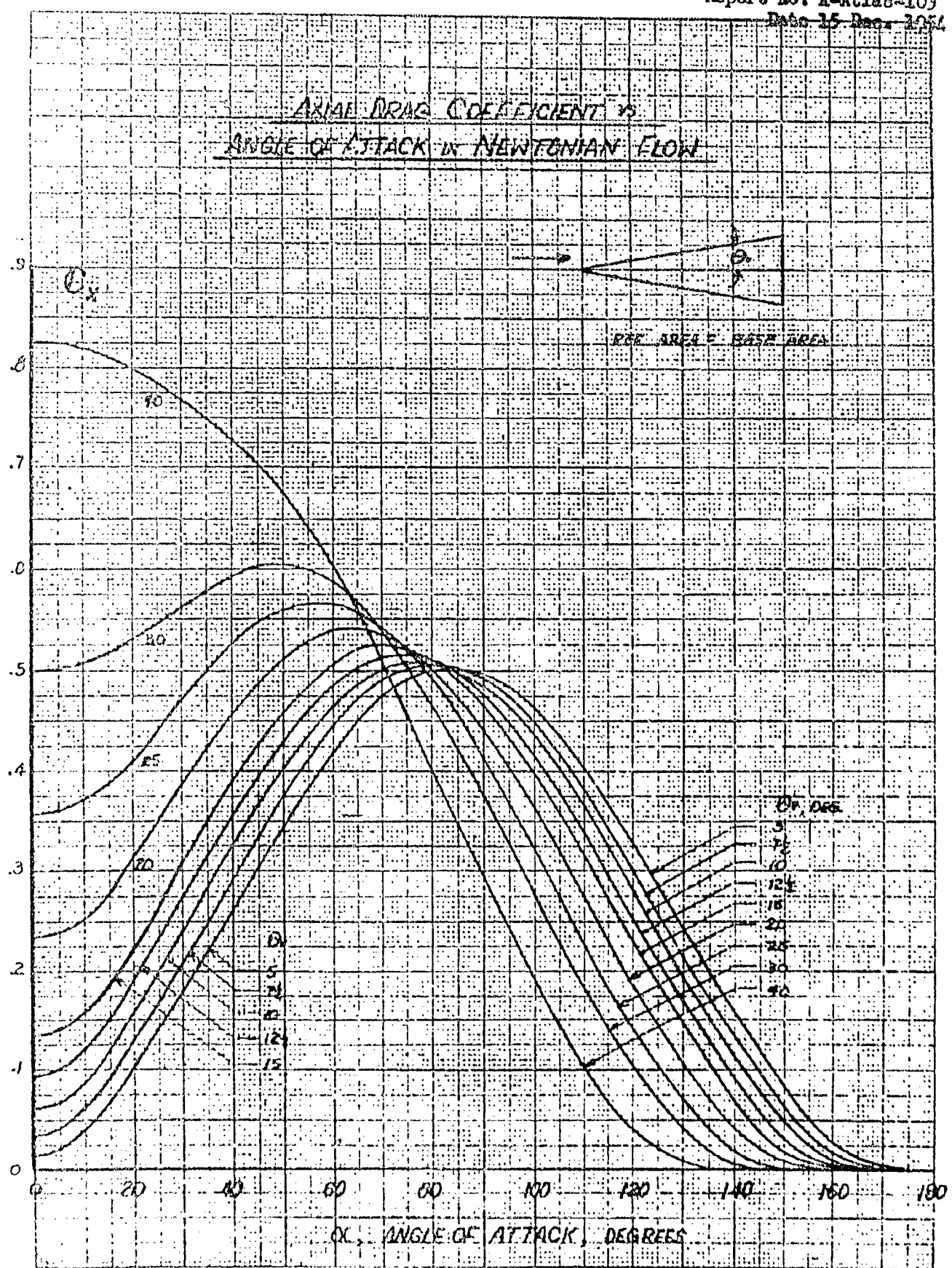
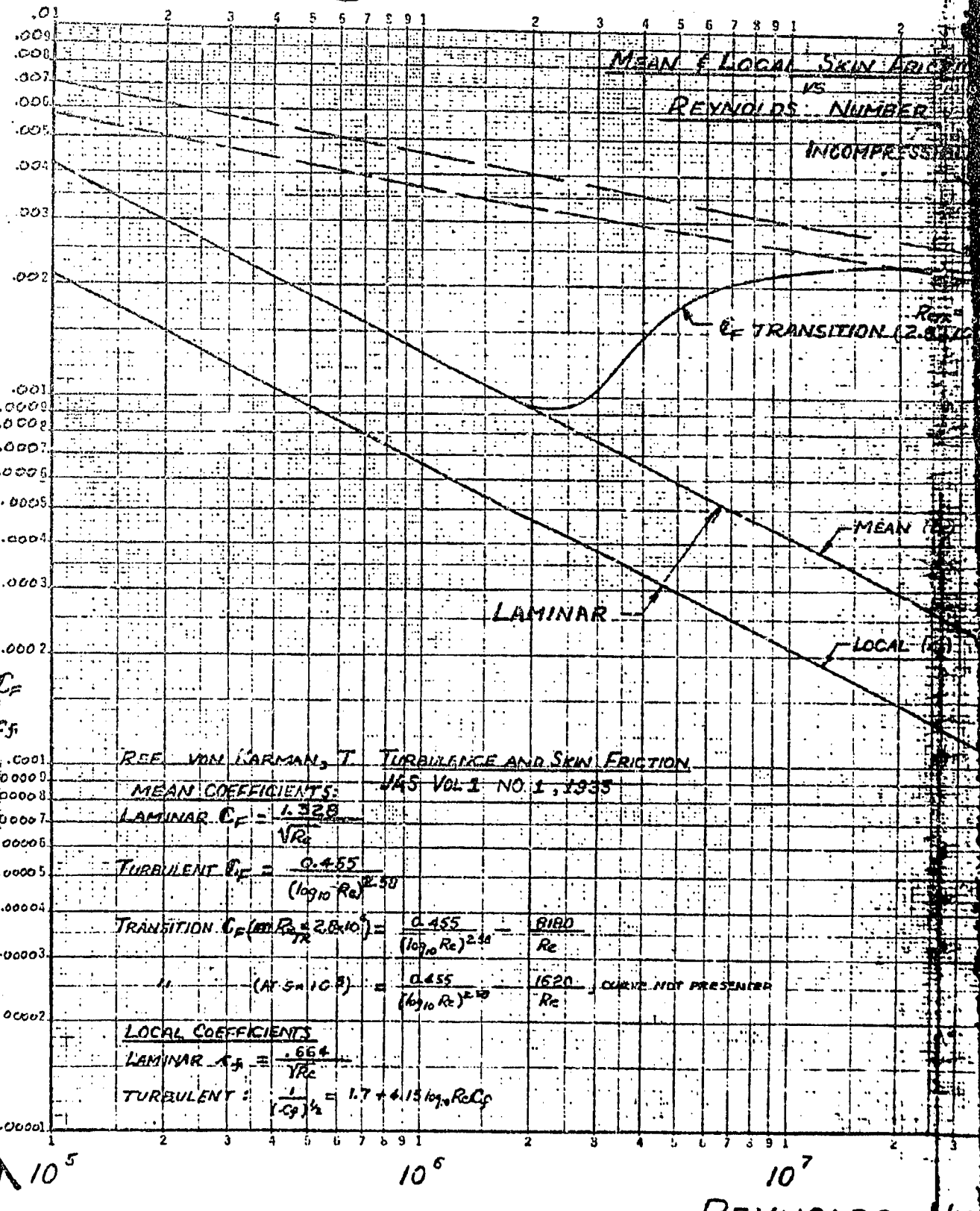
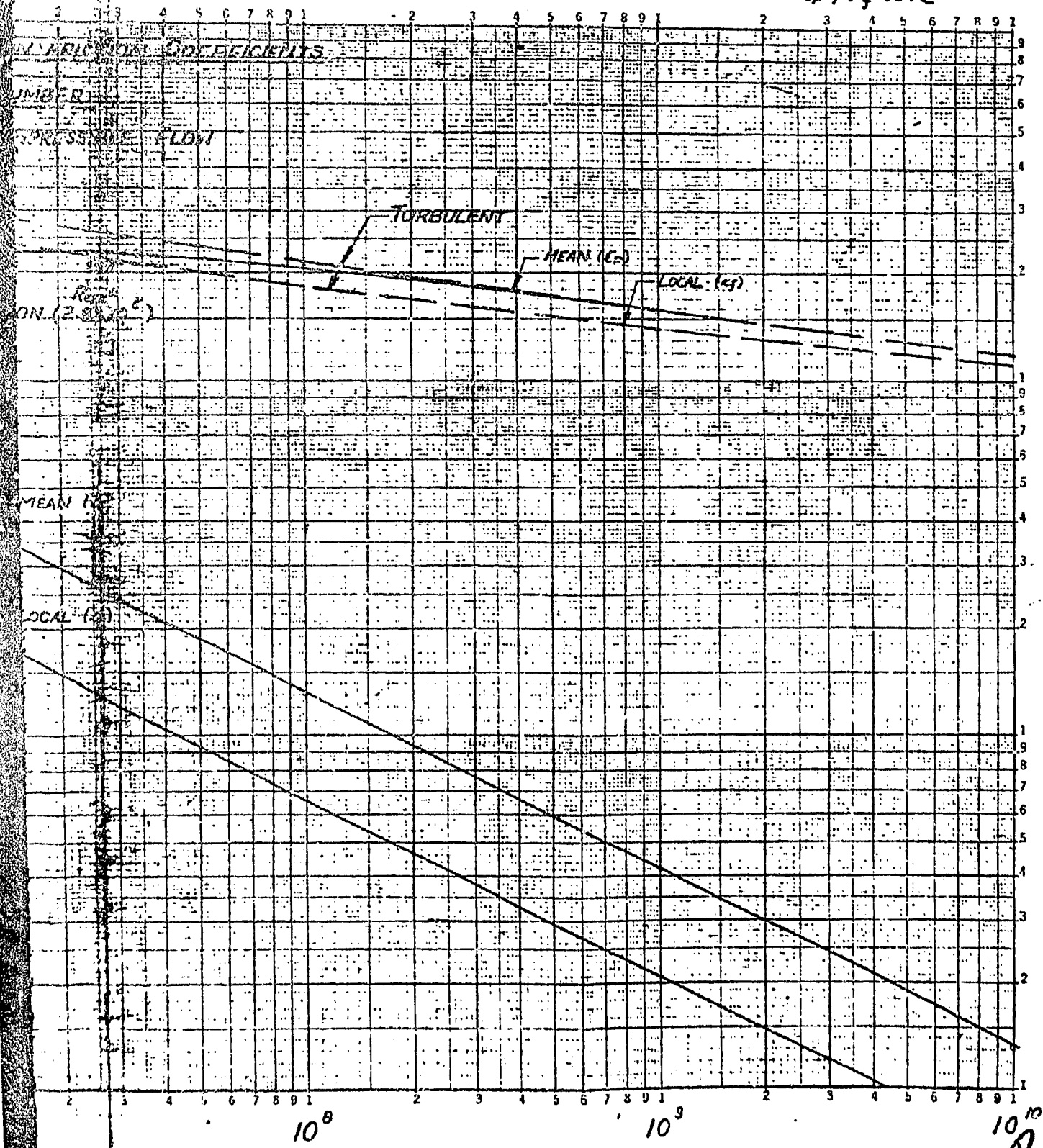


FIGURE 3.16



Report No. A-Atlas-103
Date 15 Dec. 1954

C_f & k_f vs Re



REYNOLDS NUMBER, Re

FIGURE 4.1

B

Page 70
Report No. A-Atlas-103
Date 13 Dec 1954

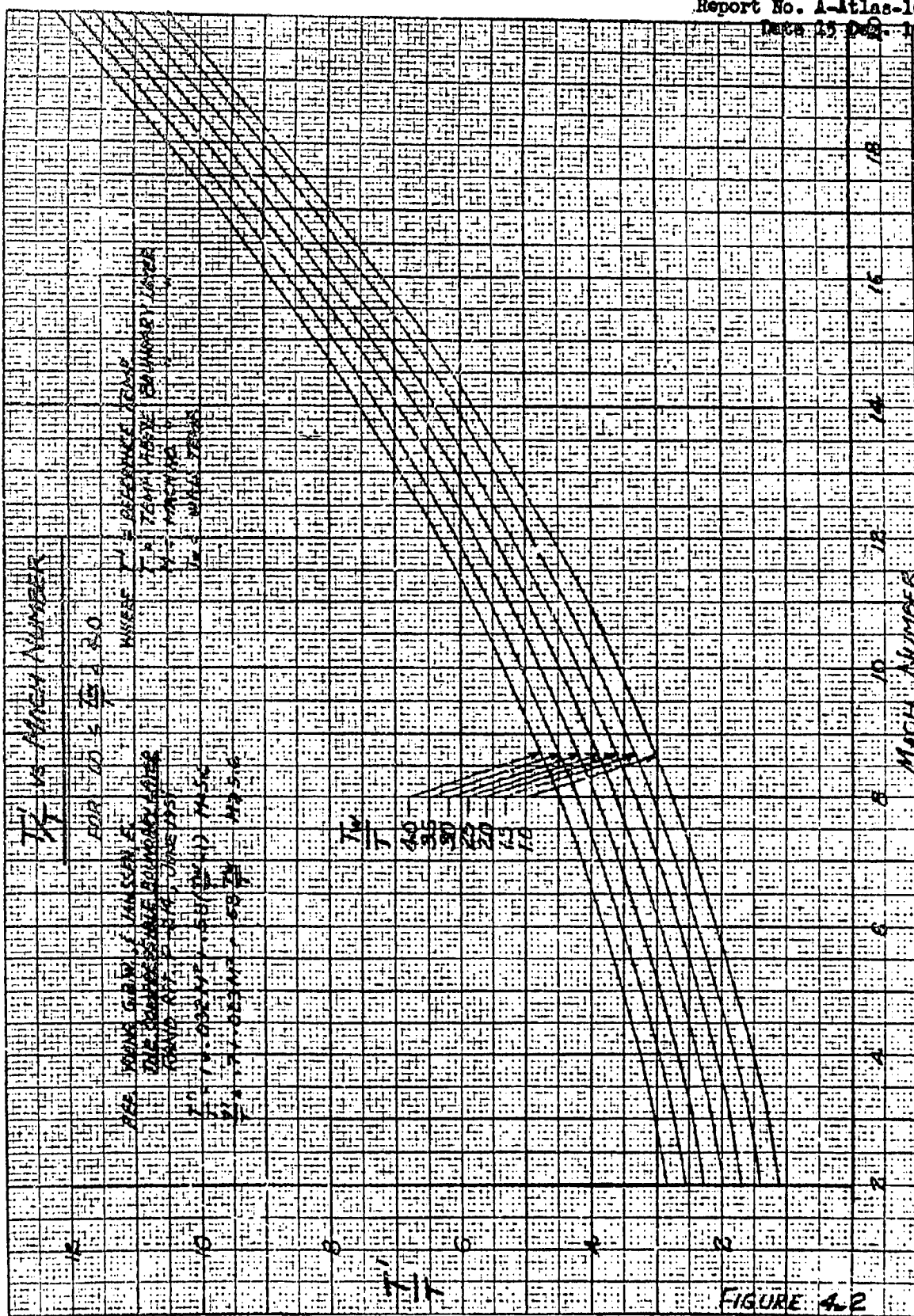
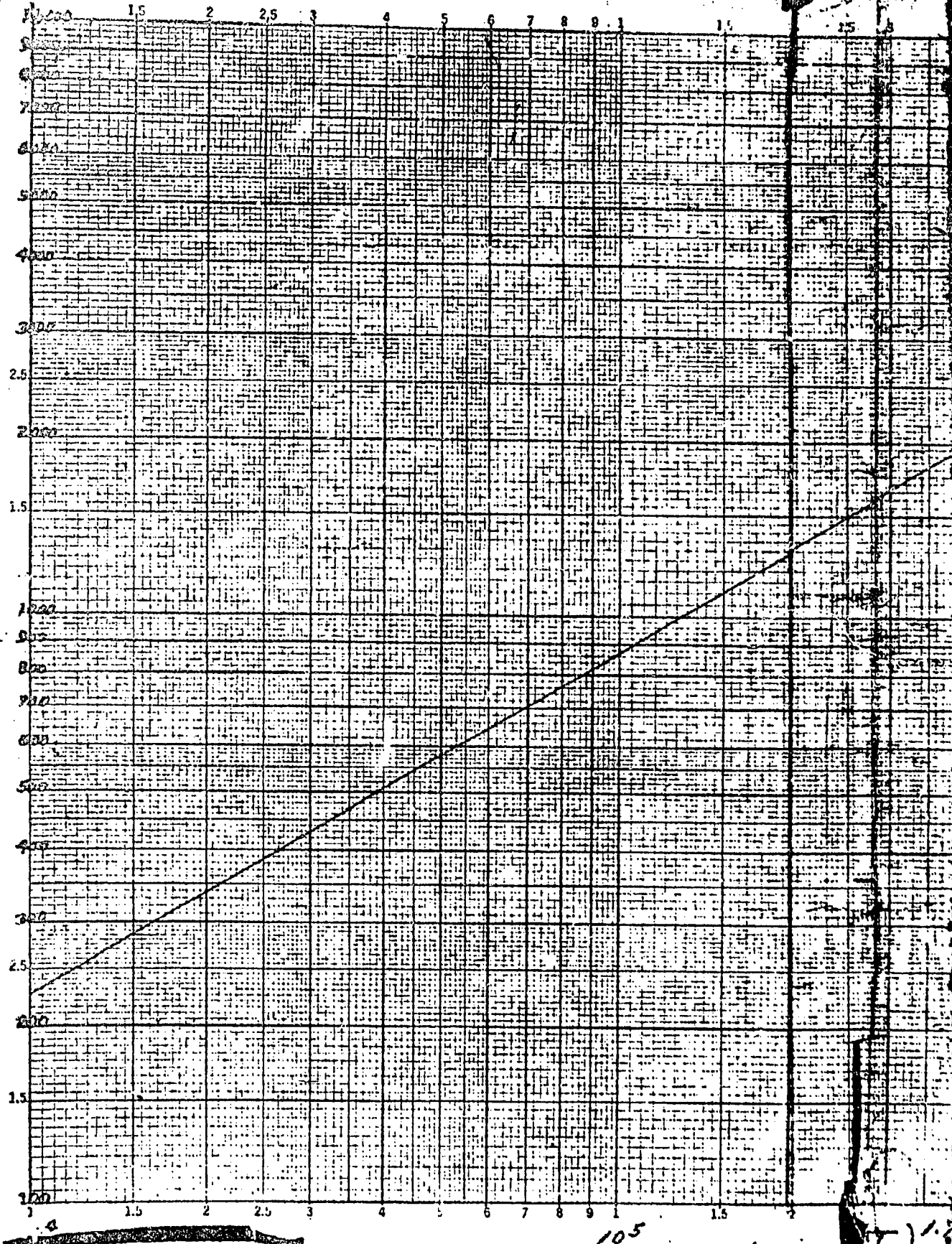


FIGURE A.2

STURTEVANT & CO., INC., No. 105, Boston,
Massachusetts, U.S.A.

TEMPERATURE, T



PILOT OF TEST

RAISED TO THE 1200

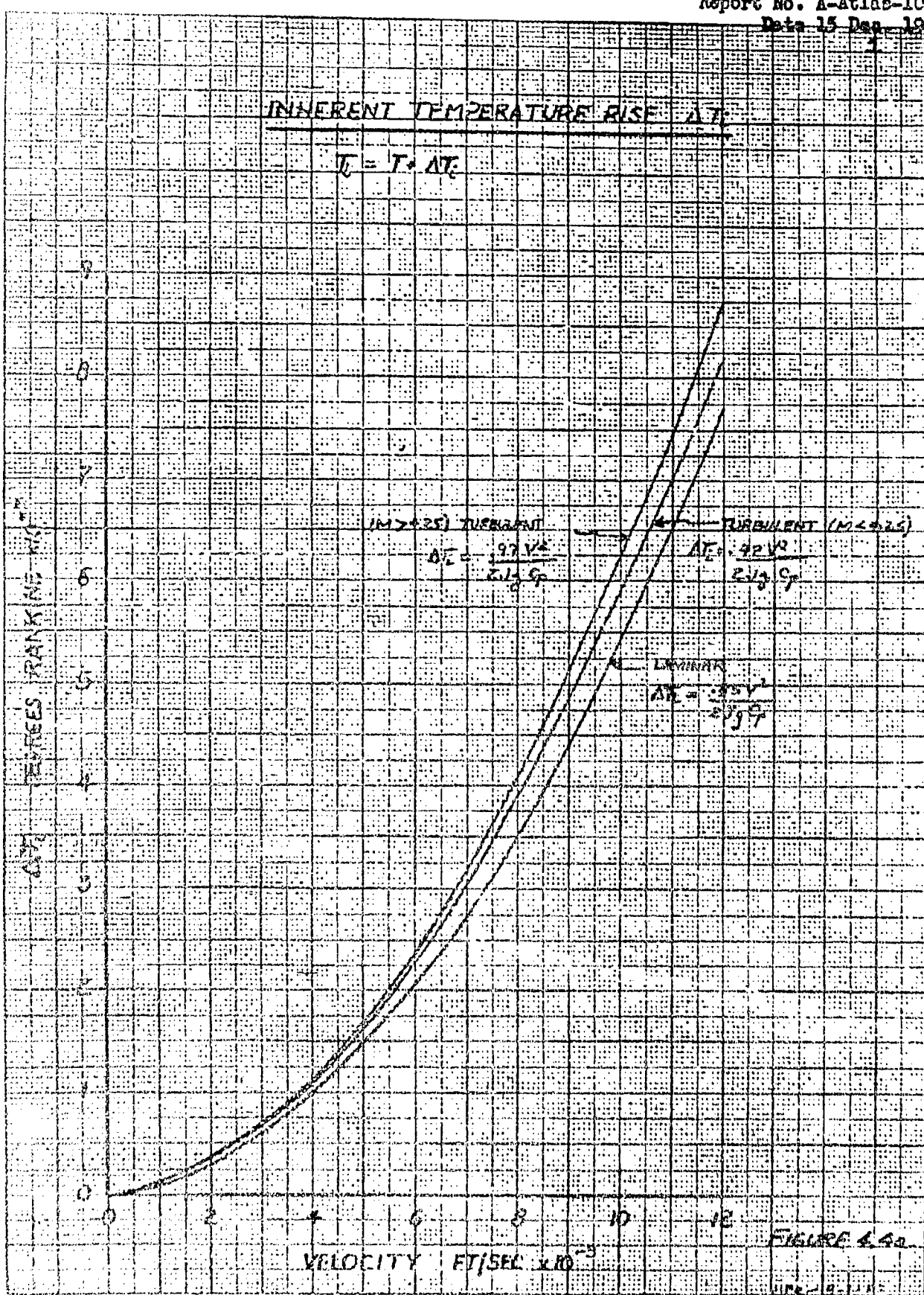
FIGURE 4.B

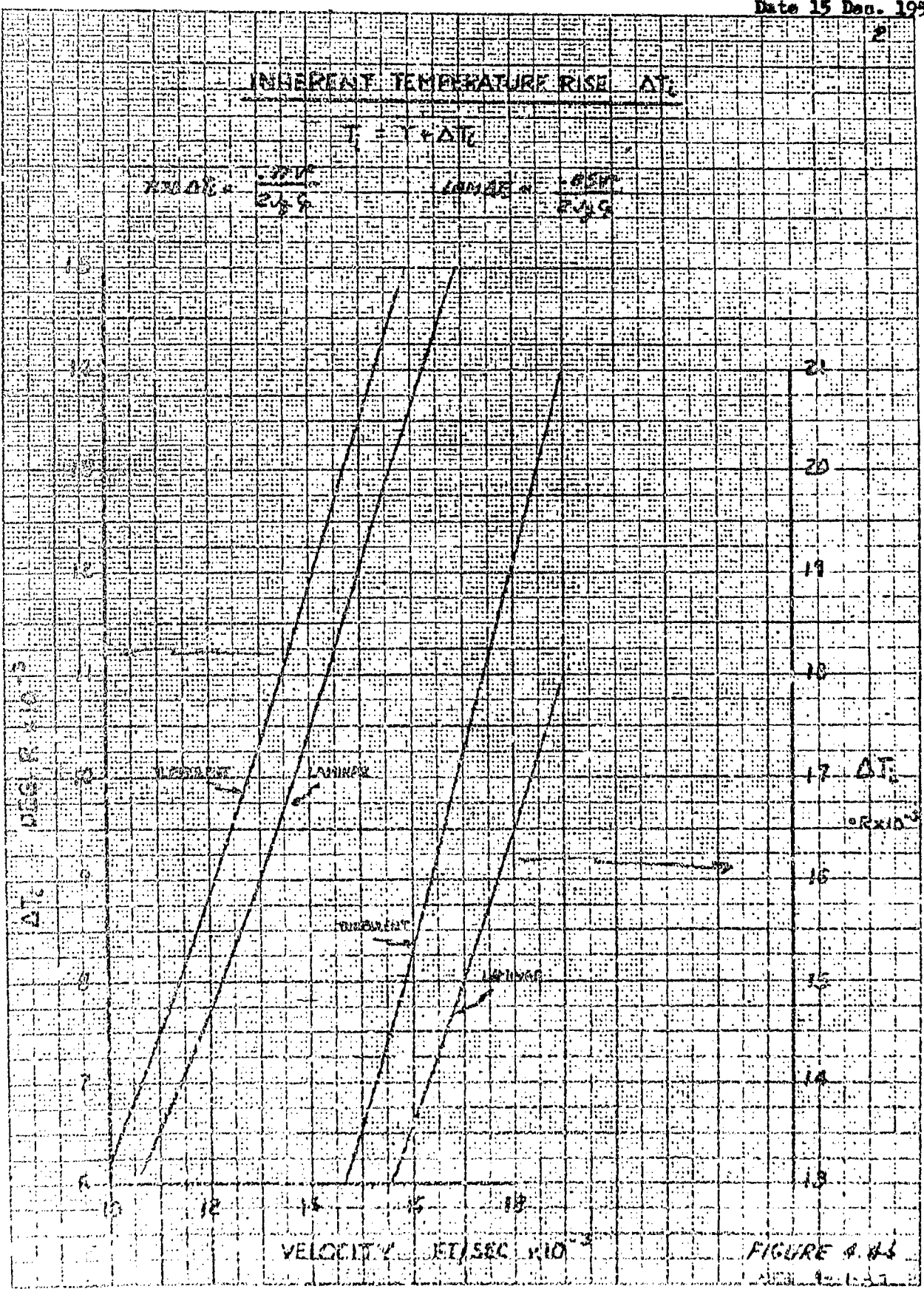
soil sample
800

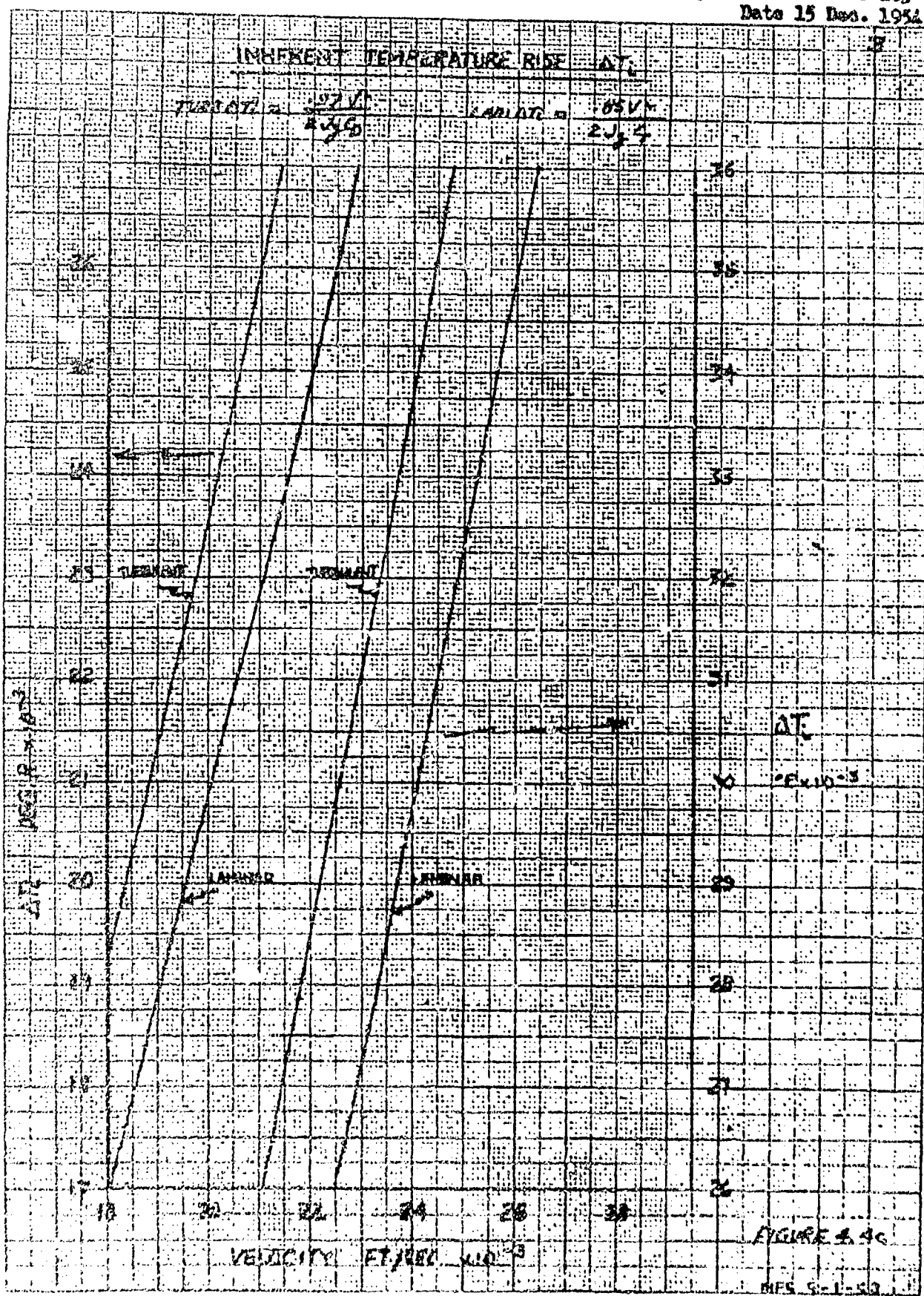
(T) 1.7

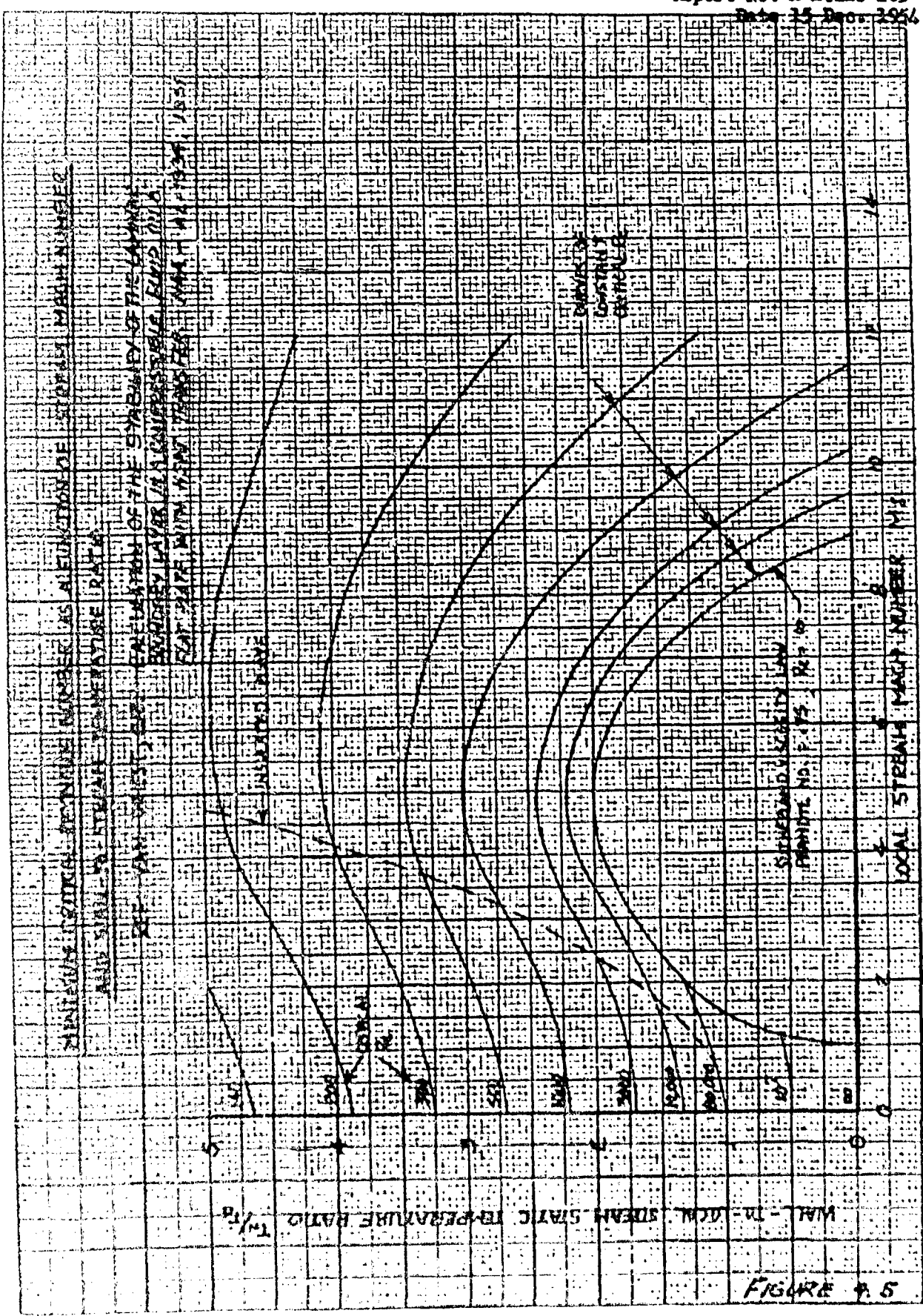
10.6

B









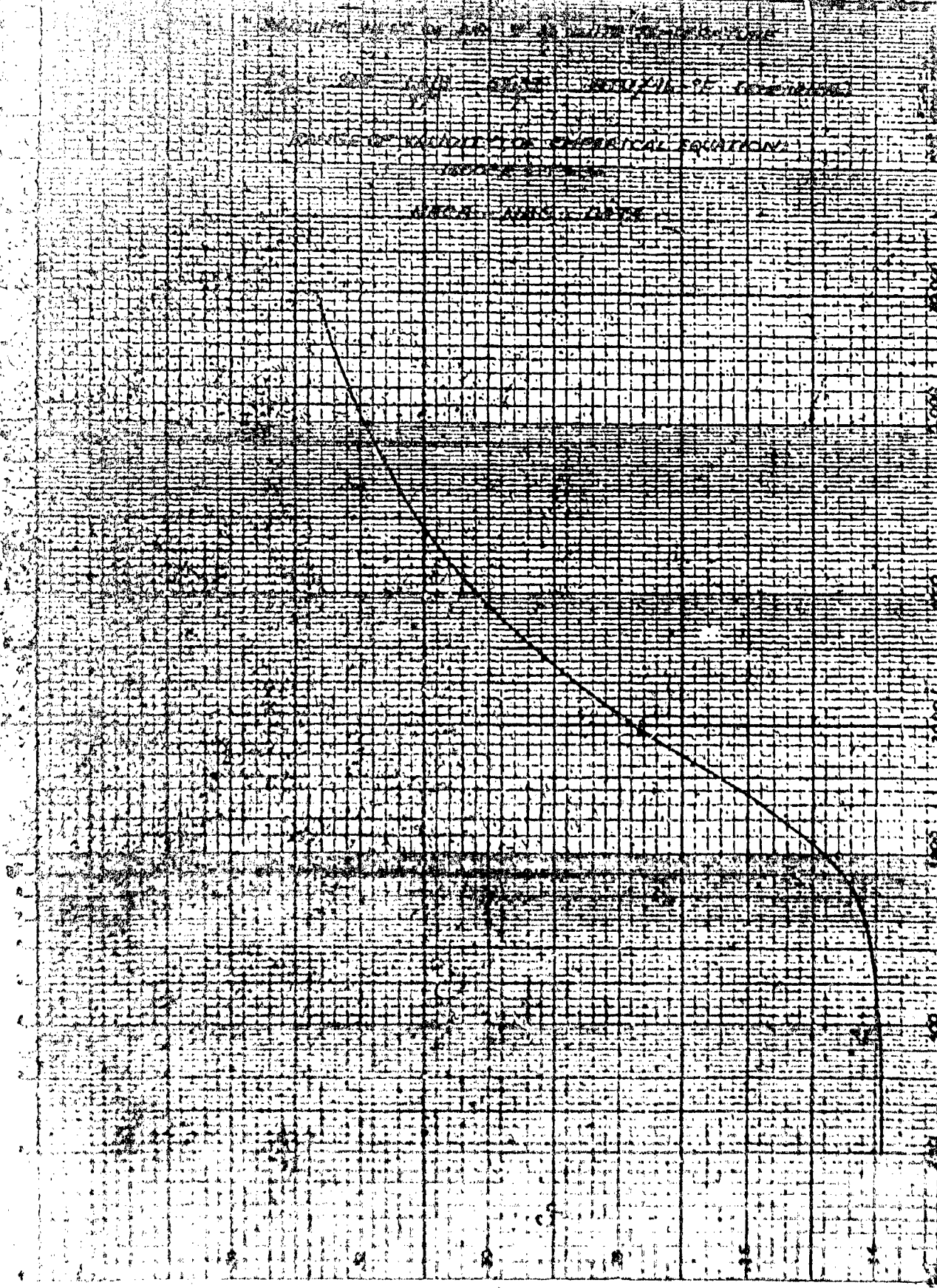


FIGURE 4.6

